RESTRICTED

CODE NO. 5
RM No. E8C02a

UNCLASSIFIED

OCT 7 1948

Copy 1

NACA

RESEARCH MEMORANDUM

EFFECT OF FUELS AND FUEL-NOZZLE CHARACTERISTICS ON PERFORMANCE OF AN ANNULAR COMBUSTOR AT SIMULATED ALTITUDE CONDITIONS

By Richard J. McCafferty

Flight Propulsion Research Laboratory
Cleveland, Ohio

CLASSIFICATION CANCELLED

Authority J.W. Crowley Date 12/14/53
EO 10501 See naca
By J. H. 1-18-54
RE 1976

CLASSIFIED DOCUMENT

This document contains classified information affecting the National Defense of the United States within the meaning of the Espionage Act, USC 50:31 and 32. Its transmission or the revelation of its contents in any manner to an unauthorized person is prohibited by law. Information so classified may be imparted only to persons in the military and naval services of the United States, appropriate civilian officers and employees of the Federal Government who have a legitimate interest therein, and to United States citizens of known loyalty and discretion who of necessity must be informed thereof.

TECHNICAL EDITING WAIVED

NATIONAL ADVISORY COMMITTEE FOR AERONAUTICS

WASHINGTON
September 28, 1948

RESTRICTED

UNCLASSIFIED

NATIONAL ADVISORY COMMITTEE FOR AERONAUTICS

RESEARCH MEMORANDUM

EFFECT OF FUELS AND FUEL-NOZZLE CHARACTERISTICS ON PERFORMANCE OF AN ANNULAR COMBUSTOR AT SIMULATED ALTITUDE CONDITIONS

By Richard J. McCafferty

SUMMARY

As part of a program to study the effects of fuel volatility, fuel composition, and fuel-injection-nozzle characteristics on the combustion performance of turbojet-engine combustors, an investigation was made with an annular combustion chamber operating under conditions simulating zero-ram operation of a turbojet engine at various altitudes and engine rotor speeds. The six fuels investigated included hydrocarbons of the paraffinic and aromatic classes having a boiling range from 104° to 664° F. They were isoheptanes, AN-F-28, AN-F-32, Diesel oil, benzene, and a high boiling aromatic (solvent 4). The fuel-injection nozzles investigated had capacities of 2.0, 3.0, 7.5, 10.5, and 17.5 gallons per hour. Investigations were made wherein the combustor-inlet-air conditions were each altered independently from conditions near the altitude ceilings.

A low-boiling-temperature fuel of either the aromatic or paraffinic classes gave higher altitude operational limits at low engine rotor speeds whereas a high-boiling-temperature fuel gave higher operational limits at high engine rotor speeds. Combustion efficiencies at various altitudes at constant engine rotor speeds indicated that the low-boiling-temperature fuels of both classes gave higher combustion efficiencies throughout the range of operational altitudes except near the altitude operational limits of these fuels.

The lower-boiling-temperature paraffinic fuels produced lower values of maximum obtainable temperature rise at severe operating conditions than did the higher boiling paraffinic fuels, but for fuel-air ratios below the point where these maximum values occurred the low-boiling-temperature paraffinic fuels gave better combustion efficiencies.

A reduction in fuel-nozzle size resulted in increased combustion efficiency of the two fuels, AN-F-28 and Diesel oil, at low heat-input or temperature-rise values but produced lower temperature-rise

limits. Performance was better with the larger nozzles at high temperature-rise ranges. In general, an optimum fuel-pressure differential (best nozzle capacity for a given temperature rise) exists for AN-F-28 or Diesel-oil fuel that provides a wide operating range of temperature rise at relatively good efficiencies for the sets of altitude operating conditions investigated.

INTRODUCTION

A program to investigate the effects of fuel volatility and hydrocarbon type on turbojet engine performance and to obtain data for devising an adequate method of rating fuels for any turbojet combustor type has been initiated at the NACA Cleveland laboratory. In the first phase of this investigation (reference 1), results obtained with a full-scale turbojet engine operating at sea-level static conditions indicated that neither fuel volatility nor hydrocarbon type had any appreciable effect on the combustion efficiency or thrust of the engine. However, a further investigation (reference 2) revealed differences in relative combustion efficiency among fuels operating in a single combustor at an altitude of 45,000 feet and indicated that combustion efficiency decreased with an increase in fuel boiling point and was relatively unaffected by difference in hydrocarbon type, except that aromatic fuels exhibited slightly lower efficiencies than the other classes. The investigation of reference 2 was made with a constant-area fuel-injection nozzle with the result that the fuel-spray characteristics changed with fuel type and with operating conditions.

The data of the present report show the effect of fuel-injection-nozzle characteristics on the variation of combustor performance with fuel volatility and hydrocarbon type for an annular combustion chamber operating at simulated conditions of zero ram throughout the altitude - engine-rotor-speed range. The data are presented as being indicative of general trends and phenomena applying to gas-turbine combustors. The engine conditions are therefore given in terms of grades of altitude (altitude in ft divided by a constant) and percentages of the military-rated engine speed. The effect of combustor-inlet parameters (temperature, pressure, and velocity) on combustor performance with various fuels was determined at operating conditions encountered near the altitude ceiling of the engine. Combustor performance characteristics that were investigated included altitude operational limits, combustion efficiencies, limits of obtainable mean temperature rise, and pressure loss. The six fuels that were studied included fuels representing paraffin and aromatic classes of hydrocarbons encompassing a wide range of fuel boiling points. The selection of fuels was limited to only those readily obtainable in quantity. Information on the combustion behavior of the fuels is also included.

APPARATUS AND INSTRUMENTATION

Combustor

933

A diagrammatic cross section of the combustor installation is shown in figure 1. The combustor in the 19XB-1 engine, which is the same as the 19B combustor, is approximately 19 inches in diameter and fills the annular space around the compressor-turbine shaft of the 19XB-1 turbojet engine. A description of an early design of the combustor, which was also used throughout most of the investigation reported herein, is given in reference 3. The basket of this combustor will be referred to in this report as basket 1. For part of the investigation a new inner liner different from the original one was used. The new liner had four additional rows of 7/16-inch holes drilled into the outer shell of the original liner near the downstream end between the existing rows of holes and 576 one-eighth inch holes located on the converging portion of the outer liner shell at the extreme downstream end of the combustor. These additional holes resulted in an open-hole-area increase of 9 percent more than the original liner. The basket of this combustor will be designated as basket 2.

Installation

A diagram of the general arrangement of the installation is shown in figure 2. The combustor was connected to the laboratory air supply and exhaust systems, and the air quantities and pressures were regulated by remote-control valves. The exhaust gases were cooled by means of water sprays in the vertical exit pipe. As some of the fuels studied were very difficult to ignite, an additional fuel line was connected to the bottom of the fuel manifold to supply AN-F-22 fuel for initiating combustion.

For regulation of inlet temperatures, a portion of the air was burned with gasoline in a preheater and then mixed uniformly with the rest of the air upstream of the combustor. The preheater was operated at conditions giving efficient combustion in order to minimize contamination of the air by combustibles. The use of such a preheater to produce a 200° F rise in the inlet temperature results in a consumption of 3.9 percent of the oxygen, an increase in the carbon-dioxide content of the inlet air by 0.80 percent of the total air weight, and an increase in the moisture content by 0.36 percent of the total air weight.

The inlet and outlet ducts were fabricated to simulate the dimensions and contours of the engine ducts leading to and from the combustor. Figure 1 shows the longitudinal cross section of the combustor and adjacent ducting and indicates the location of instrumentation planes. Observation windows for viewing the combustion were provided in the combustor housing as shown in figures 2 and 3. Another observation window, located in the vertical exit pipe (fig. 2), provided an end view of the inside of the combustor. 953

Temperature and velocity profiles at the combustor inlet were made uniform by first introducing turbulence to mix the air thoroughly with the exhaust gas from the preheater and then removing the turbulence in a calming chamber. (See fig. 2.) Maximum differences between local inlet temperatures and the mean temperatures were about 5° F. The maximum and minimum inlet velocities deviated by about 5 percent from the mean velocity for most runs. The 24 fuel nozzles in the combustor were calibrated and replaced when necessary; these nozzles were well matched, having maximum deviations of ± 3 percent from the mean fuel delivery when individually calibrated at a pressure differential of 100 pounds per square inch.

Instrumentation

The thermocouple junctions and the pressure taps in each instrumentation plane were located at centers of equal areas, as shown in figure 4. The letter positions at all instrumentation planes are arranged clockwise as seen looking upstream. A tabulation of the number and type of instruments at each plane follows:

Instruments	Instrumentation plane					
	2			3		
	Number of rakes	Probes per rake	Total number of probes	Number of rakes	Probes per rake	Total number of probes
Thermocouples	8	1	8	16	3	48
Total-pressure tubes	4	4	16	8	4	32
Wall-static pressure orifices			5			4

Instrumentation plane 2 is located at the combustor inlet, which has a cross-sectional area of 0.647 square foot; instrumentation plane 3 is at the combustor outlet where the annular cross-sectional area is 0.858 square foot. The pressure taps at plane 3 were located 1 inch downstream of the thermocouple rakes. Construction details of the temperature and pressure-measuring instruments are shown in figure 5.

933

Pressure data were obtained by photographing manometers. The thermocouples were connected through multiple switches to two calibrated self-balancing potentiometers, one with a range of -100° to 700° F to record the inlet-air temperatures and one with a range of 0° to 2400° F to record the outlet-gas temperatures. Fuel flows to the combustor and preheater were metered separately with calibrated rotameters. The pressure differential across the fuel nozzles was measured when possible by a 50-inch mercury manometer; higher pressure differentials were determined by obtaining the fuel manifold pressure with a gage that has a limit of 100 pounds per square inch and correcting for the combustor-inlet-air pressure. The air flow to the combustor was metered by a square-edge orifice installed according to A.S.M.E. specifications and located upstream of all regulating valves.

Fuels

Data on the physical properties and approximate chemical composition of the six test fuels are given in table I. Benzene and solvent 4 represent two aromatic fuels with different boiling points. Benzene and isoheptanes are similar-boiling-point fuels representing aromatic and paraffinic types of organic compounds. AN-F-28, AN-F-32 (JP-1), and Diesel oil are fuels of the paraffinic class with small percentages of aromatic-hydrocarbon constituents having a wide range of boiling points (104°-664° F).

PROCEDURE

Program

The program was divided into these principal investigations: (a) determination of altitude operational limits of the combustor equipped with standard 10.5-gallon-per-hour nozzles operating with six fuels; (b) determination of altitude operational limits of the combustor with AN-F-28 fuel for four different-capacity fuel-injection nozzles; (c) determination of combustion efficiencies at various altitudes for two engine rotor speeds with six fuels; (d) determination of the effect on combustion efficiency and temperature rise for the six fuels by varying combustor-inlet-air temperature at two conditions of altitude and engine rotor speed; (e) determination of the effect on combustor performance for AN-F-28 and Diesel-oil fuels at two conditions of altitude and engine rotor speed by varying inlet-air temperature while operating with different-capacity fuel nozzles and maintaining constant spray angle, and while operating with different spray angles and maintaining constant nozzle capacity; (f) determination of the effect on combustor performance for AN-F-28 and Diesel-oil fuels by varying inlet-air static pressure while operating with several different-capacity nozzles at conditions simulating engine operation at a maximum engine rotor speed and an altitude near the operational limits; and (g) determination of the effect on combustion efficiency and temperature rise with AN-F-28 and Diesel-oil fuels of varying the combustor-inlet velocity operating with standard capacity nozzles at conditions simulating engine operation at a maximum engine rotor speed and an altitude near the operational limits. All these investigations were made with basket 1 and investigation (g) was repeated with basket 2. 933

Estimated combustor-inlet-air conditions and combustor-outlet-gas temperatures corresponding to zero-ram operation for the 19XB-1 engine at various altitudes and engine rotor speeds were supplied by the manufacturer. These data were used to set the combustor operating conditions necessary to simulate engine operation at any desired altitude and engine rotor speed.

Altitude Operational Limits

In order to determine the altitude operational limits with any fuel or nozzle capacity, the combustor was operated with inlet conditions of air flow, pressure, and temperature simulating engine operation at various altitudes and engine rotor speeds. For each simulated altitude and engine-rotor-speed condition, the fuel flow was varied through a wide range in an attempt to obtain the combustor-outlet temperature required for nonaccelerating engine operation. All combustor-outlet temperatures were obtained by averaging individual thermocouple readings. If the required combustor-outlet temperature could be obtained, the simulated altitude and engine-rotor-speed condition was considered within the operational range of the engine; if the required combustor-outlet temperature was unobtainable, the simulated altitude and engine-rotor-speed condition was considered within the nonoperational range of the engine. In order to obtain general combustor-performance information, data were usually recorded as each of the following events occurred: (1) A combustor-outlet temperature was obtained that was equal to or slightly above the nonaccelerating-engine requirement; (2) a maximum obtainable value of combustor-outlet temperature was reached; (3) some local outlet temperatures exceeded the potentiometer limit (2400° F) and were considered unsafe for the instrumentation, making further increase in fuel flow inadvisable; and (4) combustion ceased (blow-out). The sequence and number of these events varied for different points.

Combustion Efficiencies

The combustor was operated with all six fuels over an extensive range of altitudes and engine speeds to obtain combustion efficiencies. Various altitude conditions at two engine rotor speeds (40 and 80 percent of rated engine speed) were selected for study and the air flow, pressure, and temperature at the combustor inlet were maintained constant. The fuel flow was altered to give an outlet-gas temperature approximately equal to that required for nonaccelerating-engine operation. The combustor-outlet temperature was difficult to estimate because the outlet temperature distribution was nonuniform; data were therefore usually recorded at two or more fuel flows that gave combustor-outlet temperatures slightly above and slightly below the required value. An interpolation was then made between the combustion efficiencies for these outlet temperatures to obtain the combustion efficiency for a combustor-outlet temperature equal to the nonaccelerating-engine requirement.

Effect of Combustor-Inlet Conditions on Performance

In order to determine the effect of the inlet variables on combustor performance, two altitude - engine-rotor-speed conditions were chosen slightly below the altitude operational limits (as obtained with AN-F-28 fuel); one was in the low-engine-rotor-speed range and the other was in the high-speed range. These two conditions will hereinafter be referred to as point A and point B, respectively. The combustor inlet conditions for points A and B are as follows:

Combustor inlet air	Point A	Point B
Static pressure, lb/sq in. absolute	9.2	7.7
Temperature, °F	240	35
Velocity, ft/sec	200	160
Required temperature rise, °F	1180	635

These conditions were severe enough to bring out any differences in combustion performance between the fuels and the nozzles studied. The combustor-inlet pressure, velocity, and temperature were maintained at values simulating engine operation at point A or B, the fuel flow was altered, and data were taken at each of several fuel-air ratios. In general, the fuel-air ratio was increased until the local combustor-outlet temperatures became too high for safe operation or until blow-out occurred. One of the three combustor-inlet parameters was then set at some new value, the other two parameters were maintained at the original values, and the fuel flow was again altered. This procedure was continued until each of the parameters had been varied independently of the others for each of the different fuels and fuel-injection nozzles investigated.

Methods of Calculation

The average dynamic pressures at instrumentation planes 2 and 3 were computed from the average velocities at these stations determined from the air flow, fuel flow, and the average temperatures and static pressures measured at these instrumentation planes. The total-pressure drop across the combustor was obtained as follows: Static pressures were measured, the dynamic pressures based on the average velocity at the respective stations were added to these values to give total pressures at the combustor inlet and outlet, and the difference between these values was taken as the total-pressure drop across the combustor.

The combustion efficiency is arbitrarily defined as the ratio of the actual total temperature rise to the theoretical rise in total temperature possible with the fuel and fuel-air ratio used. The charts of reference 4 were utilized for these computations. The thermocouple indications were taken as true values of the total temperatures with no corrections made for radiation or stagnation effects.

RESULTS AND DISCUSSION

Altitude Operational Limits

Effect of fuel characteristics. - Altitude operational limits of the annular combustor are presented in figure 6. The curves separate the region where the combustor-outlet temperatures attainable were sufficient from the region where the combustor-outlet temperatures attainable were insufficient for nonaccelerating operation of the engine. At a simulated speed of 50-percent rated engine rotor speed, solvent 4 gave the lowest operational ceiling of the fuels tested, and benzene gave the highest ceiling. At 95 percent rated engine rotor speed, the lowest ceiling existed with solvent 4 and the highest with AN-F-32 fuel. Diesel oil gave a higher altitude ceiling than AN-F-28 fuel in the high-engine-rotor-speed range but a lower ceiling in the low-rotor-speed range. These altitude operational limits were obtained with conditions simulating zero flight velocities. In figure 6 are also shown the altitude - engine-rotor-speed points A and B.

These results indicate that a low-boiling-temperature fuel, whether it be aromatic or paraffinic, gives better altitude performance in the low-engine-rotor-speed range (40 to 50 percent rated speed) than a high-boiling-temperature fuel. The reverse is true, however, in the high-speed range (85 to 100 percent rated speed) with the higher-boiling-temperature fuels producing in most cases higher operational ceilings. Exceptions are the AN-F-28 fuel limits occurring below the isoheptanes and benzene limits in the high-speed range and the limits obtained with solvent 4 falling several thousand feet below the other limits regardless of engine speed.

Effect of injection-nozzle orifice area. - Altitude operational limits with four different-capacity fuel nozzles using AN-F-28 fuel are presented in figure 7. The 3.0-gallon-per-hour nozzles produced the lowest ceiling in the high-rotor-speed range whereas the 17.5-gallon-per-hour nozzles gave the lowest limits in the low-rotor-speed range. When the combustor was operating with 17.5-gallon-per-hour nozzles in the low-rotor-speed range, the combustor-outlet temperature required for engine operation could be attained 2000 to 3000 feet above the limit curve as shown for this nozzle in figure 7. The combustion was unstable, however, and would cease (blow-out) in this region. Combustion near the altitude operational limits was more stable when the combustor was operating with 3.0-gallon-per-hour nozzles rather than with 10.5-gallon-per-hour nozzles (standard nozzle size for this combustion chamber) but the maximum temperature rise attainable would be reached at lower fuel-air ratios with 3.0-gallon-per-hour nozzles than with 10.5-gallon-per-hour nozzles. A more detailed explanation will be presented later in this report.

Combustion Efficiencies

Results of the combustion-efficiency investigation are shown in figure 8. The effect of increasing altitude at constant engine rotor speeds of 40 and 80 percent rated speed on the combustion efficiency for the six fuels is presented. Combustion efficiency decreased with increasing altitude at constant engine rotor speed for all the fuels investigated. AN-F-28 fuel produced the best combustion efficiency of the six fuels up to altitudes near the operational limits; at these altitudes the combustion efficiency of all the fuels decreased very rapidly and combustion ceased with further increase in altitude.

In general, combustion efficiency decreased with increase in fuel boiling temperature for both types of fuel investigated except near the altitude operational limits.

If the efficiency curves are extrapolated to sea level for the 80-percent-rated-speed condition, all the data converge close to 100-percent efficiency and show very little differences in combustion efficiency with each fuel. Previous work on a full-scale engine operated at sea level with a high engine rotor speed has shown no appreciable difference between the performance with these fuels (reference 1).

The reproducibility of results obtained in this part of the investigation is shown in figure 9. Combustion efficiencies with AN-F-28 were obtained from time to time throughout the program. Results check within ±3.5 percent for 40 percent rated speed and ±1.5 percent for 80 percent rated speed.

Effect of Inlet-Air Temperature on Fuel Performance

Effect of fuel characteristics. - The effect of combustor-inlet temperature on combustor performance is shown in figure 10, where the mean temperature rise through the combustor is plotted as a function of fuel-air ratio. Data are presented for operation with the six fuels with 10.5-gallon-per-hour fuel nozzles at inlet-air pressures and velocities corresponding to points A and B of figure 6 and for three inlet temperatures at each of these altitude - engine-rotor-speed points. The actual temperature supplied to the combustion chamber by the compressor in the engine is 240° F for point A and 35° F for point B. For estimation of combustion efficiencies, curves for various percentages of the theoretical temperature rise are included. Fuel-air ratios at which combustion ceased (blow-out) are marked on the curves with a line drawn perpendicular to the curve.

The maximum temperature rise obtainable and the fuel-air ratio at which it occurred in general decreased as the inlet-air temperature was decreased at constant pressure and velocity when operating with five of the fuels studied. Benzene, however, was less temperature sensitive than the other five fuels. The temperature-rise curves obtained with benzene for three inlet-air temperatures follow a common path for the high fuel-air ratios at point A and only the lowest temperature at point B produced a peaking of the temperature-rise curve and blow-out with increasing fuel-air ratio. (See fig. 10(e).) This lack of sensitivity to combustor-inlet-air temperature indicates why benzene produces the highest operational ceiling of the six fuels in the low-engine-speed range. Aromatic solvent 4 was more temperature sensitive than the lower boiling aromatic (benzene) or the paraffinic fuels; that is, a given decrease in inlet-air temperature had a more adverse effect on the combustion of solvent 4 than on the other fuels at the conditions studied. For the paraffinic fuels studied, combustion efficiency decreased at a less rapid rate as the boiling point of the fuel increased for the fuel-air ratios past the maximum combustion efficiency attainable.

A comparison of the performance of the combustor operating with the six fuels at points A and B for each inlet temperature is shown in figure 11. In order to place the performance of the various fuels having differences in heating values on a comparable basis, mean temperature rise against heat input is shown in figure 11, where heat input is computed as the product of the fuel-air ratio and lower heating value of the fuel.

Results show that the lower-boiling-temperature fuels (isoheptanes, AN-F-28, and benzene) produced combustion efficiencies 10 to 20 percent above the combustion efficiencies produced by the higher-boiling-temperature fuels (AN-F-32, Diesel oil, and solvent 4) at the combustor temperature rise required for nonaccelerating engine operation at point A (1180° F) and at point B (635° F). The higher-boiling paraffinic fuels, however, produced combustion efficiencies comparable to those produced by the lower-boiling paraffinic fuels at the highest heat inputs and temperature rises investigated at point A. A greater maximum temperature rise could be obtained with the higher-boiling-temperature paraffins than with the lower-boiling-temperature paraffins regardless of the amount of fuel input to the combustor. Because the higher-boiling paraffinic fuels, such as Diesel oil, continued to produce increasing temperature rise with increase in fuel-air ratio after the lower-boiling paraffinic fuels, such as AN-F-28, had produced a limiting value of temperature rise, the higher-boiling fuels produced higher altitude operational limits at maximum engine speeds.

Reproducibility of results is shown in figure 12. The combustor was operated at point A (inlet-air temperature, 240° F) with AN-F-28 fuel for various amounts of time throughout the program. The plot of temperature rise against fuel-air ratio shows a decrease of approximately 4 percent in combustion efficiency with AN-F-28 fuel from the beginning to the end of the program. The performance with solvent 4 might be slightly better therefore if these data had been obtained first instead of last. Check runs at operating conditions producing combustion efficiencies below 30 percent indicated results obtained at these conditions were not reliable; trends were reversed from time to time.

The effect of fuel boiling temperature on combustion efficiency is shown in figure 13. Combustion efficiency is presented as a function of average boiling temperature for two values of heat input for the combustor equipped with 10.5-gallon-per-hour nozzles operating at the three inlet temperatures at point A. The average boiling temperature is defined as the average of the initial boiling point, the temperatures corresponding to the distillation of each 10-percent increment of the fuel volume, and the final boiling point. At a heat input of 330 Btu per pound of air (fig. 13(a)), combustion efficiency decreased with increase in average fuel boiling point, and this trend was more pronounced with aromatic than with paraffinic fuels. At the highest heat input investigated, 580 Btu per pound (approximate fuel-air ratio of 0.032), the aromatic fuels exhibited a similar trend of decreasing efficiency with increased average boiling point (fig. 13(b)), but the increase in fuel boiling point had little effect on combustion efficiency of the paraffinic fuels at this high heat input.

The sensitivity of the combustion efficiency to boiling temperature of the paraffinic fuels was approximately the same for all the combustor inlet temperatures investigated. For the two aromatic fuels the adverse effect of increased fuel boiling temperature on combustion efficiency was much greater at the low combustor-inlet-air temperatures than at the high inlet-air temperatures.

Effect of fuel injection pressure. - The investigation presented in the remainder of this report was conducted with two paraffinic fuels, AN-F-28 and Diesel oil. The effect of fuel injection pressure is shown in figure 14 where the temperature rise through the combustor is plotted as a function of heat input for combustor operation with 17.5-, 10.5-, 7.5-, 3.0-, and 2.0-gallon-per-hour fuel nozzles at points A and B. The method of varying fuel injection pressure was to operate the combustor with different-capacity nozzles; the fuel pressure increased as the nozzle capacity decreased for the same fuel flow. In general, a decrease in inlet-air temperature at combustor conditions near the altitude operational ceiling decreased the temperature rise through the combustor at any heat input for both fuels for all the nozzle capacities examined.

A comparison of the temperature rise attainable at five inlet temperatures for various values of heat input for the combustor operating at points A and B with the several nozzle capacities investigated is shown in figure 15. The same data are plotted in figure 16, which shows the shape of the temperature-rise curve and the accompanying combustion-efficiency values as the mean temperature rise is increased by increasing fuel-air ratio. For the low-heat-input or low-temperature-rise values at point A, decreasing the nozzle capacity was beneficial to the combustion process for both fuels, particularly so for Diesel oil. At a heat-input value of 225 Btu per pound of air (fig. 15(a)), decreasing the nozzle capacity from 10.5 to 2.0 gallon per hour increased the temperature rise from 200° to 620° F (combustion efficiency increased from 20 to 75 percent) with Diesel oil, and with AN-F-28 fuel the temperature rise increased from 610° to 640° F (combustion efficiency increased from 72 to 76 percent). At these low temperature rises, corresponding to low heat-input values, the rate of combustion-efficiency increase due to larger injection pressures became greater for AN-F-28 fuel as the inlet temperature decreased (figs. 15(a) to 15(c)). With Diesel oil the inlet temperature had no appreciable effect on the rate of increase of combustion efficiency with decrease in nozzle size.

With both fuels the low-capacity fuel nozzles produced temperature-rise limits within the fuel-air-ratio range investigated; these limits occurred at lower temperature-rise values with the smaller-capacity nozzles. With nozzles of the same capacity, the temperature-rise limit occurred at a higher temperature with Diesel oil than with AN-F-28 fuel. With Diesel oil the 3.0-gallon-per-hour nozzles gave a temperature-rise increase up to a limiting value of 1330° F; with AN-F-28 they gave an increase up to 830° F. The 7.5-gallon-per-hour nozzle gave no temperature-rise limit in the range investigated with Diesel oil but did give a limit with AN-F-28. At the lower inlet-air temperatures these temperature-rise limits were low for both fuels; some nozzles produced limits at an inlet-air temperature of 90° F that did not produce a limit within the fuel-air-ratio range investigated at 240° F. These trends for point-A conditions were also indicated at point-B conditions. However, the combustion at point-B conditions had low efficiencies, and the data were inconsistent.

A comparison of Diesel oil and AN-F-28 fuels operating at point-A conditions utilizing the optimum nozzle size for each heat-input value is shown in figure 17. The combustion-efficiency and temperature-rise curves presented represent the maximum values that can be obtained with a variable-size nozzle having a capacity range of 2.0 to 17.5 gallons per hour. These curves show that Diesel oil operates at lower efficiencies for these conditions than AN-F-28 regardless of injection pressure at low heat input but that a greater amount of temperature rise is nevertheless available with Diesel oil than with AN-F-28 for inlet-air temperatures of 90° and 150° F for these nozzle sizes. The rate of decrease in temperature rise with decreasing inlet-air temperature is greater for Diesel oil than for AN-F-28.

Variation of combustion efficiency with fuel-injection pressure differential at constant heat-input values for both fuels at points A and B is shown in figure 18. Combustion efficiency for values of mean temperature rise through the combustor for constant pressure-differential curves is presented in figure 19. As either the heat input or the temperature-rise values increased, the beneficial effect of increasing injection pressure became less until a transition point was reached above which increasing injection pressure was detrimental to combustion. For each inlet temperature, an optimum fuel-pressure differential exists for each fuel that provides a wide operating range of temperature rise at relatively good efficiencies. Temperature-rise limits are encountered at successively lower values of temperature rise as the inlet-air temperature is decreased regardless of fuel volatility. 353

<u>Effect of varying fuel-nozzle spray angle at constant capacity.</u> - The results obtained by investigating the performance of the combustor operating with 3.0-gallon-per-hour nozzles and two fuels at four different fuel-nozzle spray angles is shown in figure 20. No consistent differences in data trends for the various spray angles were found. The detrimental effect of decreasing inlet-air temperature on combustion performance was similar for all angles of spray regardless of fuel used. The different-angle nozzles produced nearly identical temperature-rise limits; the limits with Diesel oil occurring at higher values of temperature rise than the limits with AN-F-28 fuel at an inlet temperature of 240° F. It may be noted that decreasing temperature has a more harmful effect on the temperature-rise limits with Diesel oil than on the limits with AN-F-28 fuel.

Effect of Inlet-Air Pressure on Fuel and Nozzle Performance

The effect of inlet pressure on temperature rise and combustion efficiency with AN-F-28 and Diesel-oil fuels operating with 17.5-, 10.5-, and 3.0-gallon-per-hour nozzles at conditions near point A is presented in figures 21 and 22. The 17.5- and 10.5-gallon-per-hour nozzles had a 45° spray angle and the 3.0-gallon-per-hour nozzle had a 30° spray angle. Data were obtained at inlet-air static pressures of 8.4, 9.2, and 10.0 pounds per square inch absolute. Comparison of the effect of inlet-air temperature and pressure indicates that a decrease in combustor-inlet-air pressure produced the same general effects on performance as a decrease in combustor-inlet-air temperature. The combustion efficiencies obtained with AN-F-28 fuel were better than those obtained with Diesel oil except at the high heat inputs where in some cases AN-F-28 produced temperature-rise limits and Diesel oil did not.

Effect of Inlet-Air Velocity on Fuel Performance

The effect of altering inlet-air velocity on AN-F-28 and Diesel-oil fuels is shown in figure 23. An increase in inlet-air velocity had the same general effect on performance as a decrease in inlet-air pressure or temperature when operating with AN-F-28. With the Diesel oil the effect of changing the inlet-air velocity was the reverse, that is, a decrease in inlet-air velocity reduced temperature rise and efficiency throughout the fuel-air-ratio range investigated.

The difference in effect of velocity on the performance of the two fuels indicates another reason why Diesel oil produces a lower altitude ceiling at 50 percent rated speed but a higher altitude ceiling at maximum rotor speeds than AN-F-28 fuel. As the engine decelerates along the altitude limits from point A to point B, the pressure, temperature, and velocity decrease at the combustor inlet. The decrease in these parameters is harmful to the combustion of Diesel oil but the decrease in velocity is helpful to the combustion of AN-F-28 fuel. Also, decreasing inlet-air temperature is less detrimental to the combustion of AN-F-28 fuel than to the combustion of Diesel oil. Diesel oil therefore produces a lower temperature-rise-limit value than AN-F-28 at low engine rotor speeds.

The effect of velocity on AN-F-28 and Diesel-oil fuels operating with basket 2 is shown in figure 24. Trends indicated are the same as those found with basket 1.

Combustion Characteristics

Observations were made during the investigation regarding the behavior of the different fuels. The color of the flames produced by the fuels was predominately yellow at low-altitude - high-engine-rotor-speed conditions, gradually changing to blue as the altitude was increased up to the altitude ceilings with the exception of benzene. Benzene produced a thin, greenish-cast flame that was very stable and difficult to extinguish at conditions near the altitude operational limits. The flames produced by solvent 4 and Diesel oil at high altitudes and low engine speeds would only partly fill the annular combustion area and the fuel delivered by the nozzles located in the noncombustion regions would be blown downstream as raw fuel. This characteristic was not evident for the other fuels even at similar combustion efficiencies.

Benzene was the only fuel to produce a significant amount of carbon deposits. Figure 25 shows the interior of the combustion chamber at the completion of the studies of solvent 4 and figure 26 shows the same view after operation with benzene. No attempt was made to measure the amount of carbon produced by the benzene fuel.

The fuels rank in the following order with regard to ease of ignition: AN-F-28, benzene, isoheptanes, solvent 4, AN-F-32, and Diesel oil.

Pressure Drop through Combustor

Representative data for the total-pressure drop from the inlet to the outlet of the combustor operating with various fuels and with nozzles of varying capacity are presented in figure 27. The ratio of the total-pressure drop to the inlet dynamic pressure $\Delta P_{2-3}/q_2$ is plotted against the ratio of the combustor-inlet air density to the combustor-outlet gas density ρ_2/ρ_3. Two scales are shown for values of $\Delta P_{2-3}/q_2$; scale A is based on q_2 values calculated for the combustor-inlet annular cross-sectional area and scale B is based on q_2 values calculated for the maximum annular cross-sectional area of the combustor. The results follow an approximately straight line as indicated by theory. Reference 3 gives a derivation of this relation and an explanation that the relation does not hold accurately for this combustor when the flame seat shifts. The data for the various fuels are plotted in figure 27(a), and the data for the various nozzle capacities are plotted in figure 27(b). The relative scatter of data in these plots indicates that the flame seat shifts with different-capacity nozzles more than with different fuels.

SUMMARY OF RESULTS

The results obtained in the investigation of fuel and nozzle performance in an annular combustor of a turbojet engine at conditions simulating zero-ram operation at two altitude - engine-speed conditions are summarized as follows:

1. A low-boiling-temperature fuel of either aromatic- or paraffinic-hydrocarbon type gave higher altitude operational limits at low engine rotor speeds whereas a high-boiling-temperature fuel gave higher altitude operational limits at high engine rotor speeds.

2. Combustion efficiency of all the fuels investigated decreased with increasing altitude at constant engine rotor speeds, and the low-boiling-temperature fuels of either class produced the higher efficiencies

up to the vicinity of their altitude operational limits. With further increase in altitude the combustion efficiency of all the fuels dropped sharply.

3. At operating conditions near the altitude operational limits, the temperature rise through the combustor passed through a maximum value as fuel-air ratio was increased. The maximum temperature rise obtainable and the fuel-air ratio at which it occurred decreased as the inlet temperature was decreased at constant pressure and velocity with all of the fuels studied except benzene.

4. Benzene was the least sensitive and solvent 4 (a higher-boiling-temperature aromatic fuel) the most sensitive of the fuels to decreasing inlet temperature at the two altitude conditions investigated.

5. At low fuel-air ratios or heat-input rates, the combustion efficiencies of the high-boiling-temperature fuels were considerably below those of the low-boiling-temperature fuels; but as the fuel-air ratio was increased, the combustion efficiencies of the high-boiling-temperature paraffinic fuels increased and tended to approach those for the low-boiling-temperature fuels for the conditions investigated.

6. At the high altitude conditions, the low-boiling-temperature fuels tended to attain a lower maximum temperature-rise limit and at a lower fuel-air ratio than did the high-boiling-point fuels in spite of having higher combustion efficiencies at temperatures below the temperature-rise limit. Benzene, however, was an exception in that it maintained both a better combustion efficiency and a higher temperature-rise limit than the high-boiling-temperature fuels tested.

7. Increasing fuel injection pressure by decreasing fuel-nozzle orifice area increased the combustion efficiency with AN-F-28 and Diesel-oil fuels at low heat-input or temperature-rise values, but produced lower temperature-rise limits. The larger nozzles gave higher combustion efficiencies at high values of heat input or temperature rise. For each inlet-air temperature, an optimum fuel-pressure differential across the injector system was found to exist for each fuel (AN-F-28 and Diesel oil) that provides a wide operating range of temperature rise at relatively good efficiencies.

8. No consistent differences were found in performance with various spray angles of 3.0-gallon-per-hour capacity fuel nozzles, operating with AN-F-28 and Diesel-oil fuels at conditions encountered near the altitude operational limits.

9. Decreasing combustor-inlet-air static pressure decreased the maximum temperature rise obtainable and the fuel-air ratio at which it occurred for any injection nozzle capacity at altitude operating conditions.

10. Increasing the combustor-inlet-air velocity had a detrimental effect on combustion performance with AN-F-28 fuel similar to the effect of decreasing inlet-air pressure and temperature. However, an opposite effect was observed with Diesel-oil fuel, as increasing velocity over the range investigated had a beneficial effect on the combustion performance with this fuel.

11. As expected from theoretical considerations, a straight-line correlation was obtained when the ratio of the total-pressure drop through the combustor to the combustor-inlet dynamic pressure was plotted as a function of the ratio of the combustor-inlet air density to the combustor-outlet gas density.

Flight Propulsion Research Laboratory,
National Advisory Committee for Aeronautics,
Cleveland, Ohio.

REFERENCES

1. Bolz, Ray E., and Meigs, John B.: Fuel Tests on an I-16 Jet-Propulsion Engine at Static Sea-Level Conditions. NACA RM
933 No. E7B01, 1947.

2. Zettle, Eugene V., Bolz, Ray E., and Dittrich, R. T.: Effect of Fuel on Performance of a Single Combustor of an I-16 Turbojet Engine at Simulated Altitude Conditions. NACA RM No. E7A24, 1947.

3. Childs, J. Howard, McCafferty, Richard J., and Surine, Oakley W.: Effect of Combustor-Inlet Conditions on Performance of an Annular Turbojet Combustor. NACA TN No. 1357, 1947.

4. Turner, L. Richard, and Lord, Albert M.: Thermodynamic Charts for the Computation of Combustion and Mixture Temperatures at Constant Pressure. NACA TN No. 1086, 1946.

TABLE I - PHYSICAL DATA AND APPROXIMATE COMPOSITION OF FUELS INVESTIGATED

Fuel	Boiling range (°F)	Average boiling point (°F)	Specific gravity at 60°/60°F	Hydrogen-carbon ratio	Lower heating value (Btu/lb)	Viscosity (centistokes at 70° F)	Composition (percent by volume)	
							Aromatics	Paraffins and/or cyclo-paraffins
Isoheptanes	170-206	181	0.727	0.177	18,900	0.650	1.0	99
AN-F-28	104-328	210	.725	.174	18,600	.608	14.0	86
AN-F-32	314-480	373	.791	.172	18,700	1.69	10.8	89.2
Diesel oil	364-664	482	.825	.158	18,559	3.04	19.2	80.8
Benzene	170-175	172	.883	.084	17,400	.745	100.0	0
Solvent 4	310-362	329	.874	.115	17,600	1.116	99.0	1

NACA

176-614

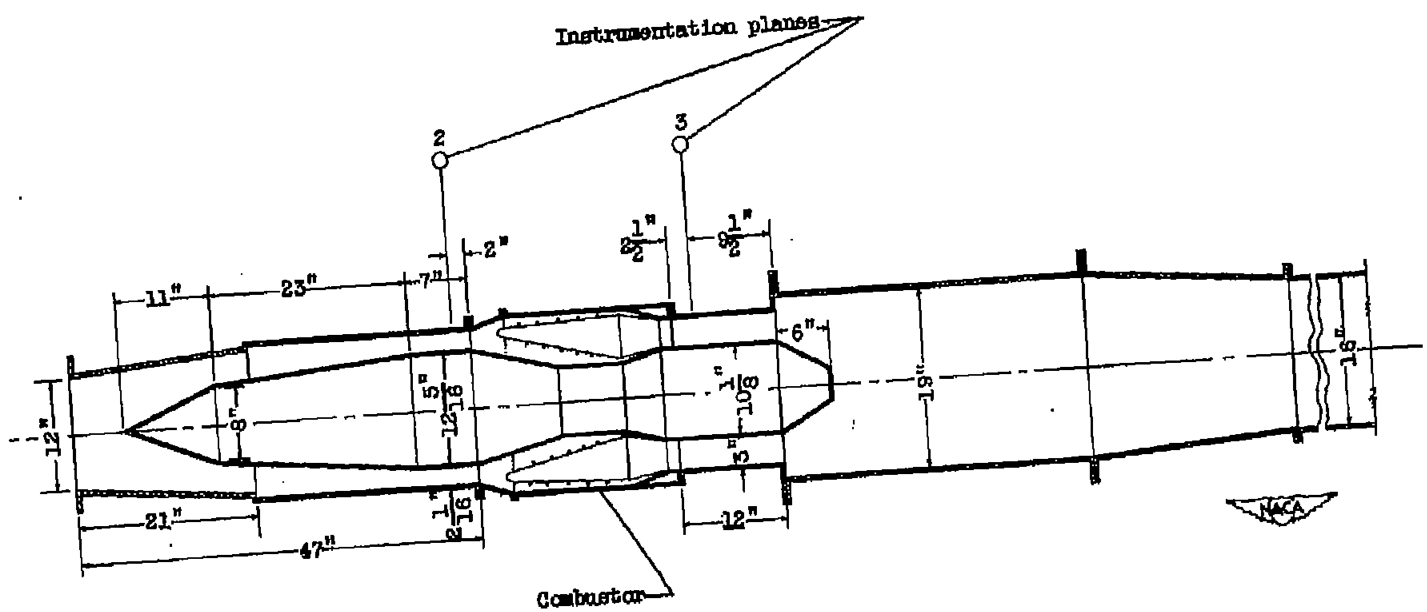

Figure 1. - Diagrammatic sketch of annular combustor showing inlet and outlet ducts and locations of instrumentation planes.

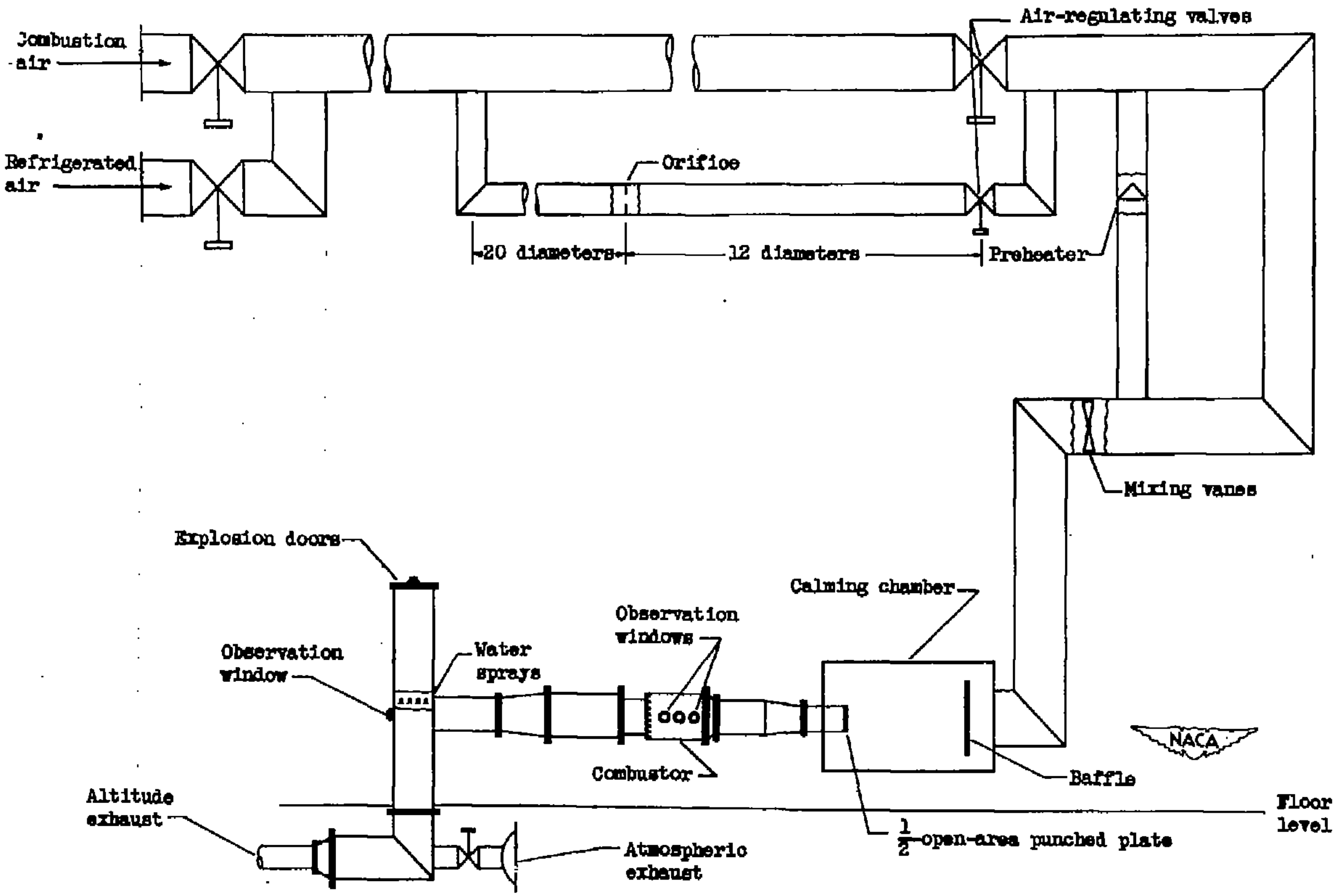

Figure 2. - Diagrammatic sketch of the arrangement of annular combustor test setup.

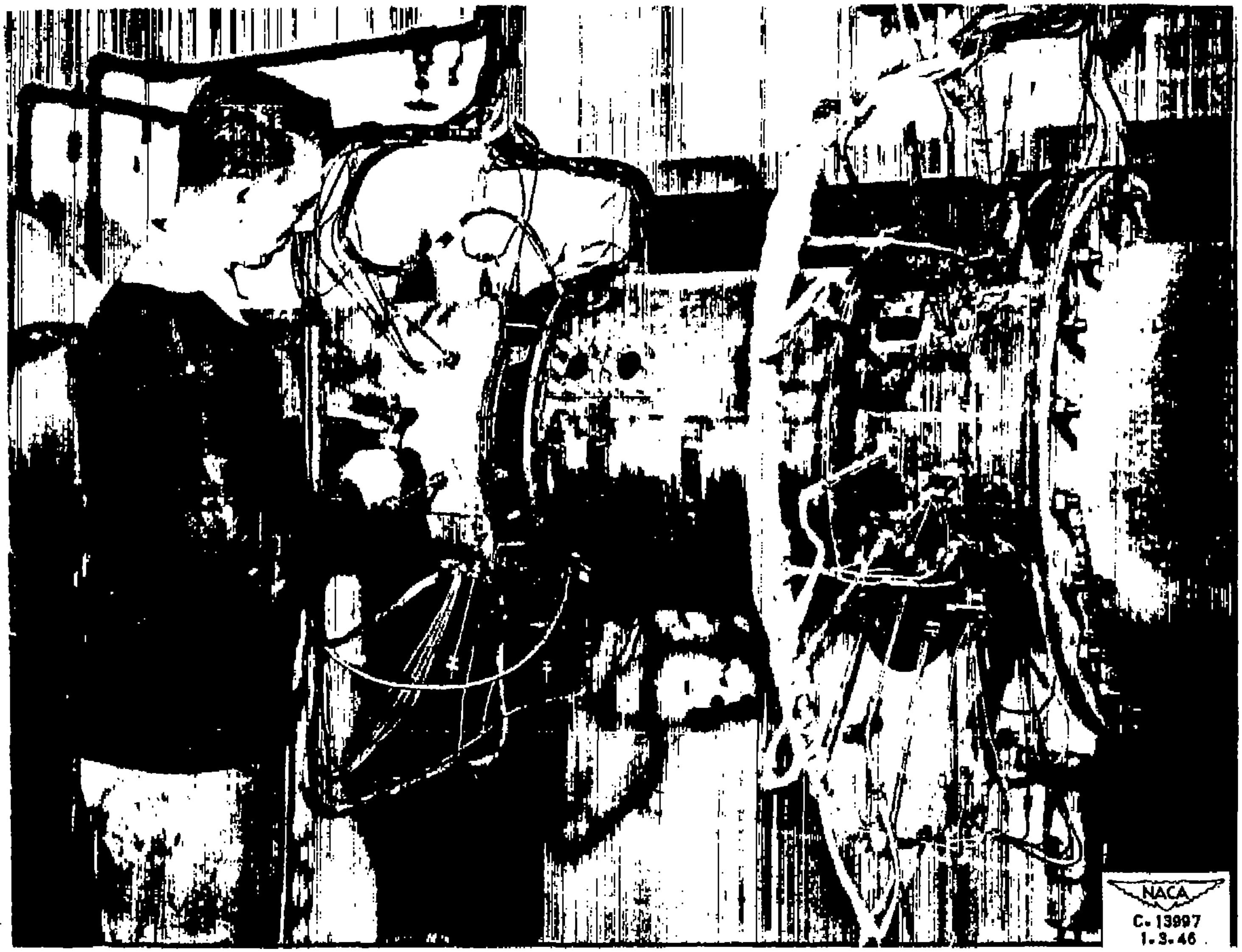

Figure 3. - Side view of installation of annular combustor for turbojet engine.

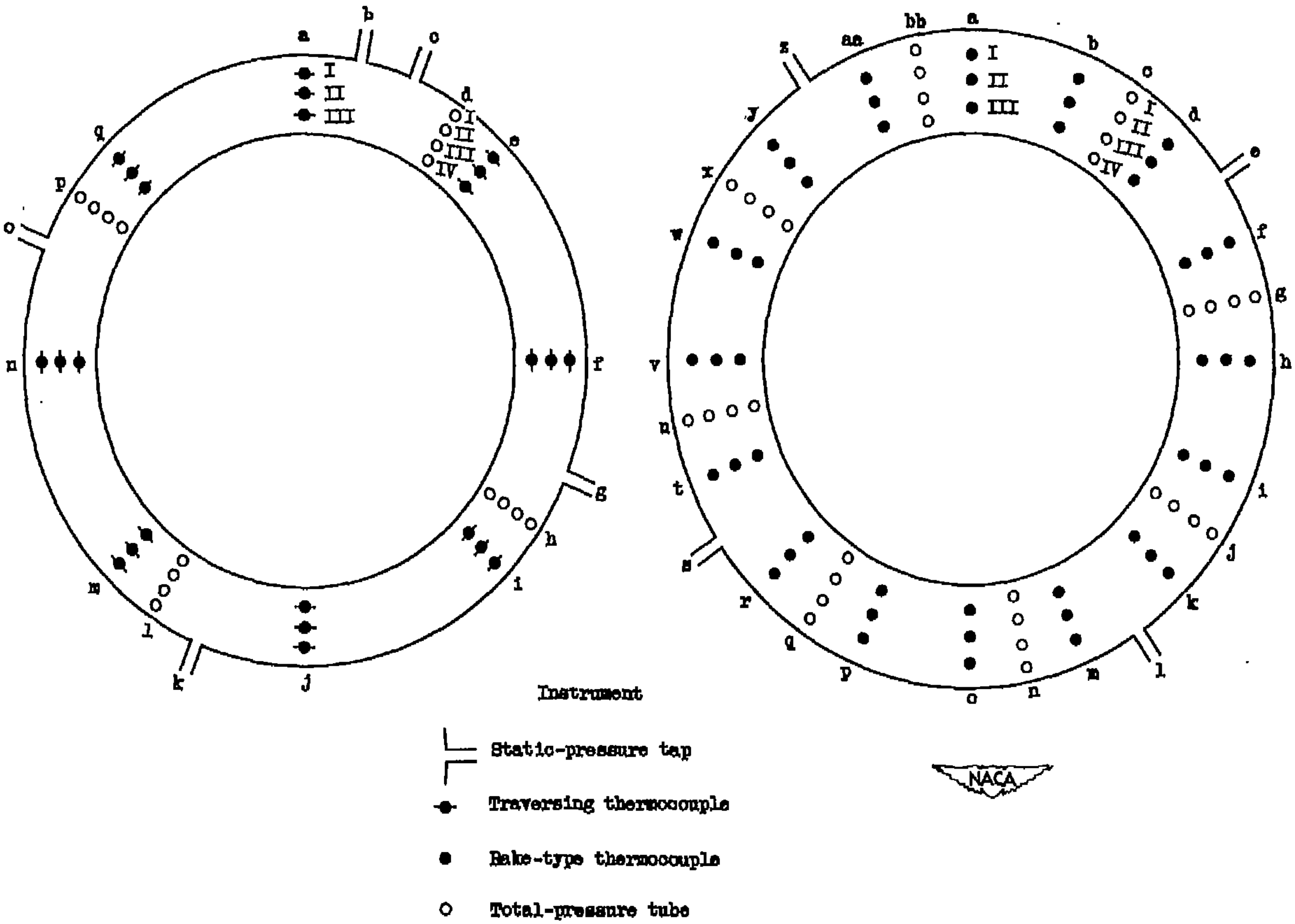

(a) Instrumentation plane 2.

(b) Instrumentation plane 3.

Figure 4. - Stations of measurement at the instrumentation planes shown in figure 1.

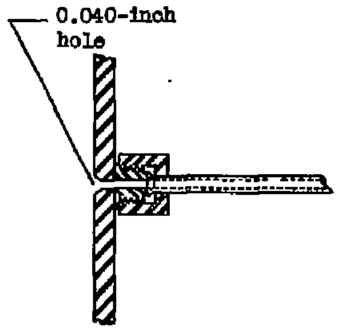

Static-pressure tap used at instrumentation planes 2 and 3

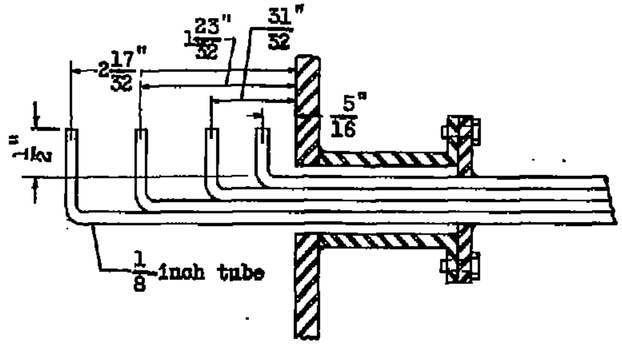

Total-pressure rake used at instrumentation plane 3

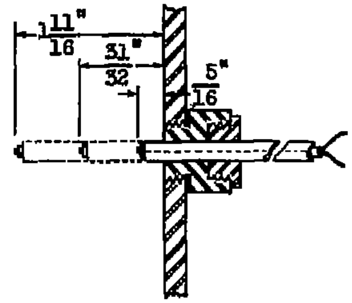

Traversing thermocouple (iron-constantan) used at instrumentation plane 2

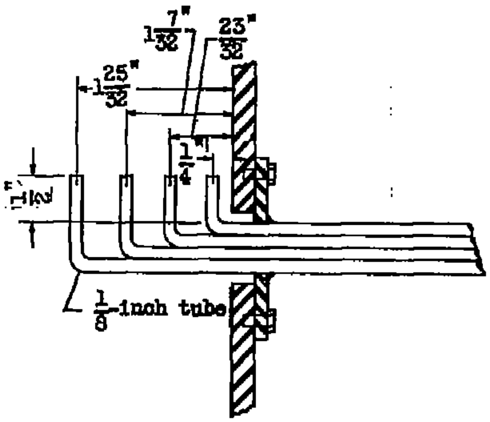

Total-pressure rake used at instrumentation plane 2

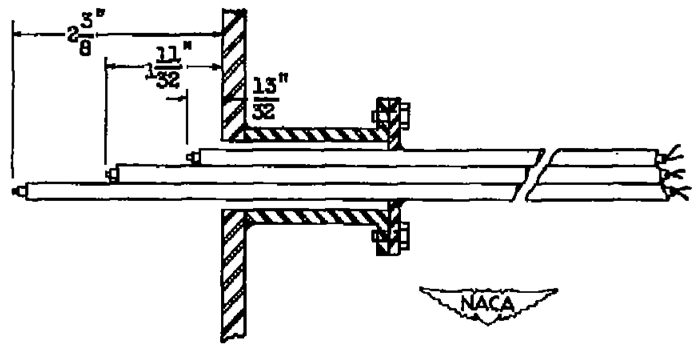

Rake-type bare thermocouple (chromel-alumel) used at instrumentation plane 3

Figure 5. - Details of the temperature- and pressure-measuring instruments used at instrumentation planes 2 and 3.

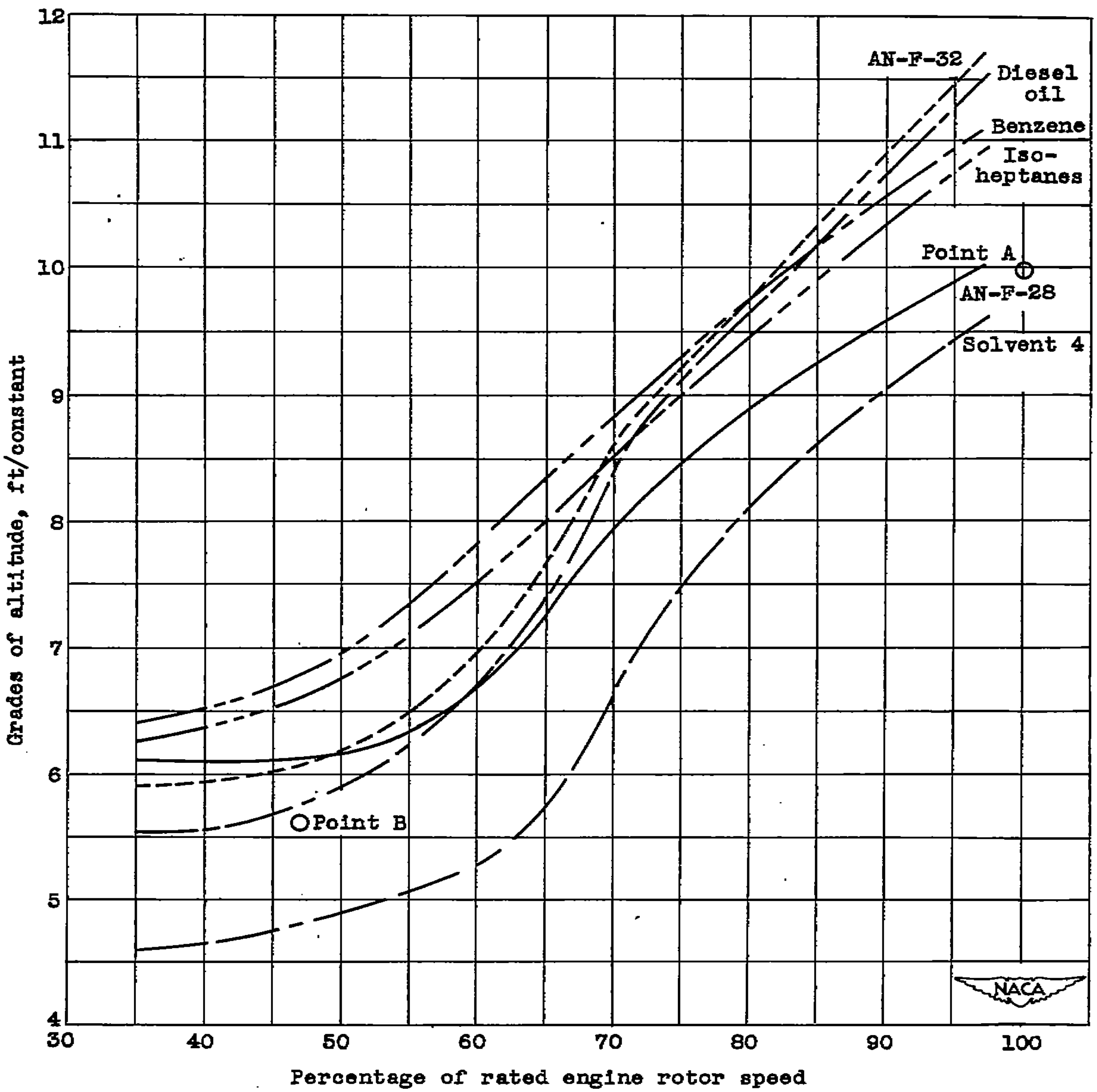

Figure 6. - Comparison of altitude operational limits of turbojet engine as determined by performance of annular combustor at simulated flight conditions with six fuels. Zero ram.

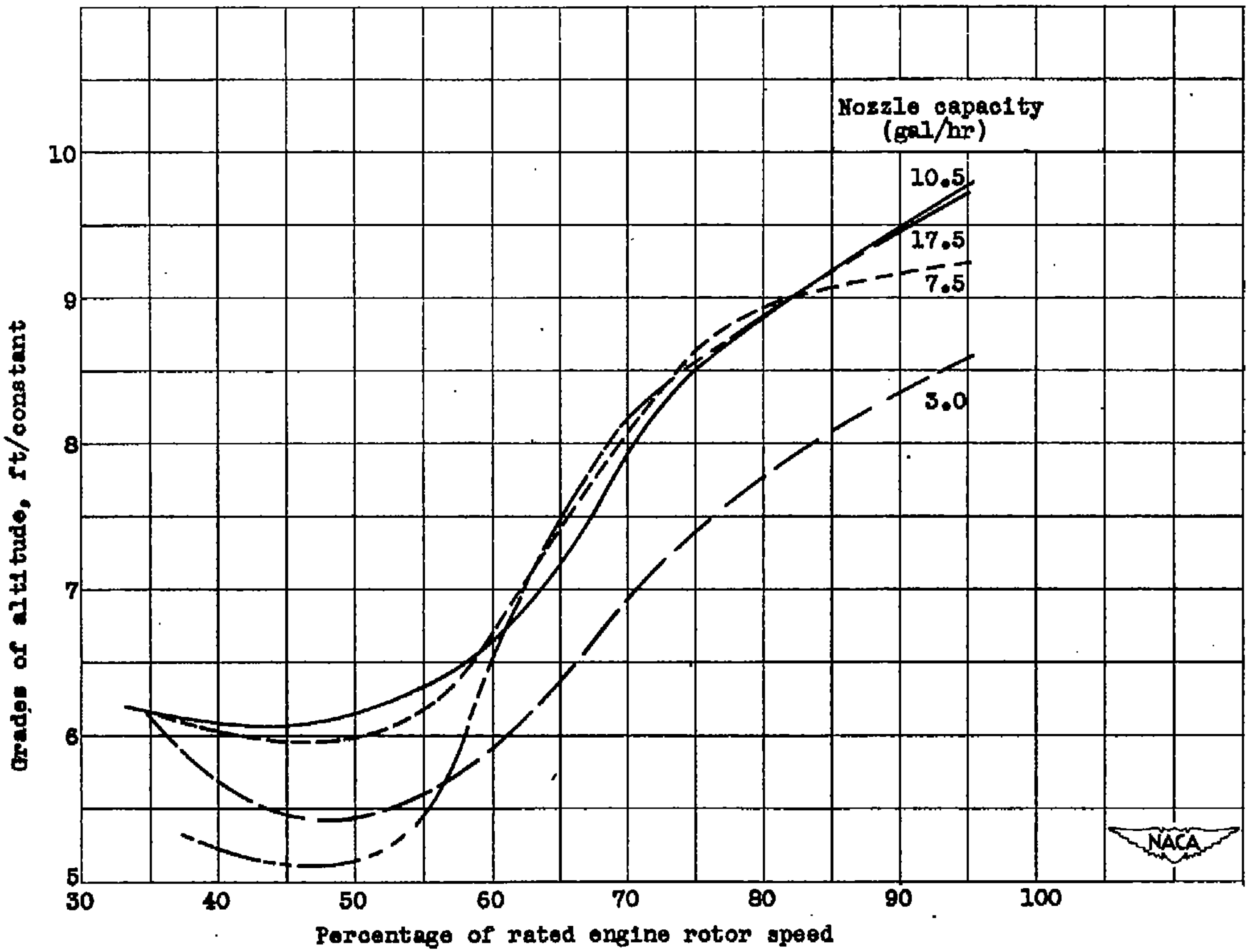

Figure 7. - Altitude operational limits of annular combustor determined by operation with different-capacity fuel-injection nozzles. Fuel, AN-F-28; zero ram.

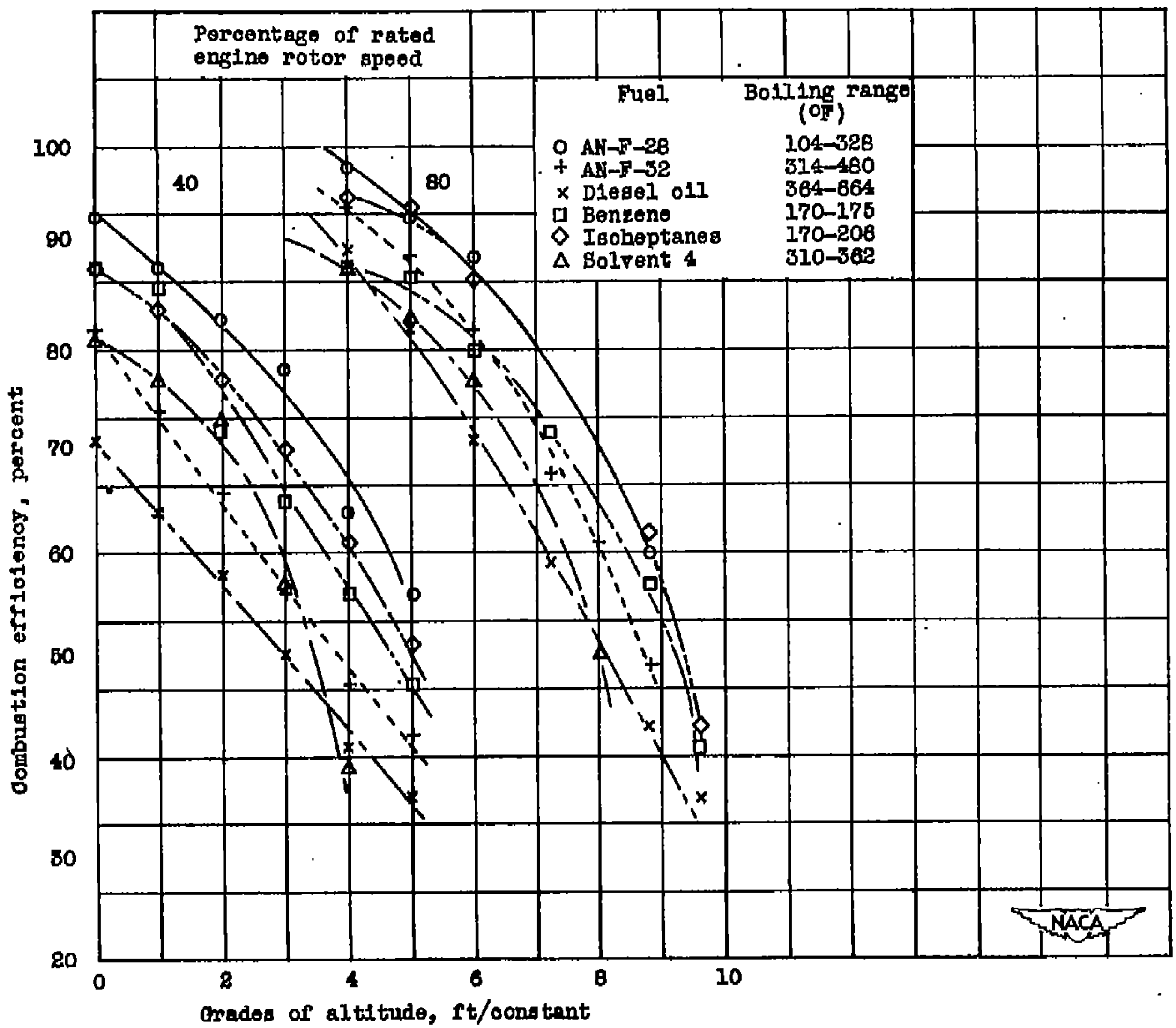

Figure 8. - Combustion-efficiency decrease with altitude increase at two constant engine-rotor-speed values for six different fuels in annular combustor. Zero ram.

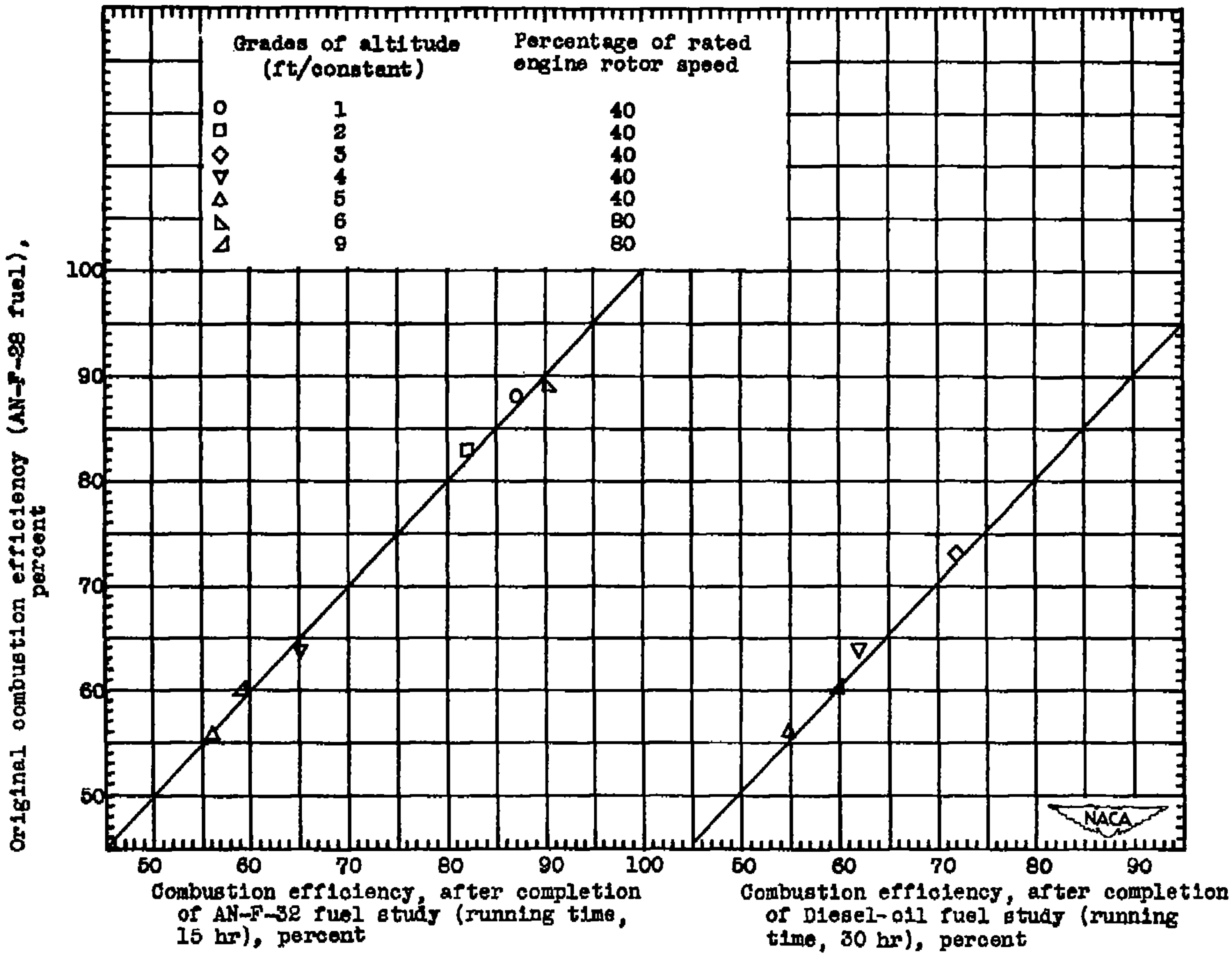

Figure 9. - Differences in combustor performance with AN-F-28 fuel over period of combustion-efficiency investigation.

933

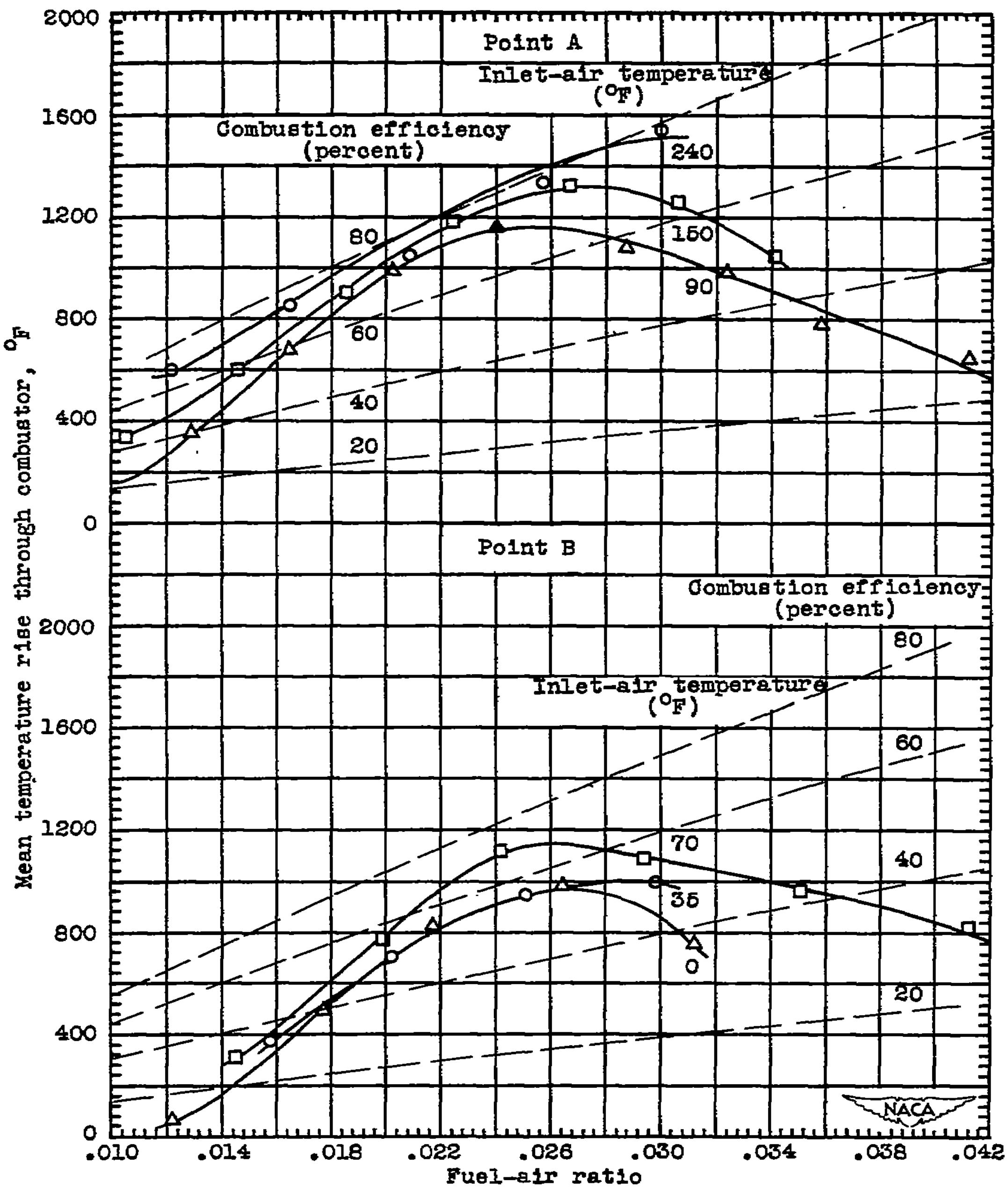

(a) Fuel, isoheptanes.

Figure 10. - Variation of mean temperature rise through annular combustor with fuel-air ratio for combustor-inlet-air temperature independently altered from values simulating engine operation with six fuels. Simulated engine operating conditions: Point A, inlet-air static pressure, 9.2 pounds per square inch absolute; inlet-air velocity, 200 feet per second; Point B, inlet-air static pressure, 7.7 pounds per square inch absolute; inlet-air velocity, 160 feet per second.

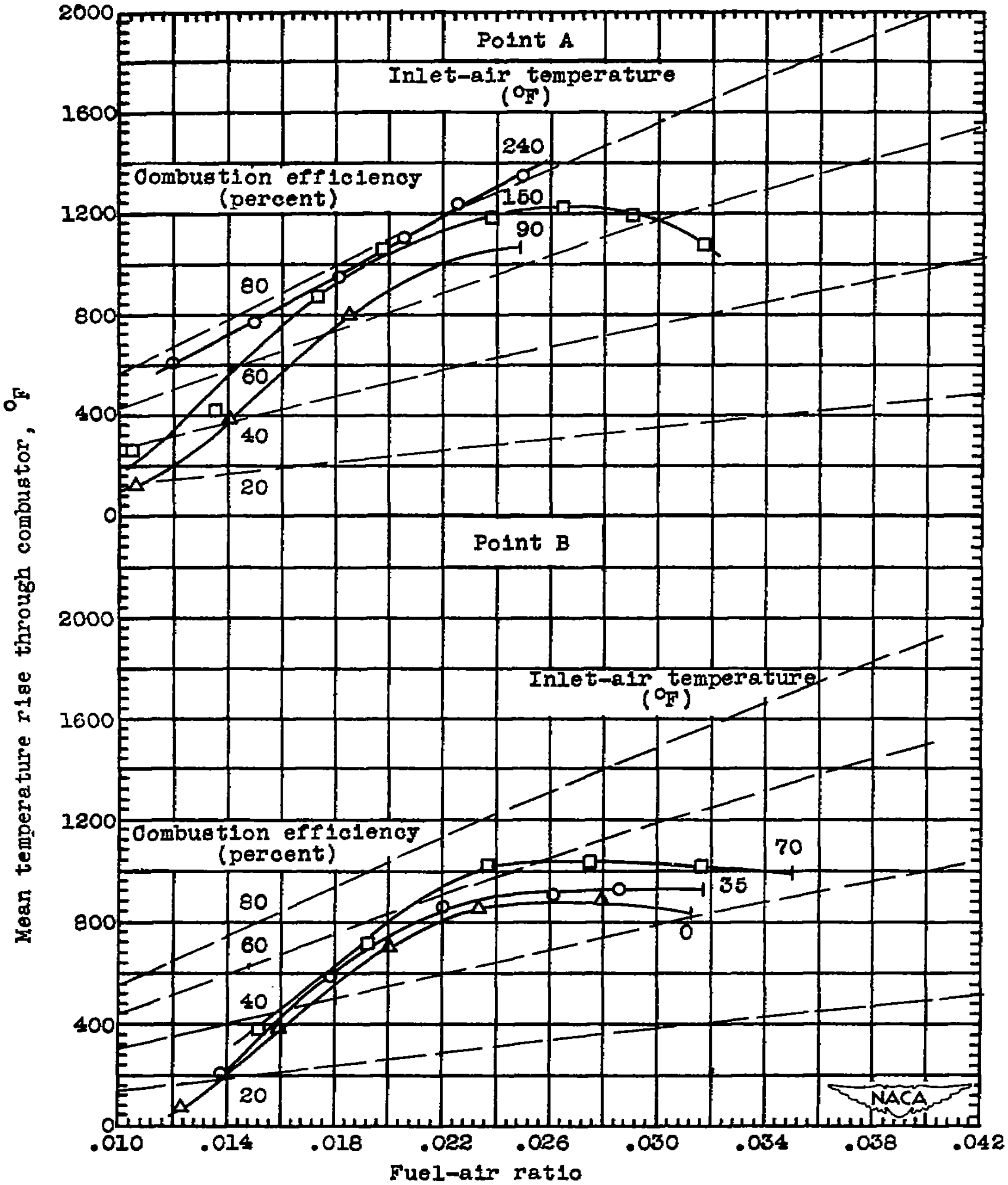

(b) Fuel, AN-F-28.

Figure 10. - Continued. Variation of mean temperature rise through annular combustor with fuel-air ratio for combustor-inlet-air temperature independently altered from values simulating engine operation with six fuels. Simulated engine operating conditions: Point A, inlet-air static pressure, 9.2 pounds per square inch absolute; inlet-air velocity, 200 feet per second; Point B, inlet-air static pressure, 7.7 pounds per square inch absolute; inlet-air velocity, 160 feet per second.

933

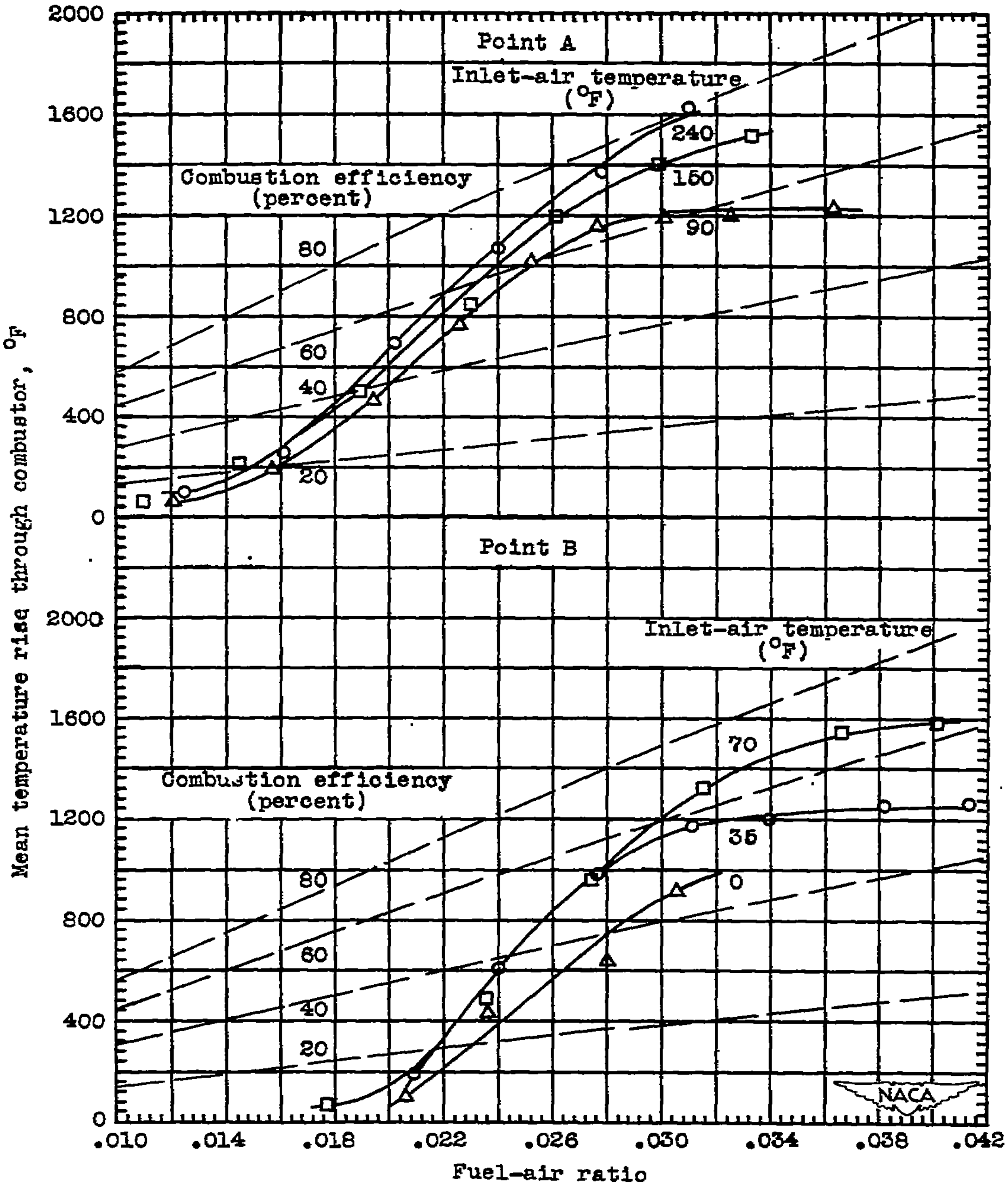

(c) Fuel, AN-F-32.

Figure 10. - Continued. Variation of mean temperature rise through annular combustor with fuel-air ratio for combustor-inlet-air temperature independently altered from values simulating engine operation with six fuels. Simulated engine operating conditions: Point A, inlet-air static pressure, 9.2 pounds per square inch absolute; inlet-air velocity, 200 feet per second; Point B, inlet-air static pressure, 7.7 pounds per square inch absolute; inlet-air velocity, 160 feet per second.

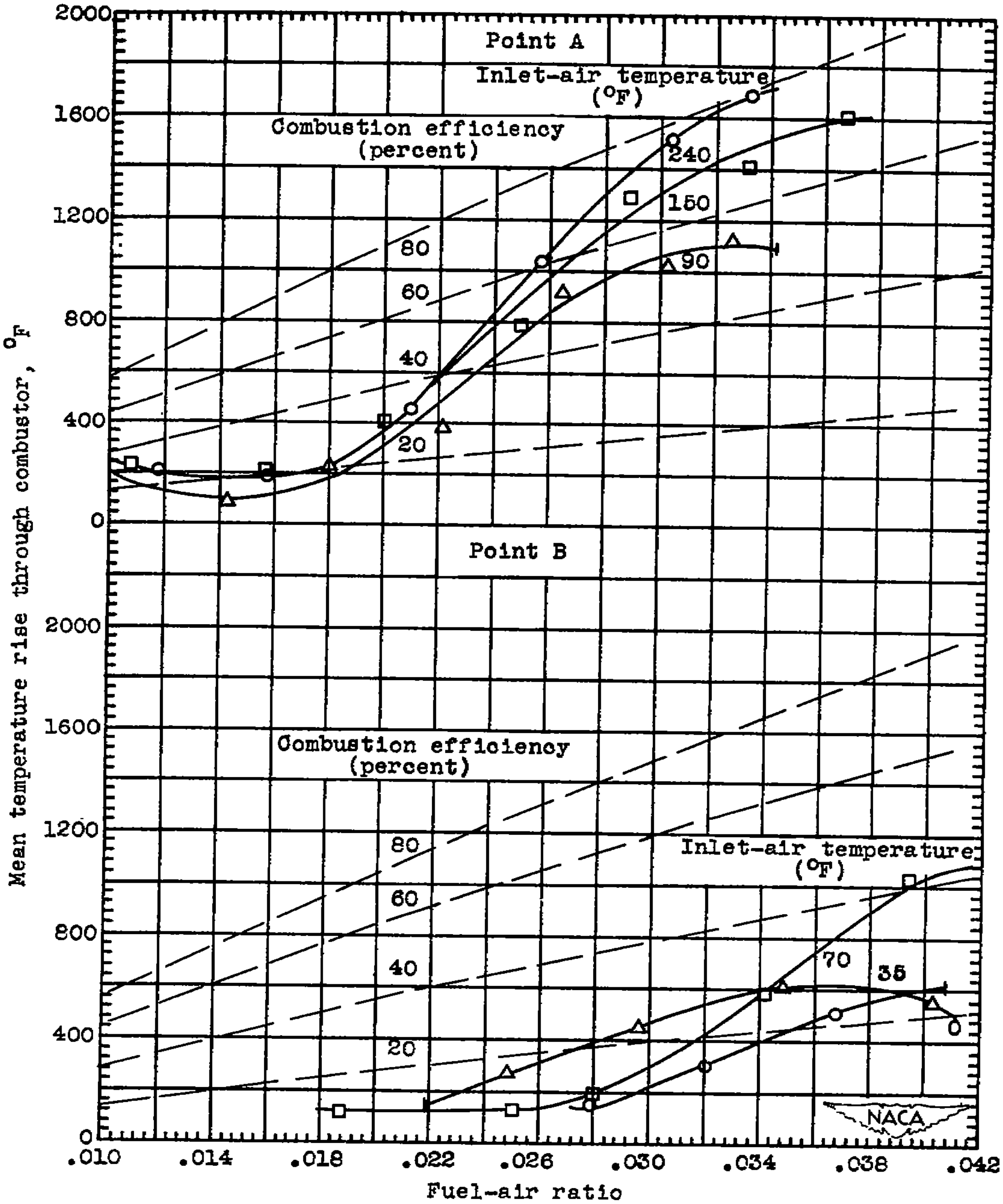

(d) Fuel, Diesel oil.

Figure 10. - Continued. Variation of mean temperature rise through annular combustor with fuel-air ratio for combustor-inlet-air temperature independently altered from values simulating engine operation with six fuels. Simulated engine operating conditions: Point A, inlet-air static pressure, 9.2 pounds per square inch absolute; inlet-air velocity, 200 feet per second; Point B, inlet-air static pressure, 7.7 pounds per square inch absolute; inlet-air velocity, 160 feet per second.

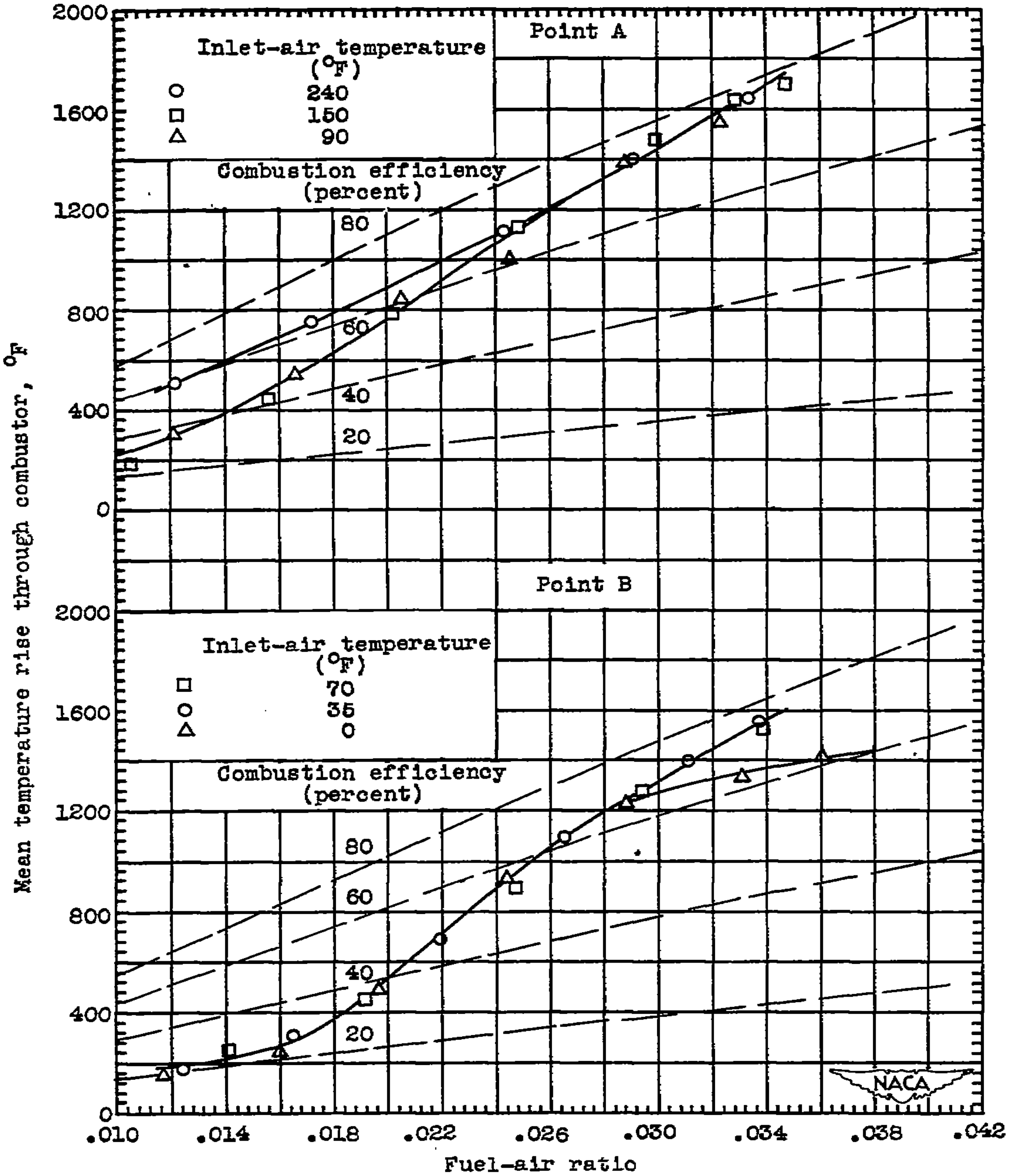

(e) Fuel, benzene.

Figure 10. - Continued. Variation of mean temperature rise through annular combustor with fuel-air ratio for combustor-inlet-air temperature independently altered from values simulating engine operation with six fuels. Simulated engine operating conditions: Point A, inlet-air static pressure, 9.2 pounds per square inch absolute; inlet-air velocity, 200 feet per second; Point B, inlet-air static pressure, 7.7 pounds per square inch absolute; inlet-air velocity, 160 feet per second.

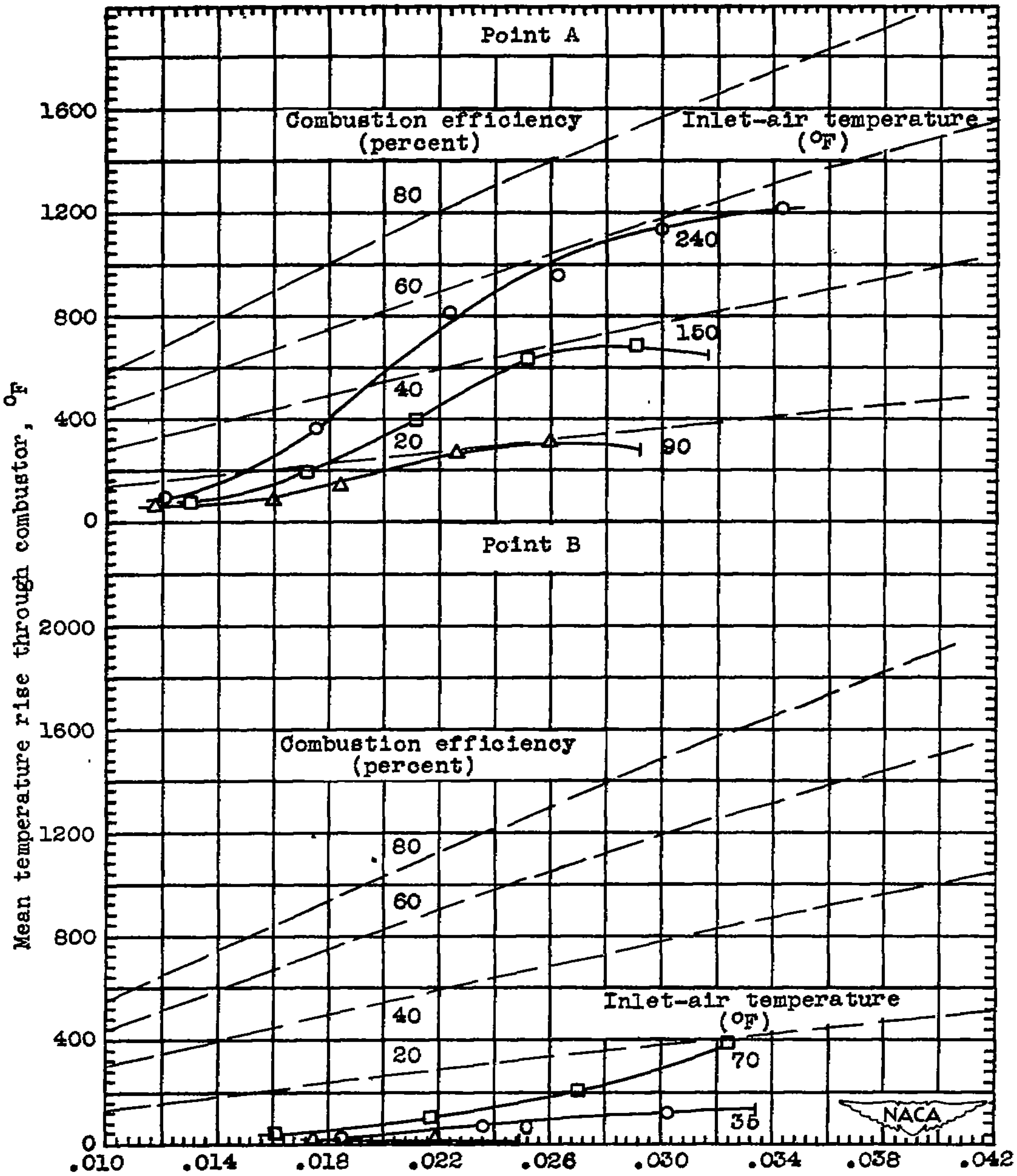

(f) Fuel, solvent 4.

Figure 10. - Concluded. Variation of mean temperature rise through annular combustor with fuel-air ratio for combustor-inlet-air temperature independently altered from values simulating engine operation with six fuels. Simulated engine operating conditions: Point A, inlet-air static pressure, 9.2 pounds per square inch absolute; inlet-air velocity, 200 feet per second; Point B, inlet-air static pressure, 7.7 pounds per square inch absolute; inlet-air velocity, 160 feet per second.

933

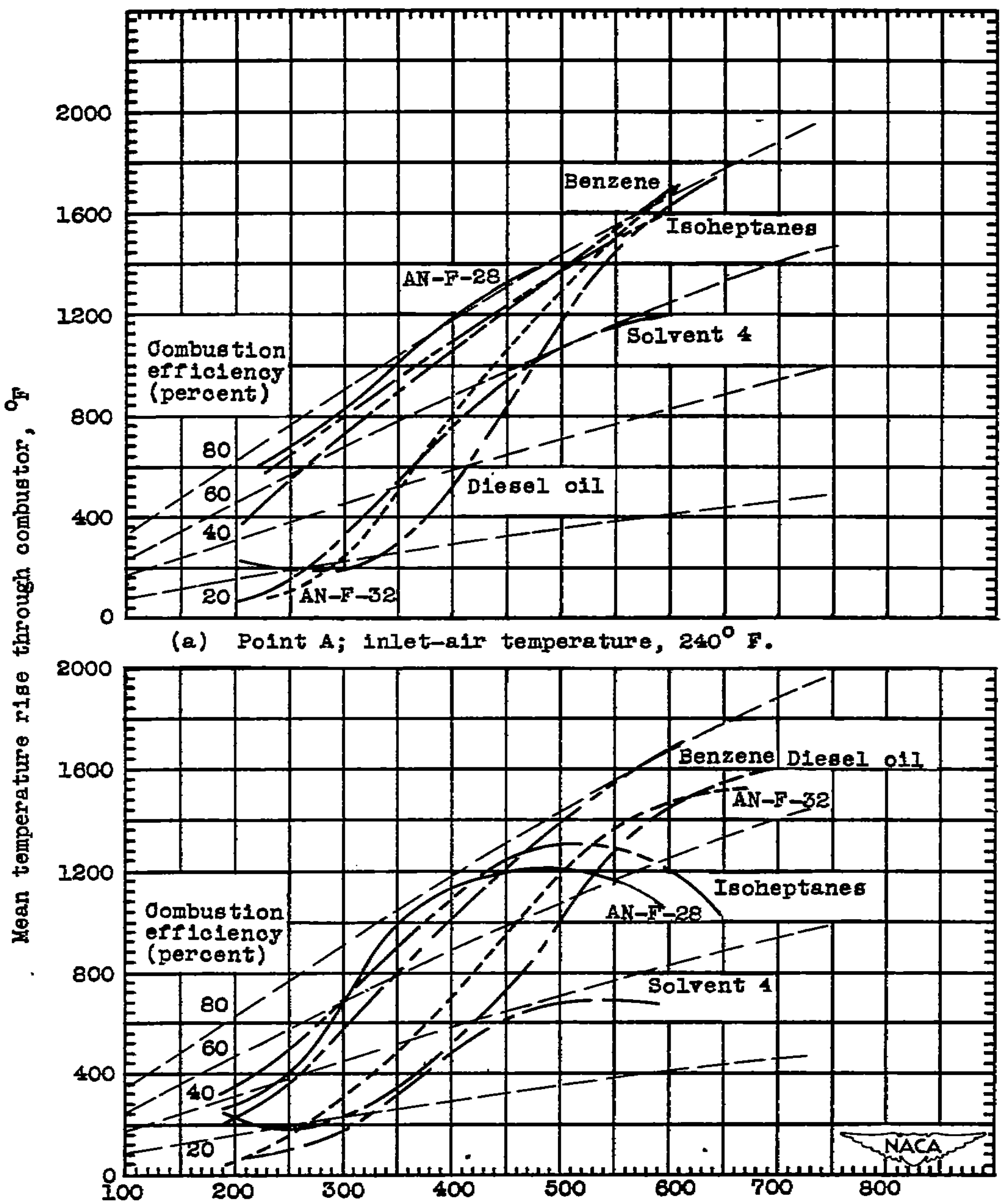

(b) Point A; inlet-air temperature, 150° F.

Figure 11. - Comparison of mean temperature rise through annular combustor for various heat-input values for six fuels and several inlet-air temperatures. Simulated engine operating conditions: Point A, inlet-air static pressure, 9.2 pounds per square inch absolute; inlet-air velocity, 200 feet per second; Point B, inlet-air static pressure, 7.7 pounds per square inch absolute; inlet-air velocity, 160 feet per second.

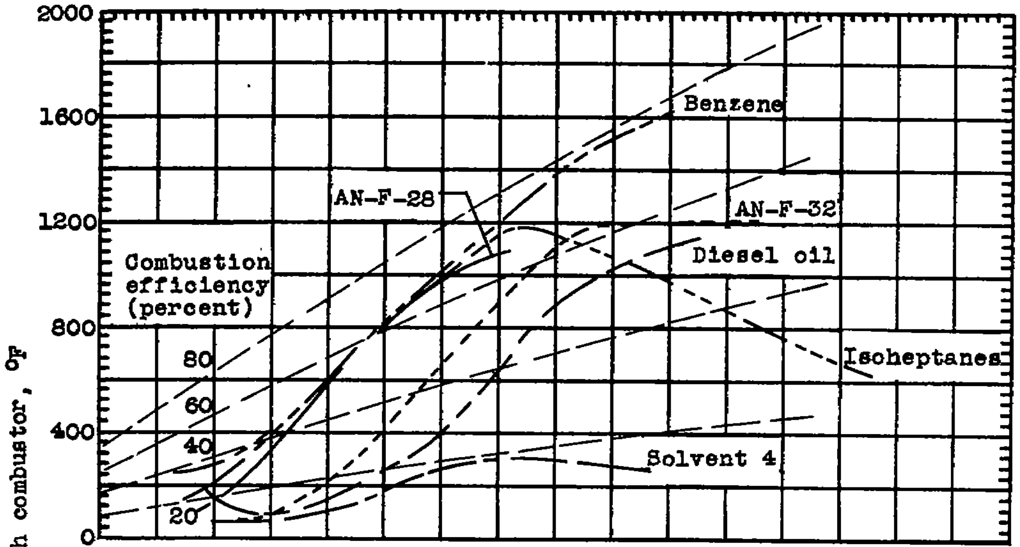

(c) Point A; inlet-air temperature, 90° F.

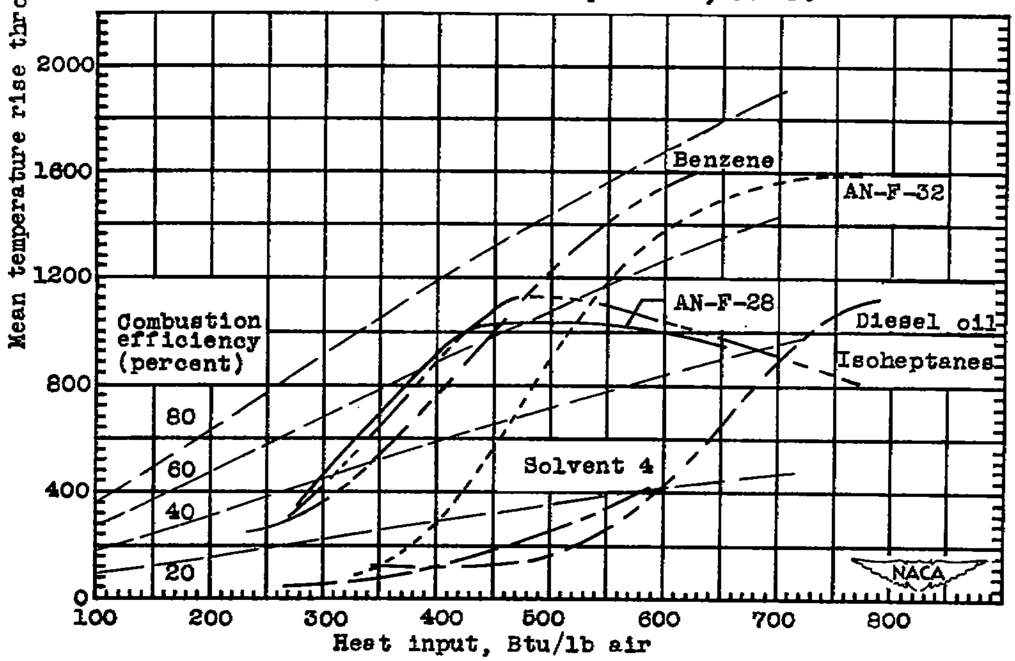

(d) Point B; inlet-air temperature, 70° F.

Figure 11. - Continued. Comparison of mean temperature rise through annular combustor for various heat-input values for six fuels and several inlet-air temperatures. Simulated engine operating conditions: Point A, inlet-air static pressure, 9.2 pounds per square inch absolute; inlet-air velocity, 200 feet per second; Point B, inlet-air static pressure, 7.7 pounds per square inch absolute; inlet-air velocity, 160 feet per second.

933

933

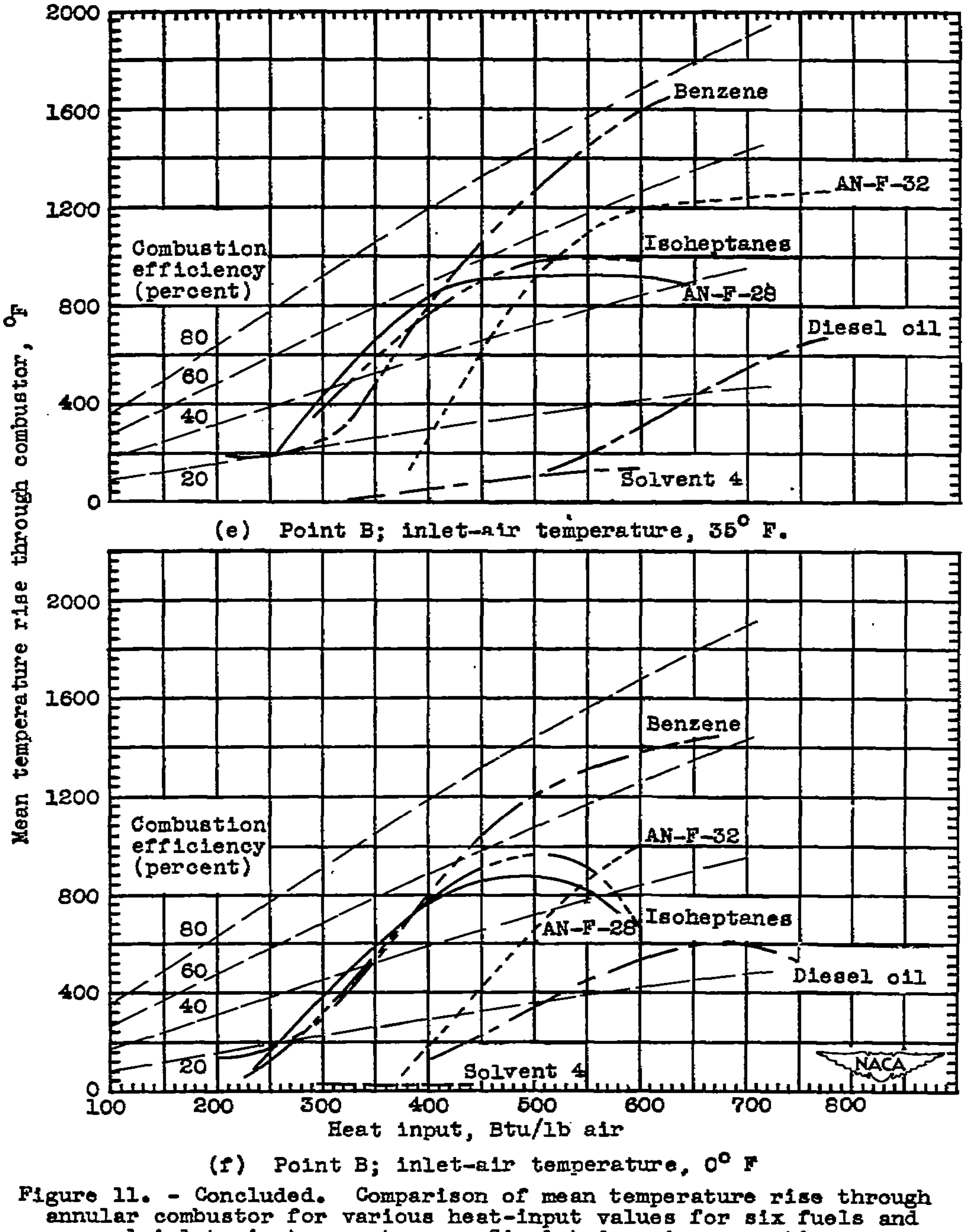

(f) Point B; inlet-air temperature, 0° F

Figure 11. - Concluded. Comparison of mean temperature rise through annular combustor for various heat-input values for six fuels and several inlet-air temperatures. Simulated engine operating conditions: Point A, inlet-air static pressure, 9.2 pounds per square inch absolute; inlet-air velocity, 200 feet per second; Point B, inlet-air static pressure, 7.7 pounds per square inch absolute; inlet-air velocity, 160 feet per second.

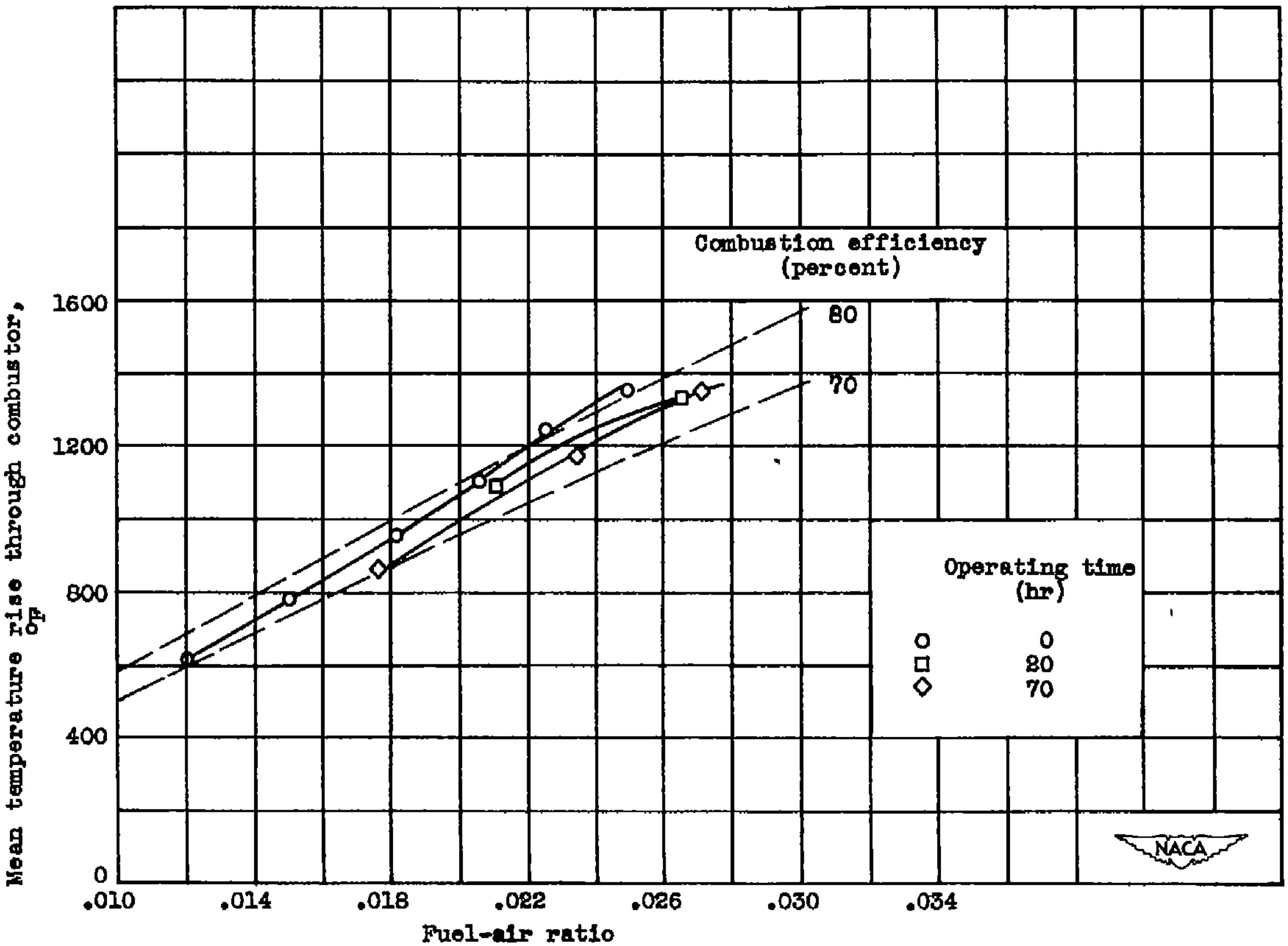

Figure 12. - Effect of hours of operation on mean temperature rise through annular combustor. Fuel, AN-F-28. Point A: inlet-air static pressure, 9.2 pounds per square inch absolute; inlet-air velocity, 200 feet per second.

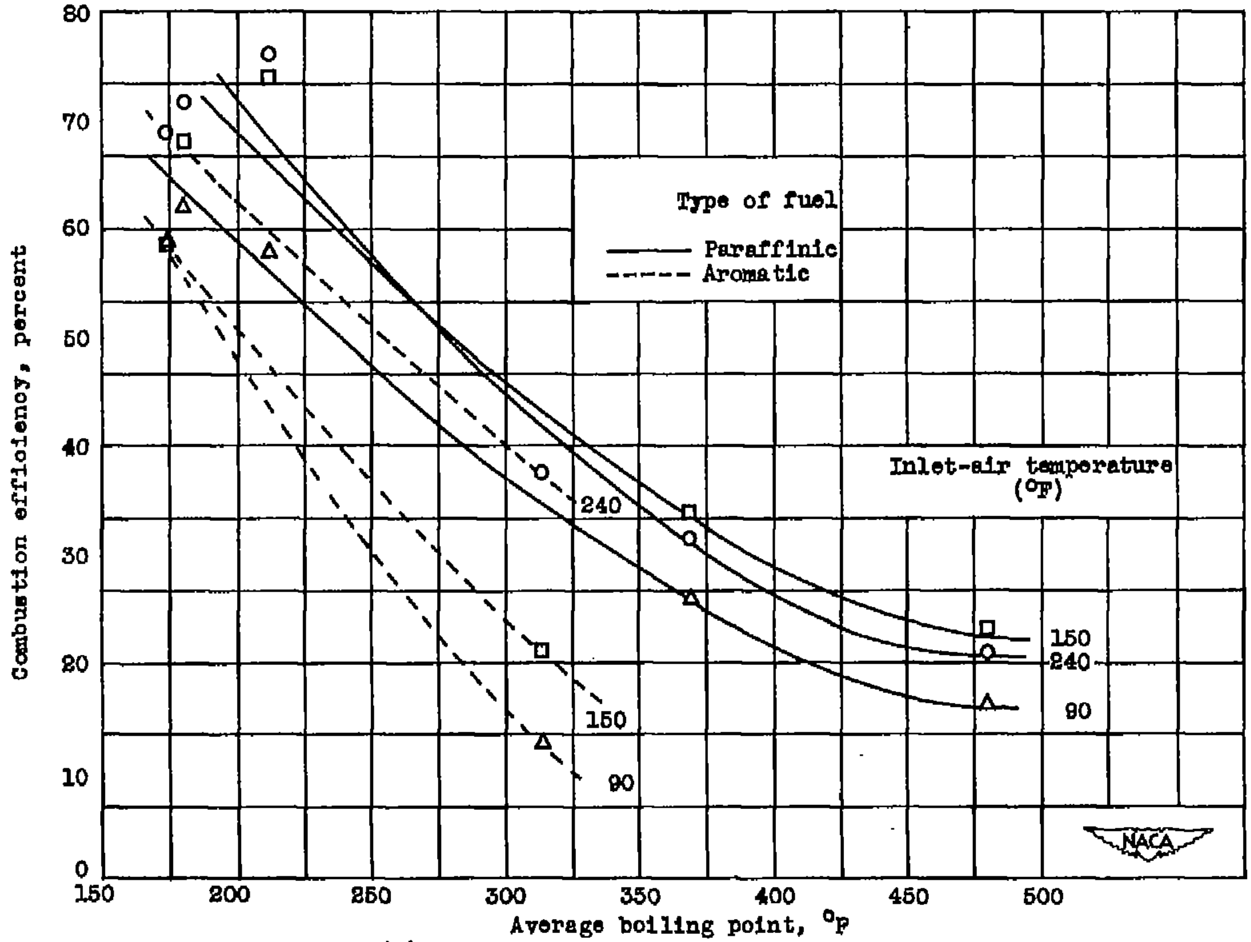

(a) Heat input, 330 Btu per pound of air.

Figure 13. - Variation of combustion efficiency with average boiling point of different fuels operating at two heat-input values at conditions simulating engine operation. Point A: inlet-air static pressure, 9.2 pounds per square inch absolute; inlet-air velocity, 200 feet per second.

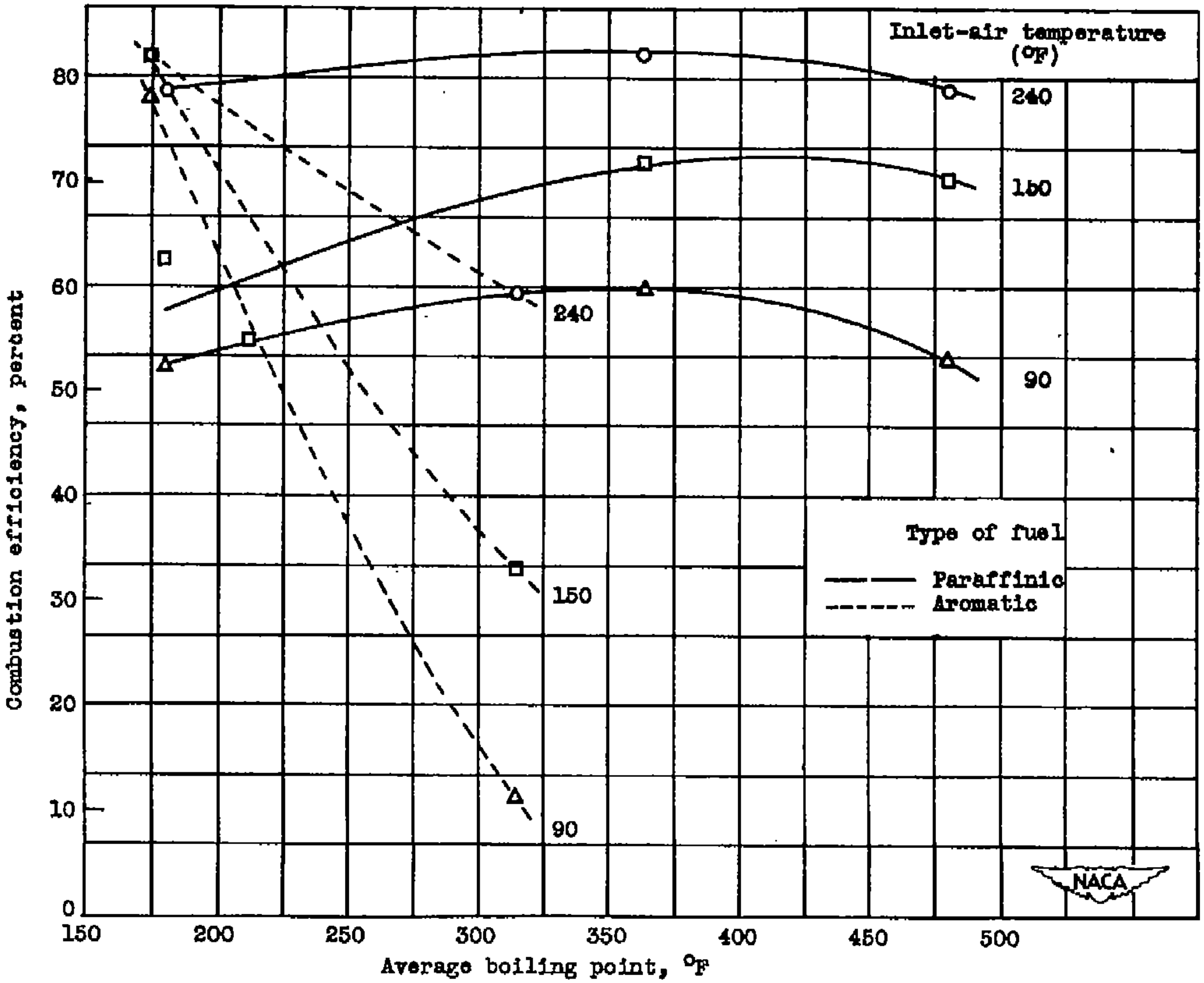

(b) Heat input, 580 Btu per pound of air.

Figure 13. - Concluded. Variation of combustion efficiency with average boiling point of different fuels operating at two heat-input values at conditions simulating engine operation. Point A: inlet-air static pressure, 9.2 pounds per square inch absolute; inlet-air velocity, 200 feet per second.

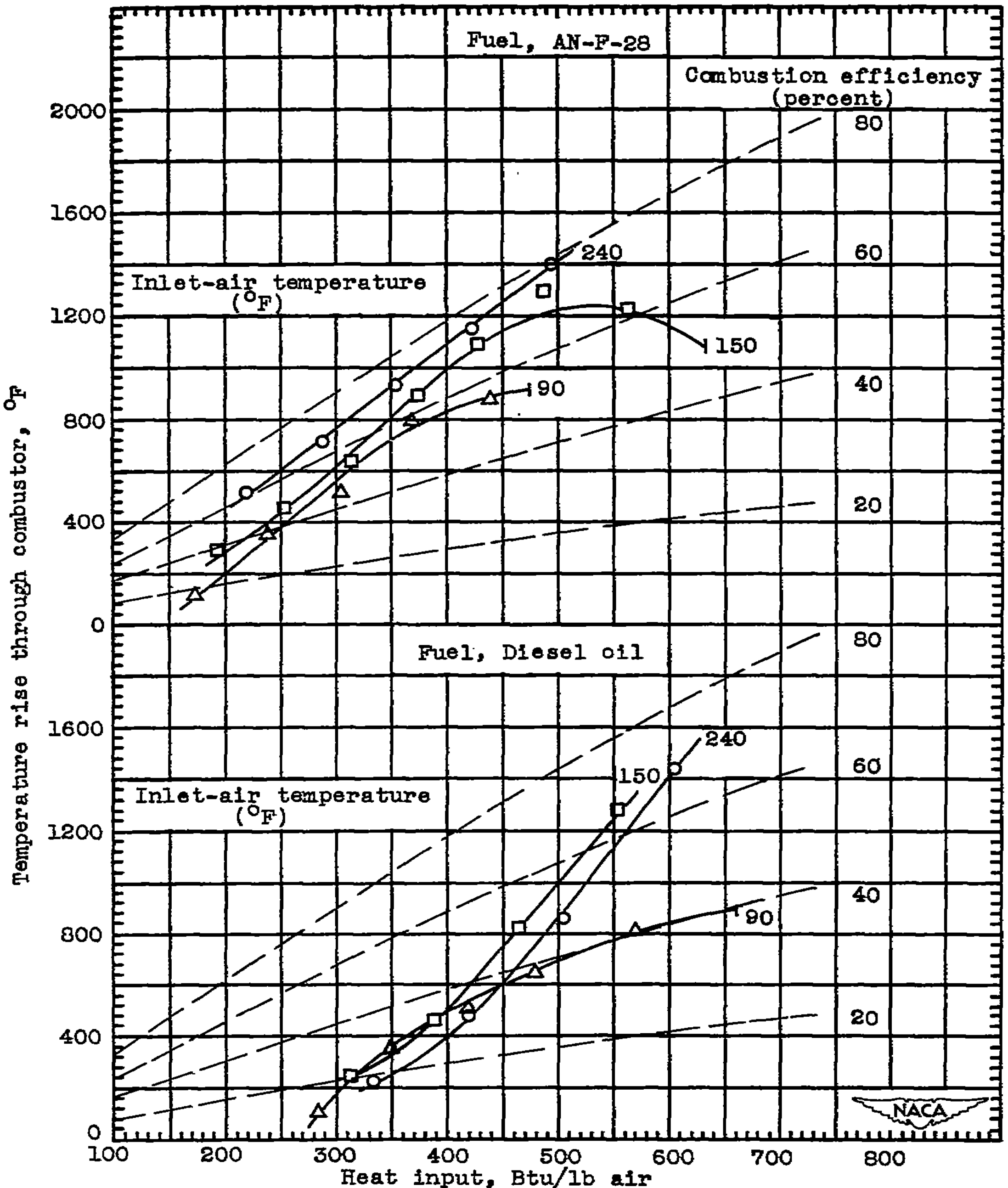

(a) Point A; 17.5-gallon-per-hour nozzles.

Figure 14. - Variation of mean temperature rise through annular combustor with heat input for several different-capacity fuel-injection nozzles operating with inlet-air temperature independently altered from values simulating engine operation. Simulated engine operating conditions: Point A, inlet-air static pressure, 9.2 pounds per square inch absolute; inlet-air velocity, 200 feet per second; Point B: inlet-air static pressure, 7.7 pounds per square inch absolute; inlet-air velocity, 160 feet per second.

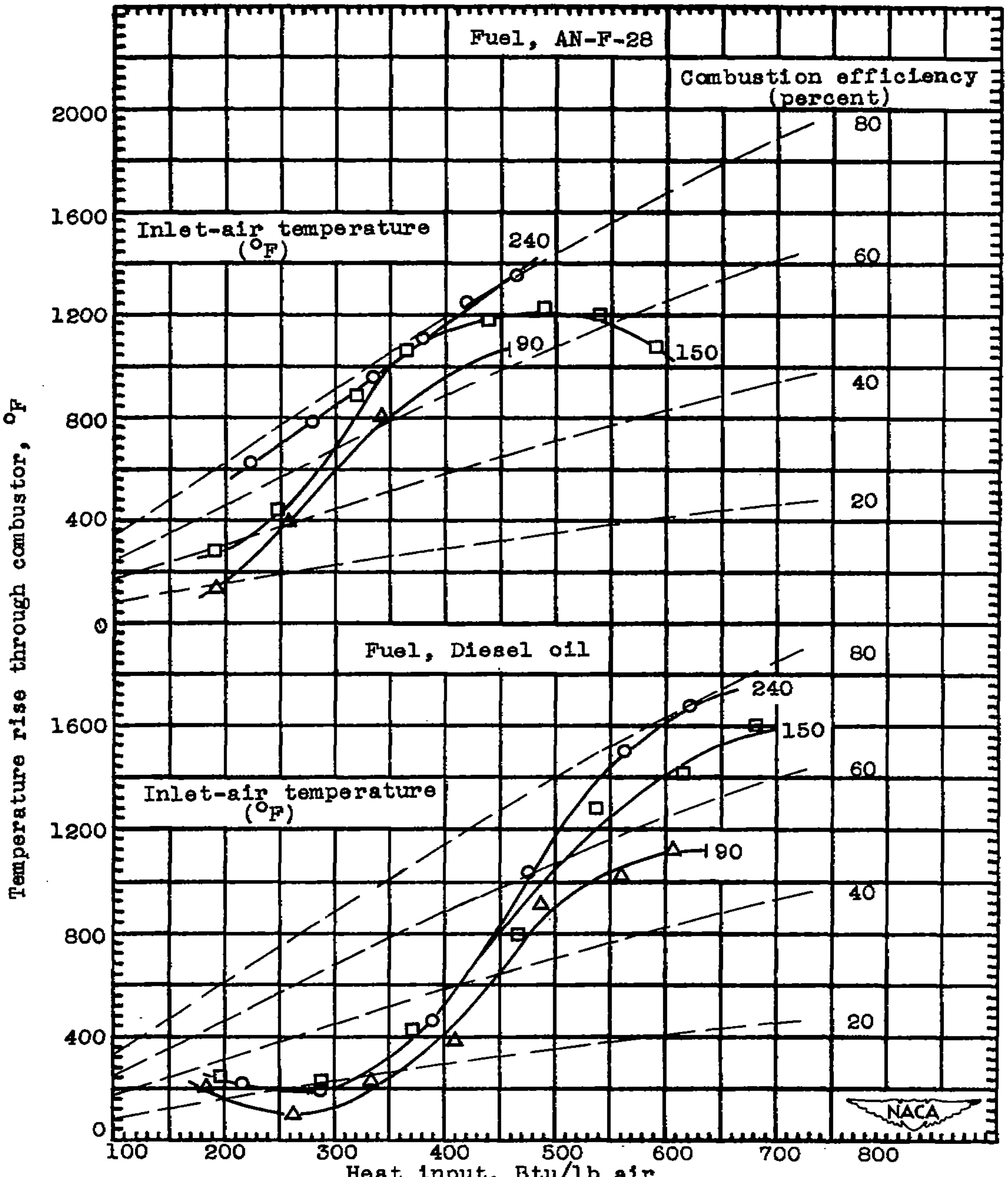

(b) Point A; 10.5-gallon-per-hour nozzles.

Figure 14. - Continued. Variation of mean temperature rise through annular combustor with heat input for several different-capacity fuel-injection nozzles operating with inlet-air temperature independently altered from values simulating engine operation. Simulated engine operating conditions: Point A, inlet-air static pressure, 9.2 pounds per square inch absolute; inlet-air velocity, 200 feet per second; Point B, inlet-air static pressure, 7.7 pounds per square inch absolute; inlet-air velocity, 160 feet per second.

953

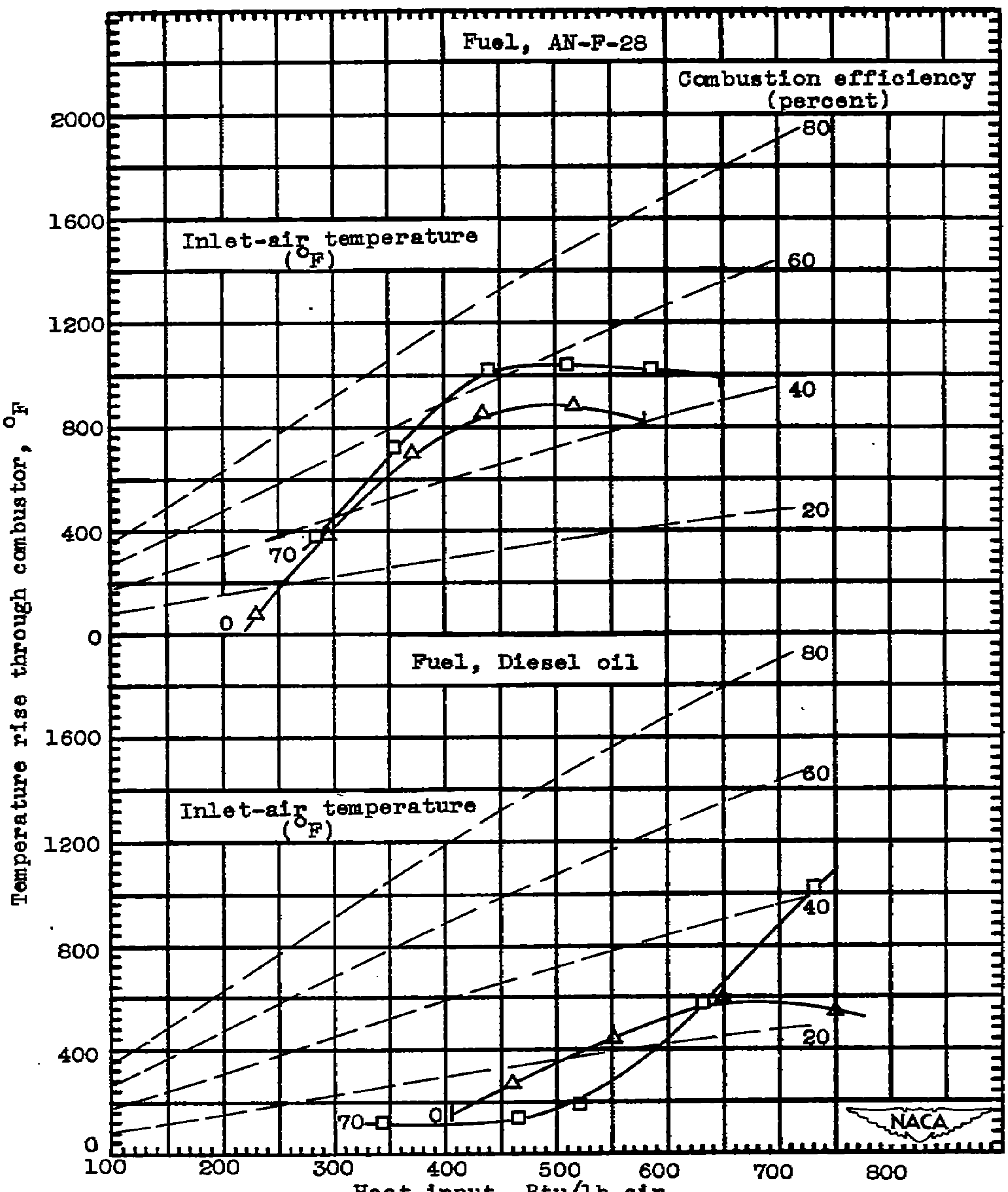

(c) Point B; 10.5-gallon-per-hour nozzles.

Figure 14. - Continued. Variation of mean temperature rise through annular combustor with heat input for several different-capacity fuel-injection nozzles operating with inlet-air temperature independently altered from values simulating engine operation. Simulated engine operating conditions: Point A, inlet-air static pressure, 9.2 pounds per square inch absolute; inlet-air velocity, 200 feet per second, Point B, inlet-air static pressure, 7.7 pounds per square inch absolute; inlet-air velocity, 160 feet per second.

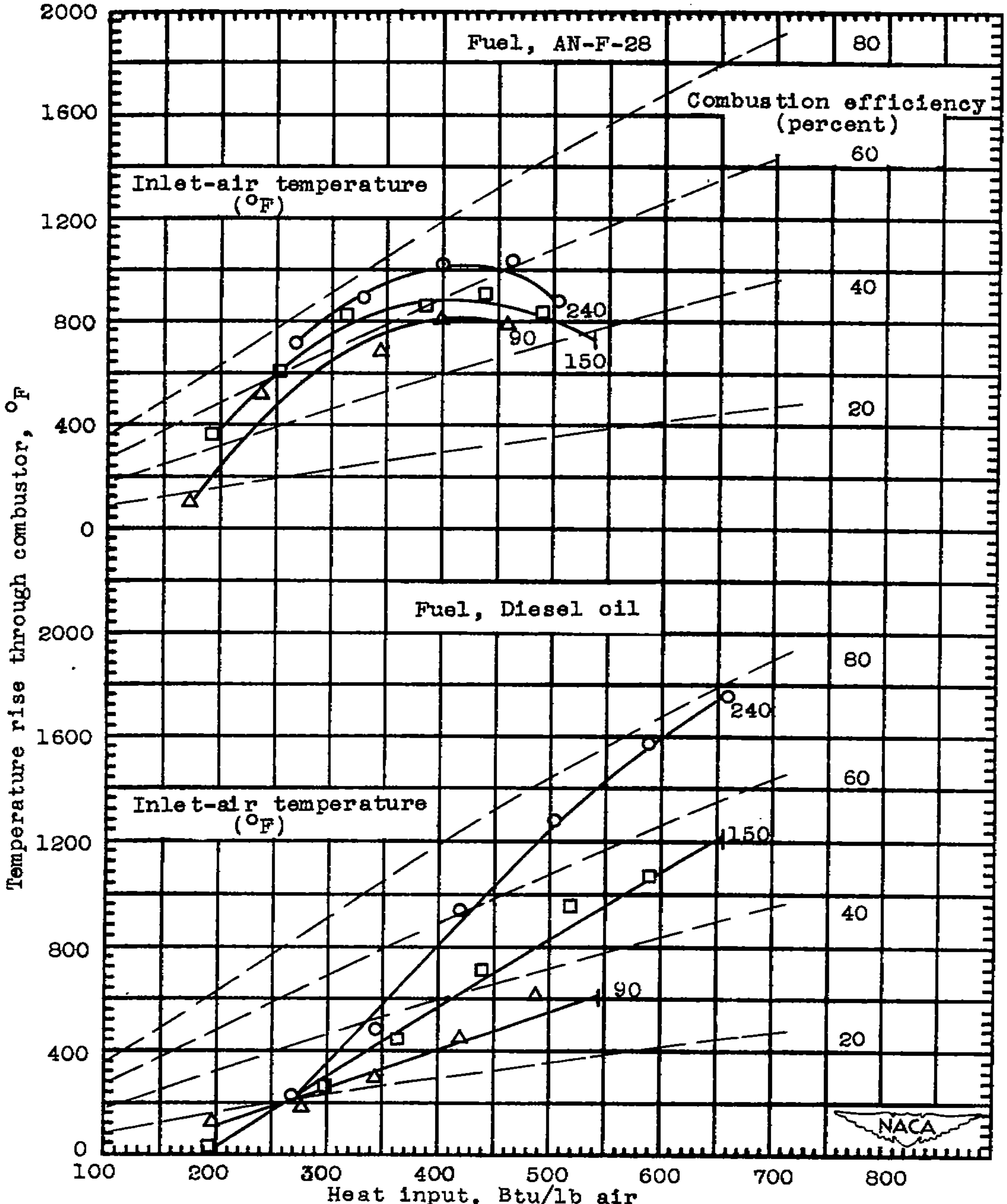

(d) Point A; 7.5-gallon-per-hour nozzles.

Figure 14. - Continued. Variation of mean temperature rise through annular combustor with heat input for several different-capacity fuel-injection nozzles operating with inlet-air temperature independently altered from values simulating engine operation. Simulated engine operating conditions: Point A, inlet-air static pressure, 9.2 pounds per square inch absolute; inlet-air velocity, 200 feet per second; Point B, inlet-air static pressure, 7.7 pounds per square inch absolute; inlet-air velocity, 160 feet per second.

933

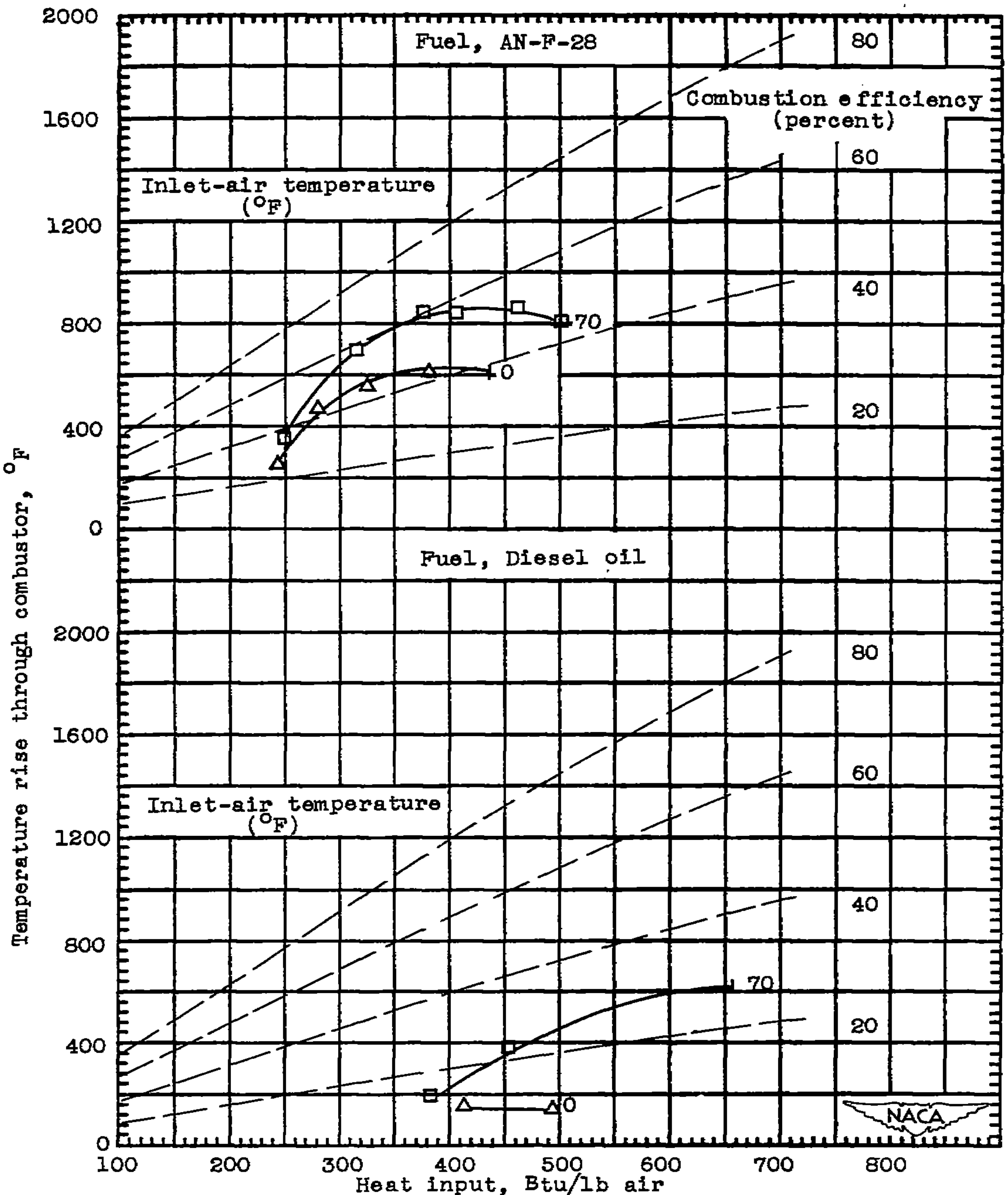

(e) Point B; 7.5-gallon-per-hour nozzles.

Figure 14. - Continued. Variation of mean temperature rise through annular combustor with heat input for several different-capacity fuel-injection nozzles operating with inlet-air temperature independently altered from values simulating engine operation. Simulated engine operating conditions: Point A, inlet-air static pressure, 9.2 pounds per square inch absolute; inlet-air velocity, 200 feet per second; Point B, inlet-air static pressure, 7.7 pounds per square inch absolute; inlet-air velocity, 160 feet per second.

933

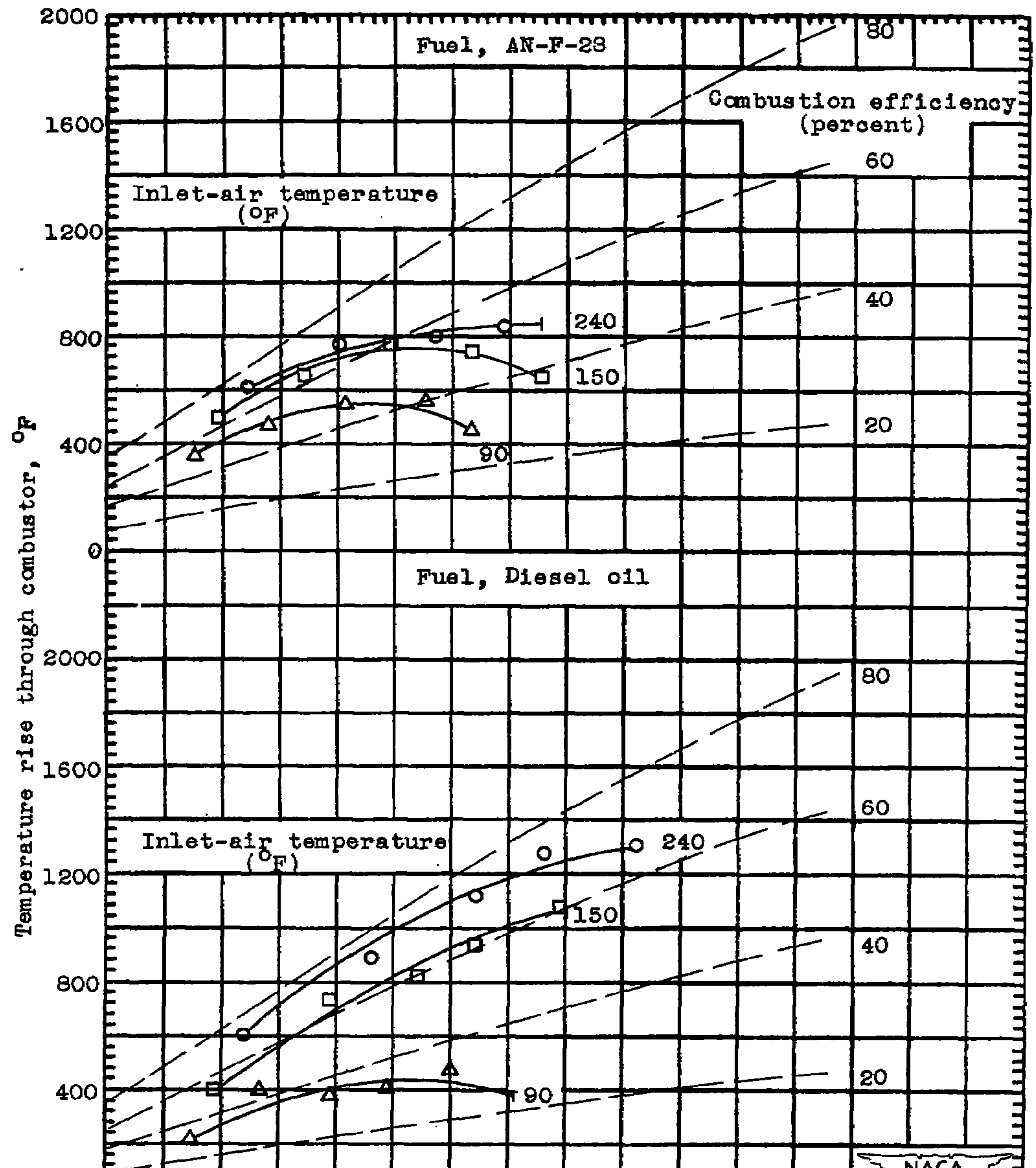

(f) Point A; 3.0-gallon-per-hour nozzles.

Figure 14. - Continued. Variation of mean temperature rise through annular combustor with heat input for several different-capacity fuel-injection nozzles operating with inlet-air temperature independently altered from values simulating engine operation. Simulated engine operating conditions: Point A, inlet-air static pressure, 9.2 pounds per square inch absolute; inlet-air velocity, 200 feet per second; Point B, inlet-air static pressure, 7.7 pounds per square inch absolute; inlet-air velocity, 160 feet per second.

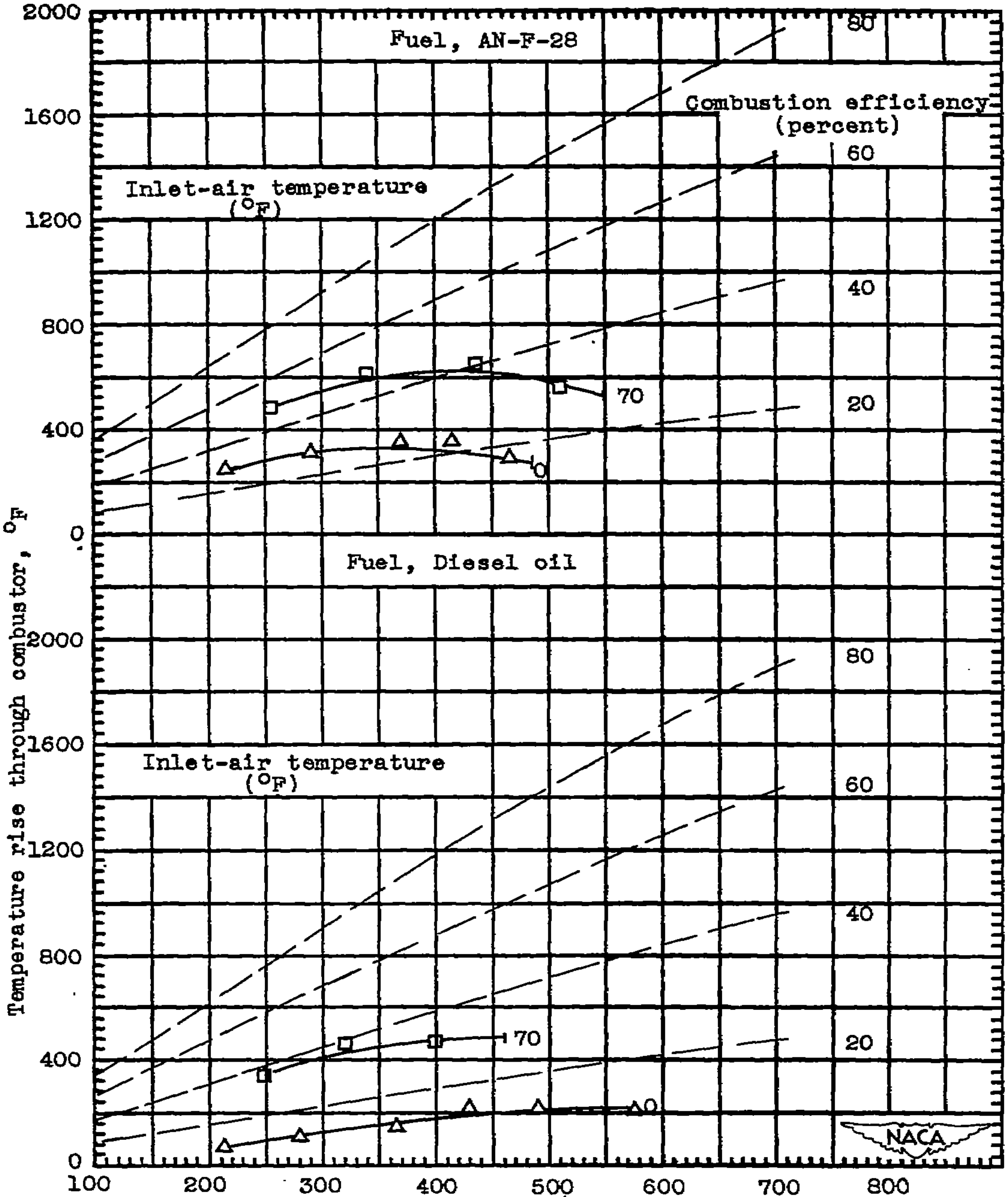

(g) Point B; 3.0-gallon-per-hour nozzles.

Figure 14. - Continued. Variation of mean temperature rise through annular combustor with heat input for several different-capacity fuel-injection nozzles operating with inlet-air temperature independently altered from values simulating engine operation. Simulated engine operating conditions: Point A, inlet-air static pressure, 9.2 pounds per square inch absolute; inlet-air velocity, 200 feet per second; Point B, inlet-air static pressure, 7.7 pounds per square inch absolute; inlet-air velocity, 160 feet per second.

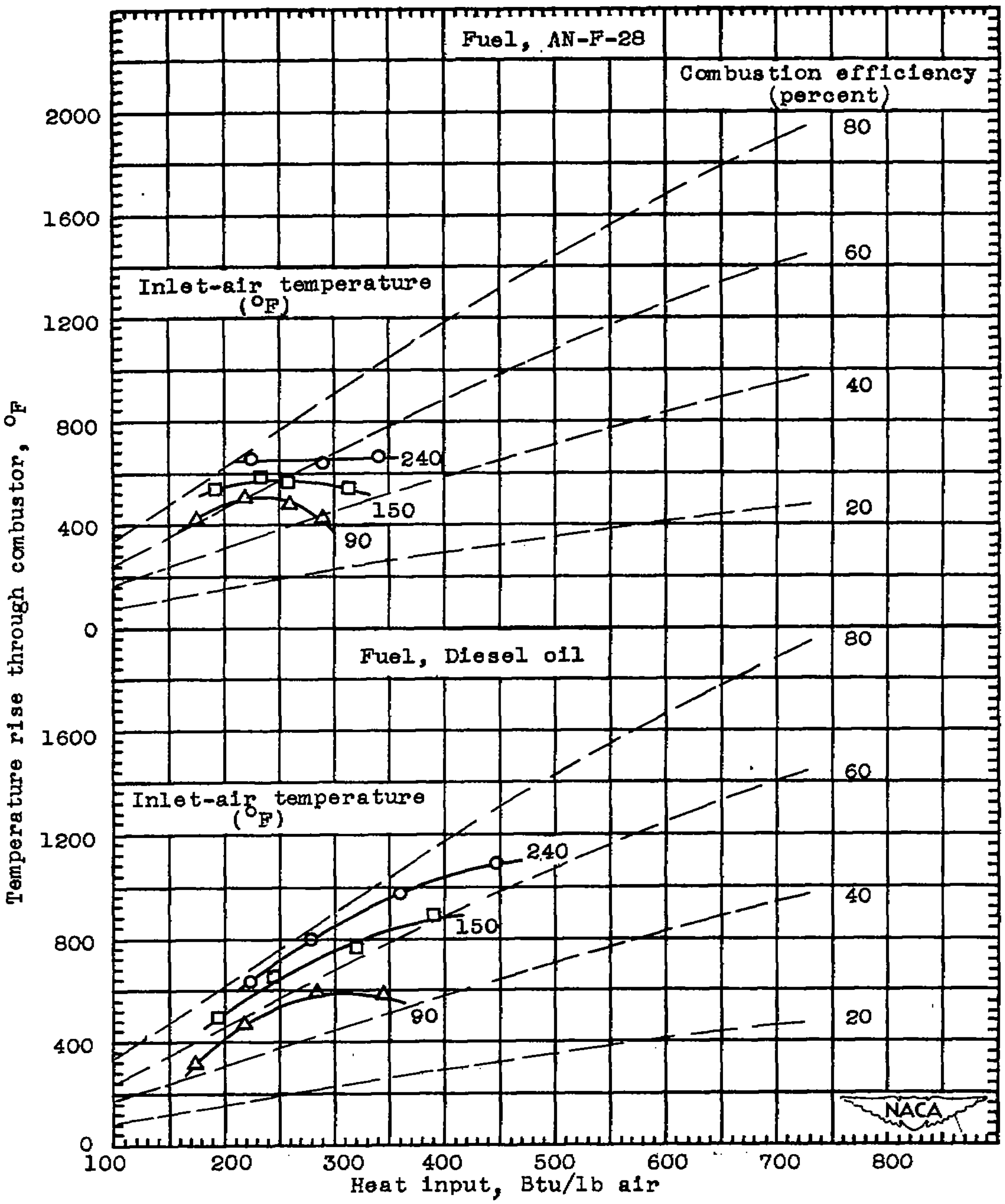

(h) Point A; 2.0-gallon-per-hour nozzles.

Figure 14. - Concluded. Variation of mean temperature rise through annular combustor with heat input for several different-capacity fuel-injection nozzles operating with inlet-air temperature independently altered from values simulating engine operation. Simulated engine operating conditions: Point A, inlet-air static pressure, 9.2 pounds per square inch absolute; inlet-air velocity, 200 feet per second; Point B, inlet-air static pressure, 7.7 pounds per square inch absolute; inlet-air velocity, 160 feet per second.

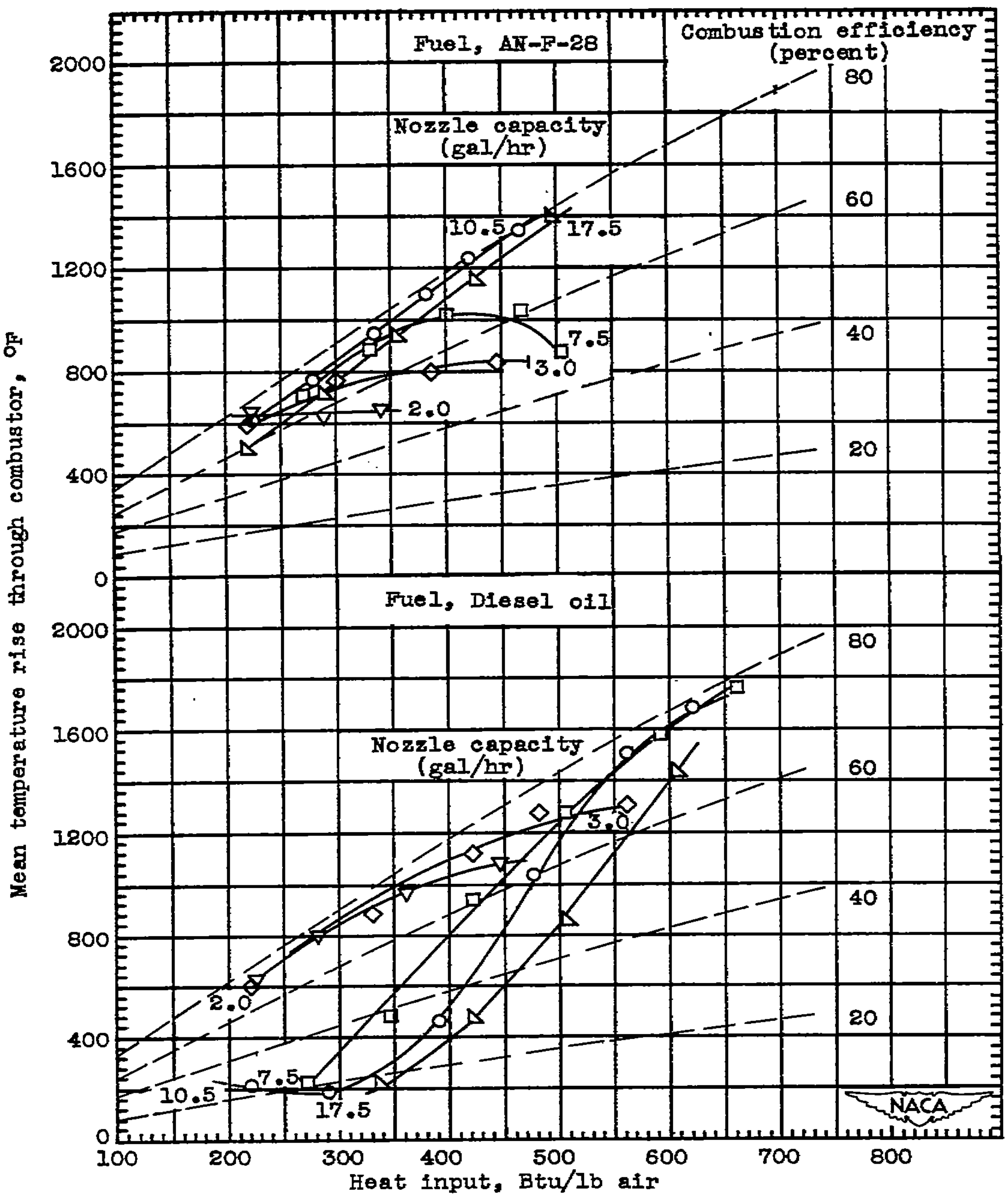

(a) Point A; inlet-air temperature, 240° F.

Figure 15. - Comparison of mean temperature rise through annular combustor for various heat-input values for several different-capacity fuel-injection nozzles. Simulated engine operating conditions: Point A, inlet-air static pressure, 9.2 pounds per square inch absolute; inlet-air velocity, 200 feet per second; Point B, inlet-air static pressure, 7.7 pounds per square inch absolute; inlet-air velocity, 160 feet per second. Fuels, AN-F-28 and Diesel oil.

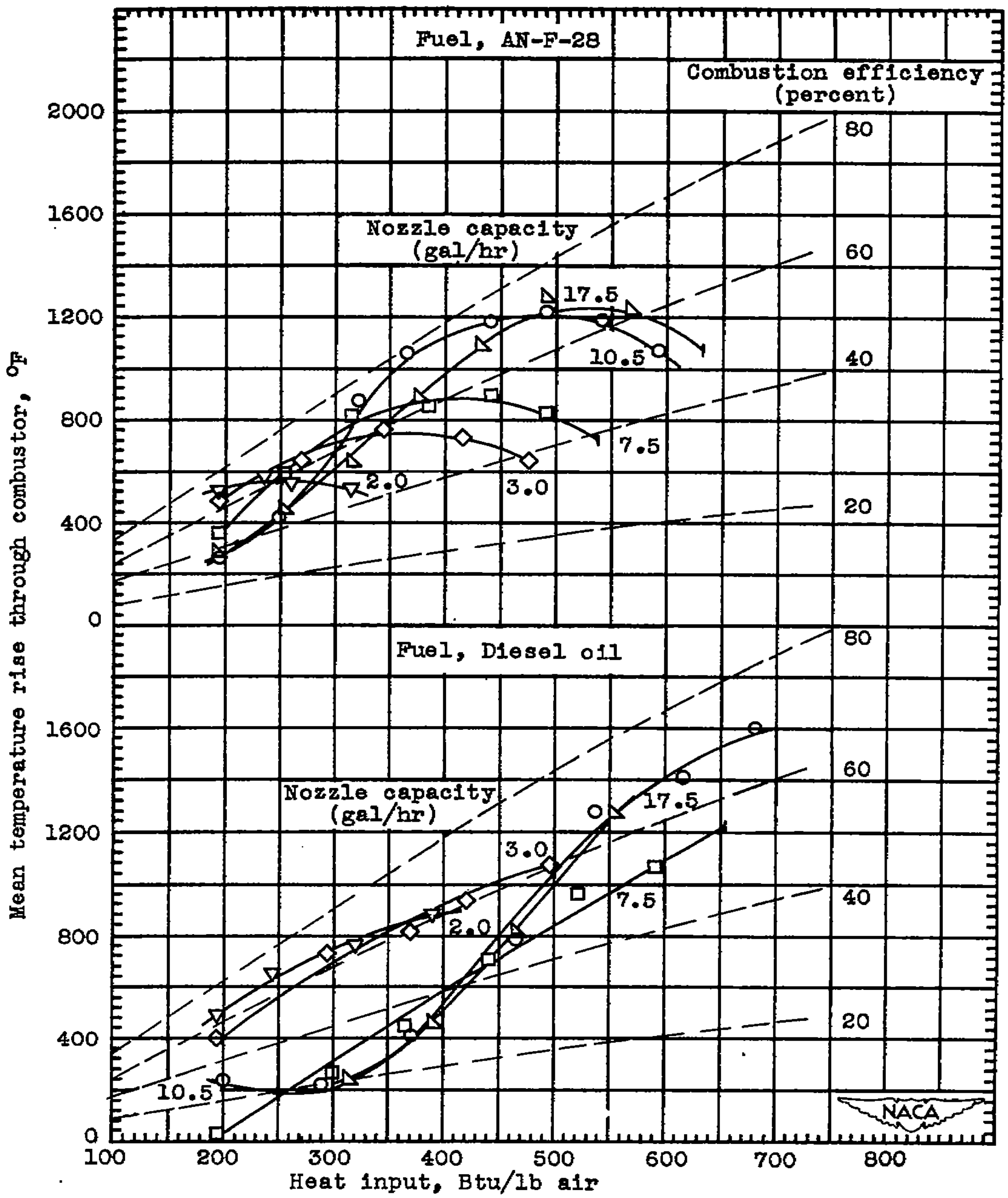

(b) Point A; inlet-air temperature, 150° F.

Figure 15. - Continued. Comparison of mean temperature rise through annular combustor for various heat-input values for several different-capacity fuel-injection nozzles. Simulated engine operating conditions: Point A, inlet-air static pressure, 9.2 pounds per square inch absolute; inlet-air velocity, 200 feet per second; Point B, inlet-air static pressure, 7.7 pounds per square inch absolute; inlet-air velocity, 160 feet per second. Fuels, AN-F-28 and Diesel oil.

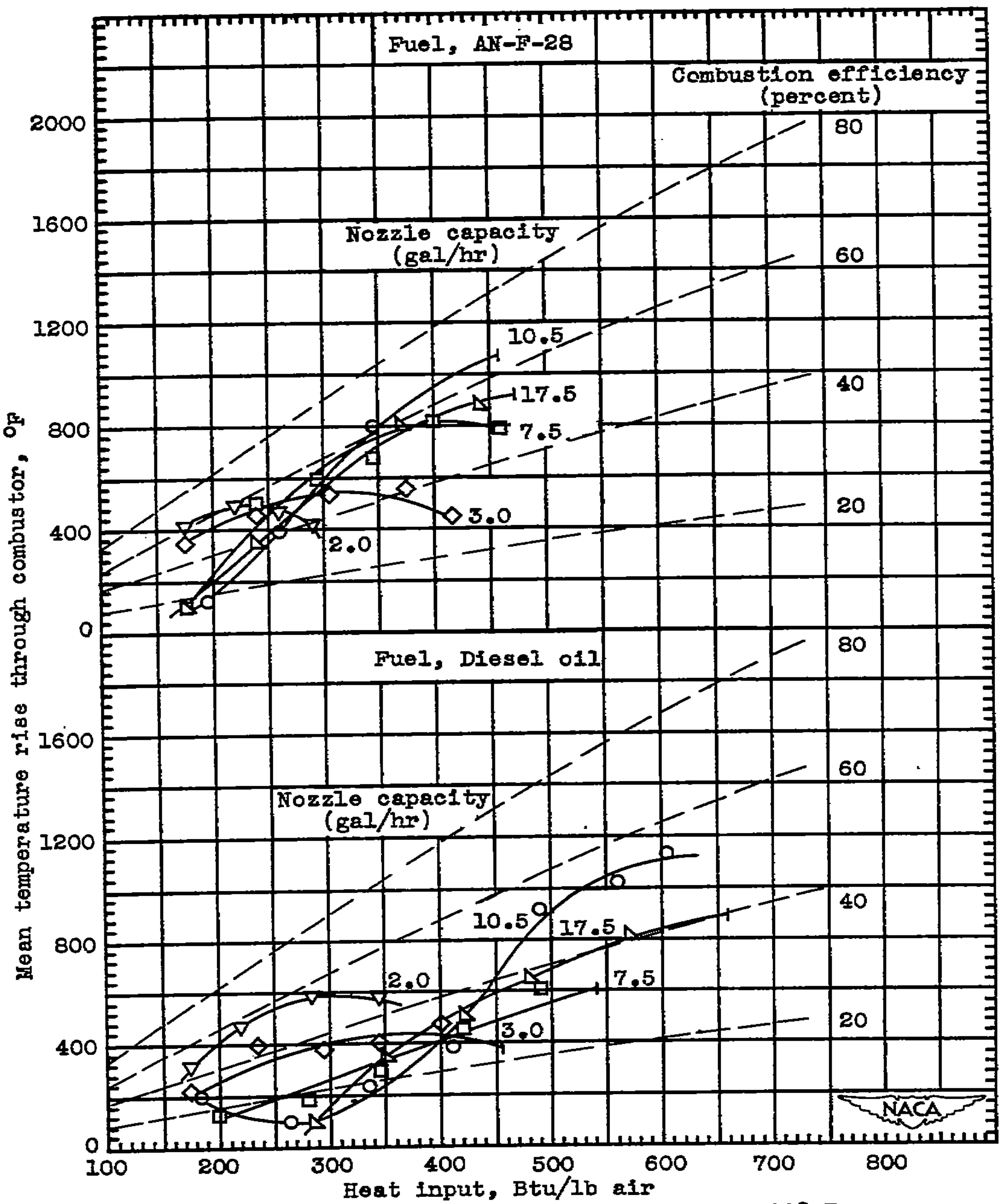

(c) Point A; inlet-air temperature, 90° F.

Figure 15. - Continued. Comparison of mean temperature rise through annular combustor for various heat-input values for several different-capacity fuel-injection nozzles. Simulated engine operating conditions: Point A, inlet-air static pressure, 9.2 pounds per square inch absolute; inlet-air velocity, 200 feet per second; Point B, inlet-air static pressure, 7.7 pounds per square inch absolute; inlet-air velocity, 160 feet per second. Fuels, AN-F-28 and Diesel oil.

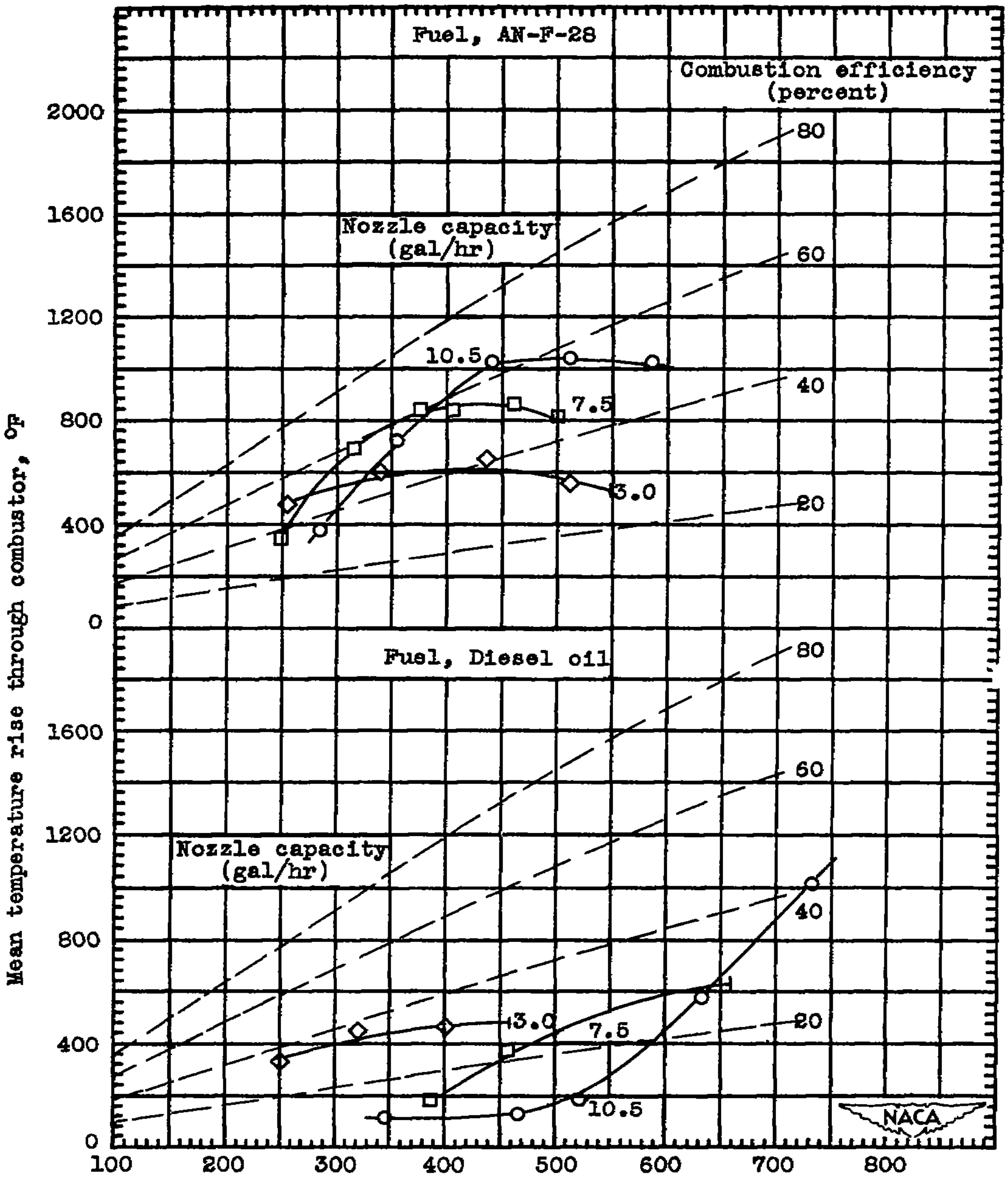

(d) Point B; inlet-air temperature, 70° F.

Figure 15. - Continued. Comparison of mean temperature rise through annular combustor for various heat-input values for several different-capacity fuel-injection nozzles. Simulated engine operating conditions: Point A, inlet-air static pressure, 9.2 pounds per square inch absolute; inlet-air velocity, 200 feet per second; Point B, inlet-air static pressure, 7.7 pounds per square inch absolute; inlet-air velocity, 160 feet per second. Fuels, AN-F-28 and Diesel oil.

933

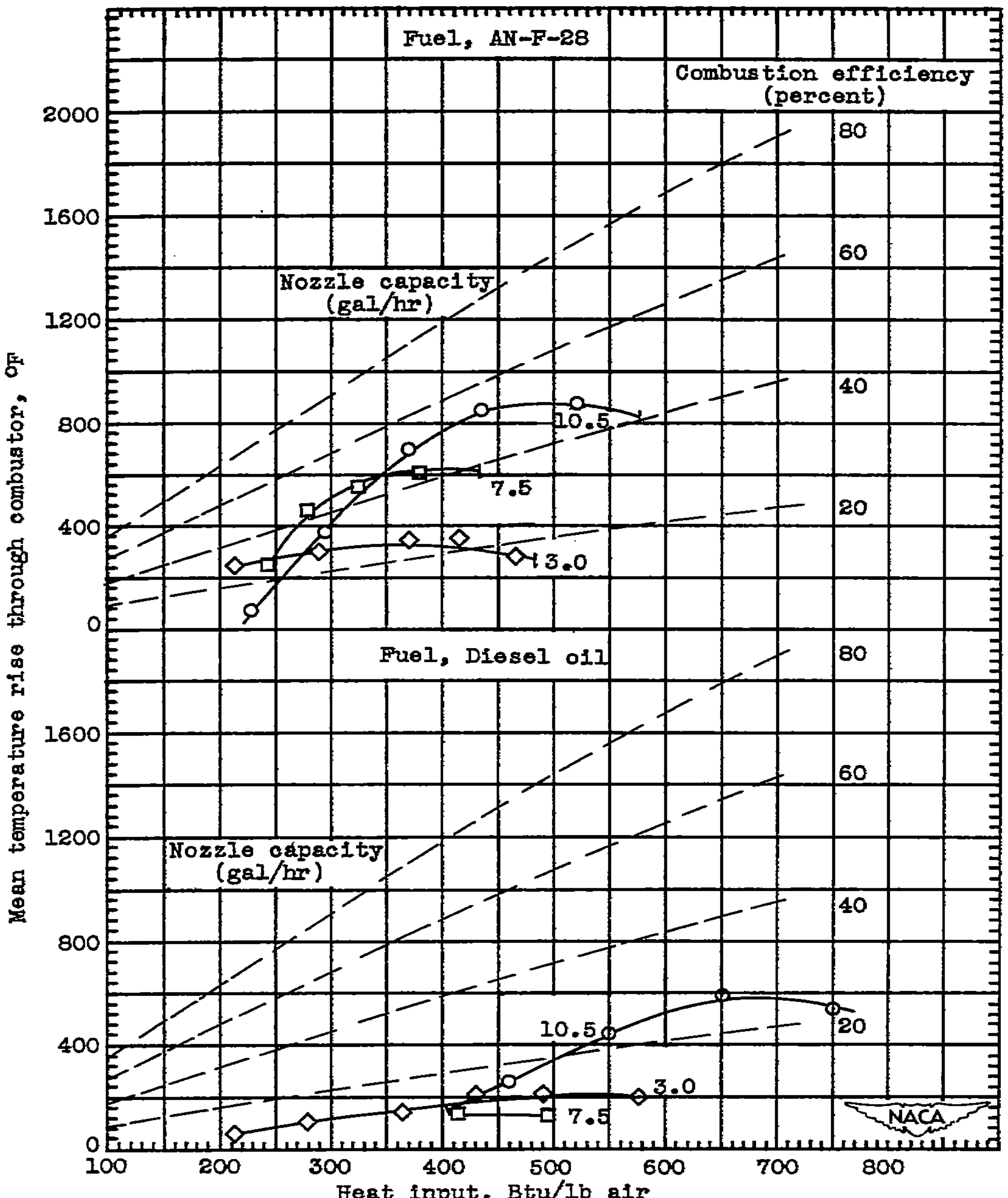

(e) Point B; inlet-air temperature, 0° F.

Figure 15. - Concluded. Comparison of mean temperature rise through annular combustor for various heat-input values for several different-capacity fuel-injection nozzles. Simulated engine operating conditions: Point A, inlet-air static pressure, 9.2 pounds per square inch absolute; inlet-air velocity, 200 feet per second; Point B, inlet-air static pressure, 7.7 pounds per square inch absolute; inlet-air velocity, 160 feet per second. Fuels, AN-F-28 and Diesel oil.

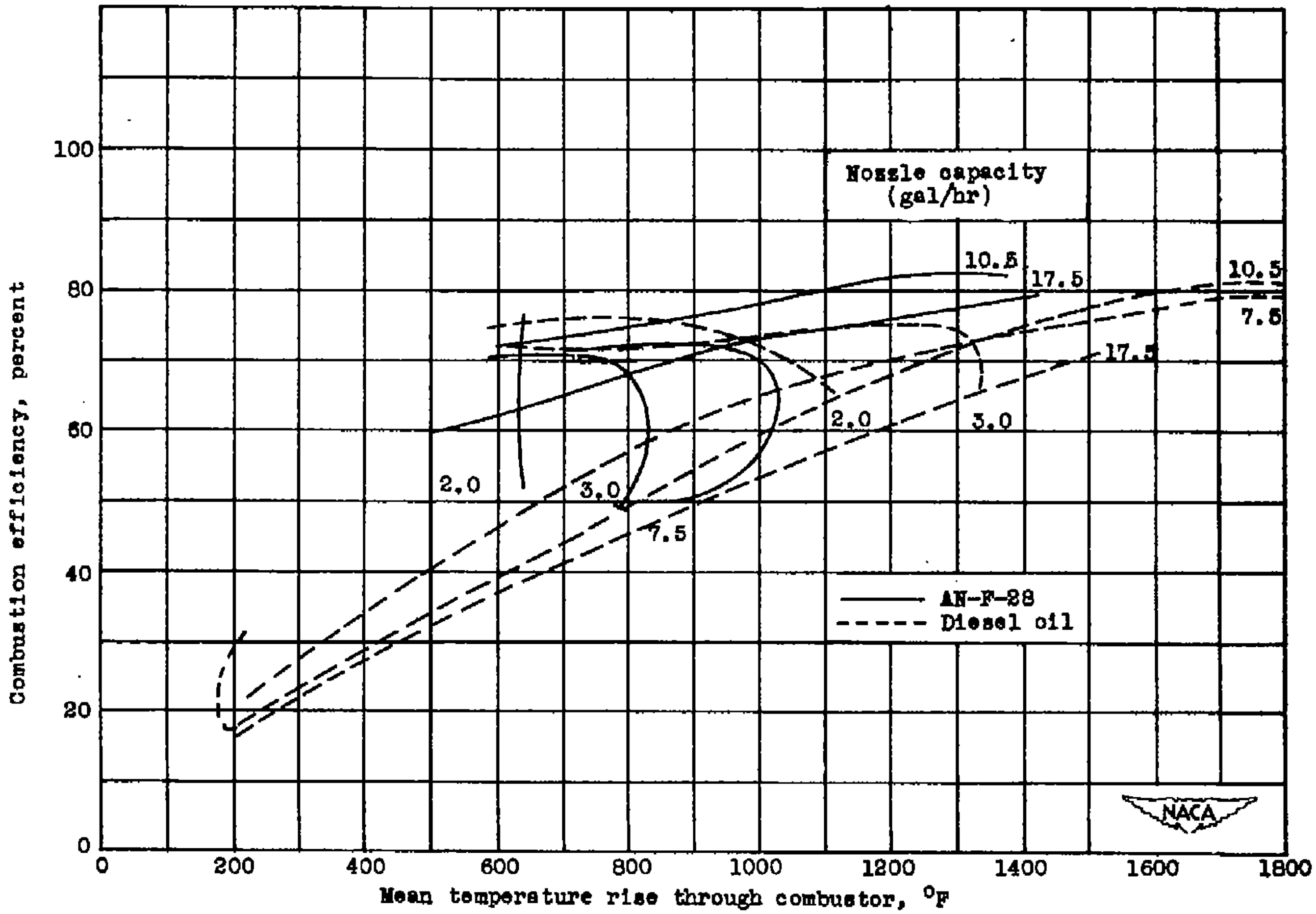

(a) Point A; inlet-air temperature, 240° F.

Figure 16. - Comparison of combustion efficiencies obtainable for various values of mean temperature rise through annular combustor for several different-capacity fuel-injection nozzles. Simulated engine operating conditions: Point A, inlet-air static pressure, 9.2 pounds per square inch absolute; inlet-air velocity, 200 feet per second; Point B, inlet-air static pressure, 7.7 pounds per square inch; inlet-air velocity, 160 feet per second. Fuels, AN-F-28 and Diesel oil.

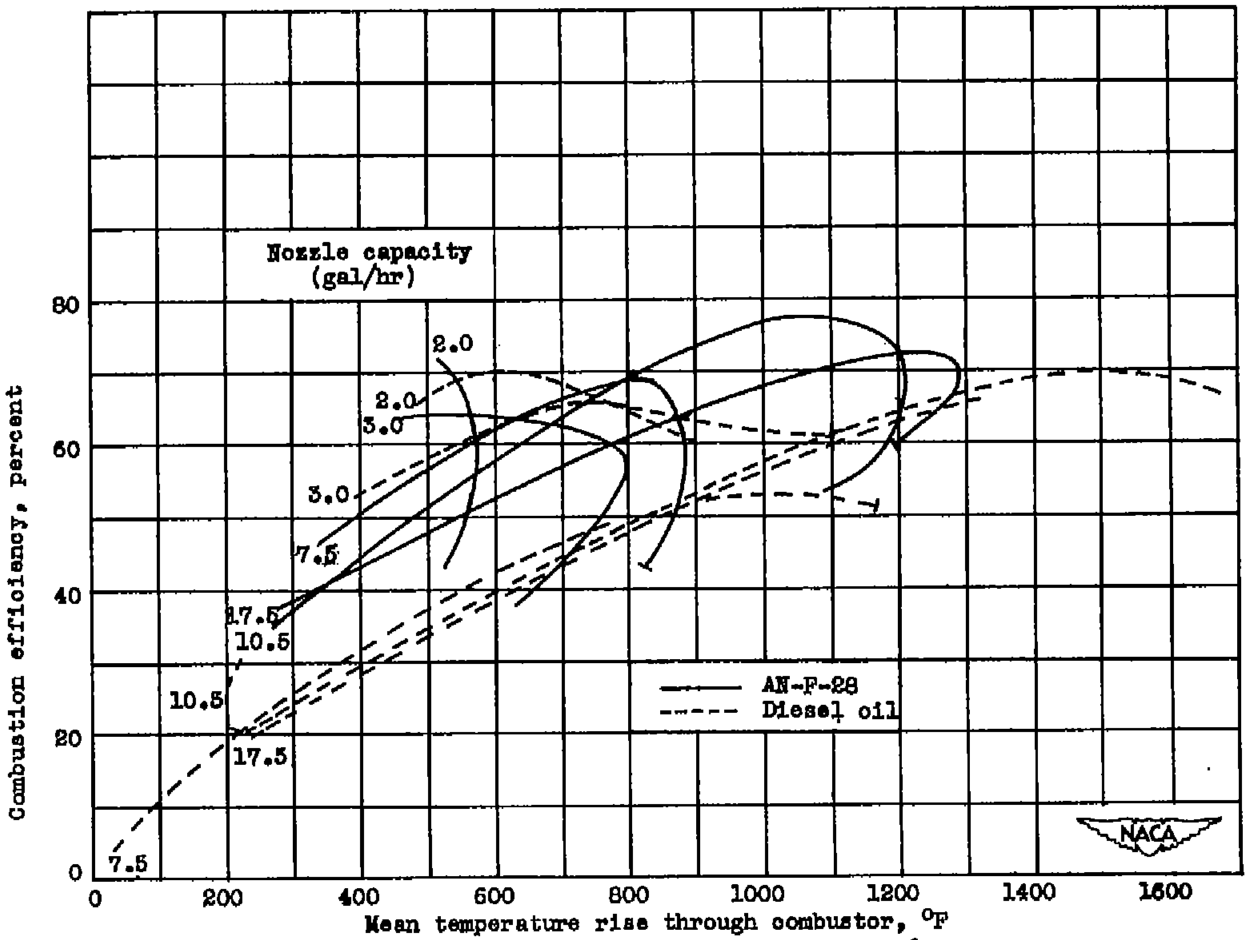

(b) Point A; inlet-air temperature, 150° F.

Figure 16. - Continued. Comparison of combustion efficiencies obtainable for various values of mean temperature rise through annular combustor for several different-capacity fuel-injection nozzles. Simulated engine operating conditions: Point A, inlet-air static pressure, 9.2 pounds per square inch absolute; inlet-air velocity, 200 feet per second; Point B, inlet-air static pressure, 7.7 pounds per square inch; inlet-air velocity, 160 feet per second. Fuels, AN-F-28 and Diesel oil.

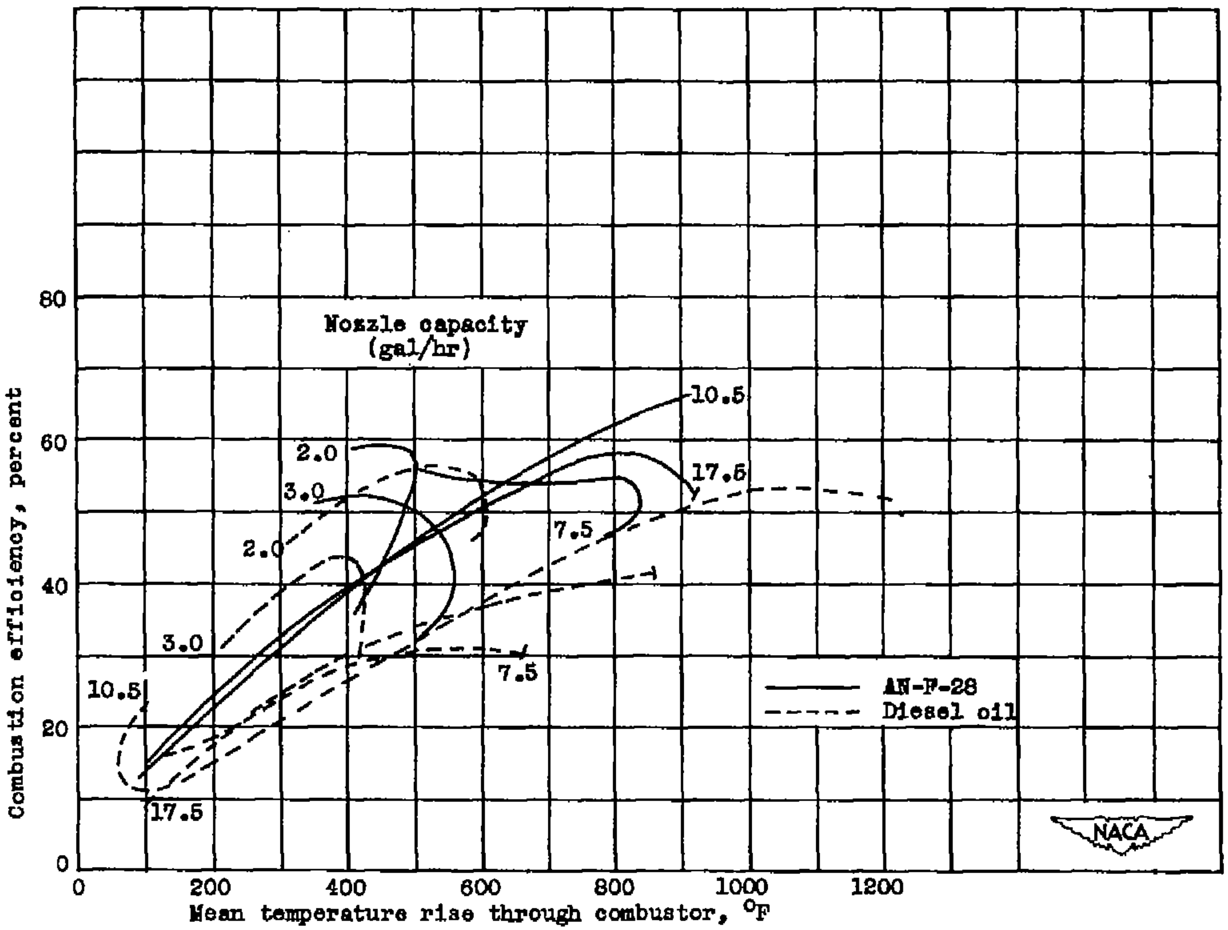

(c) Point A; inlet-air temperature, 90° F.

Figure 16. - Continued. Comparison of combustion efficiencies obtainable for various values of mean temperature rise through annular combustor for several different-capacity fuel-injection nozzles. Simulated engine operating conditions: Point A, inlet-air static pressure, 9.2 pounds per square inch absolute; inlet-air velocity, 200 feet per second; Point B, inlet-air static pressure, 7.7 pounds per square inch; inlet-air velocity, 160 feet per second. Fuels, AN-F-28 and Diesel oil.

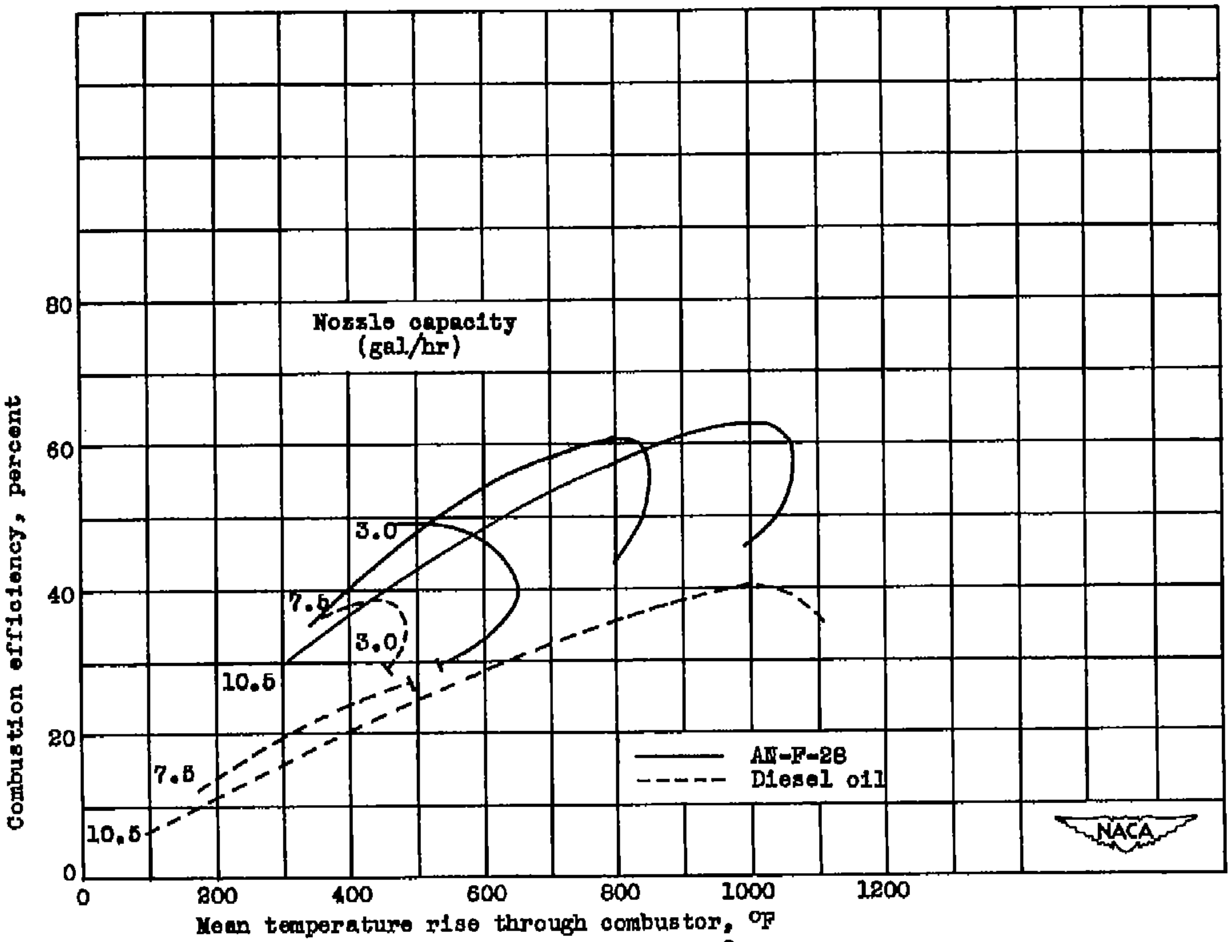

(d) Point B; inlet-air temperature, 70° F.

Figure 16. - Continued. Comparison of combustion efficiencies obtainable for various values of mean temperature rise through annular combustor for several different-capacity fuel-injection nozzles. Simulated engine operating conditions: Point A, inlet-air static pressure, 9.2 pounds per square inch absolute; inlet-air velocity, 200 feet per second; Point B, inlet-air static pressure, 7.7 pounds per square inch; inlet-air velocity, 160 feet per second. Fuels, AN-F-28 and Diesel oil.

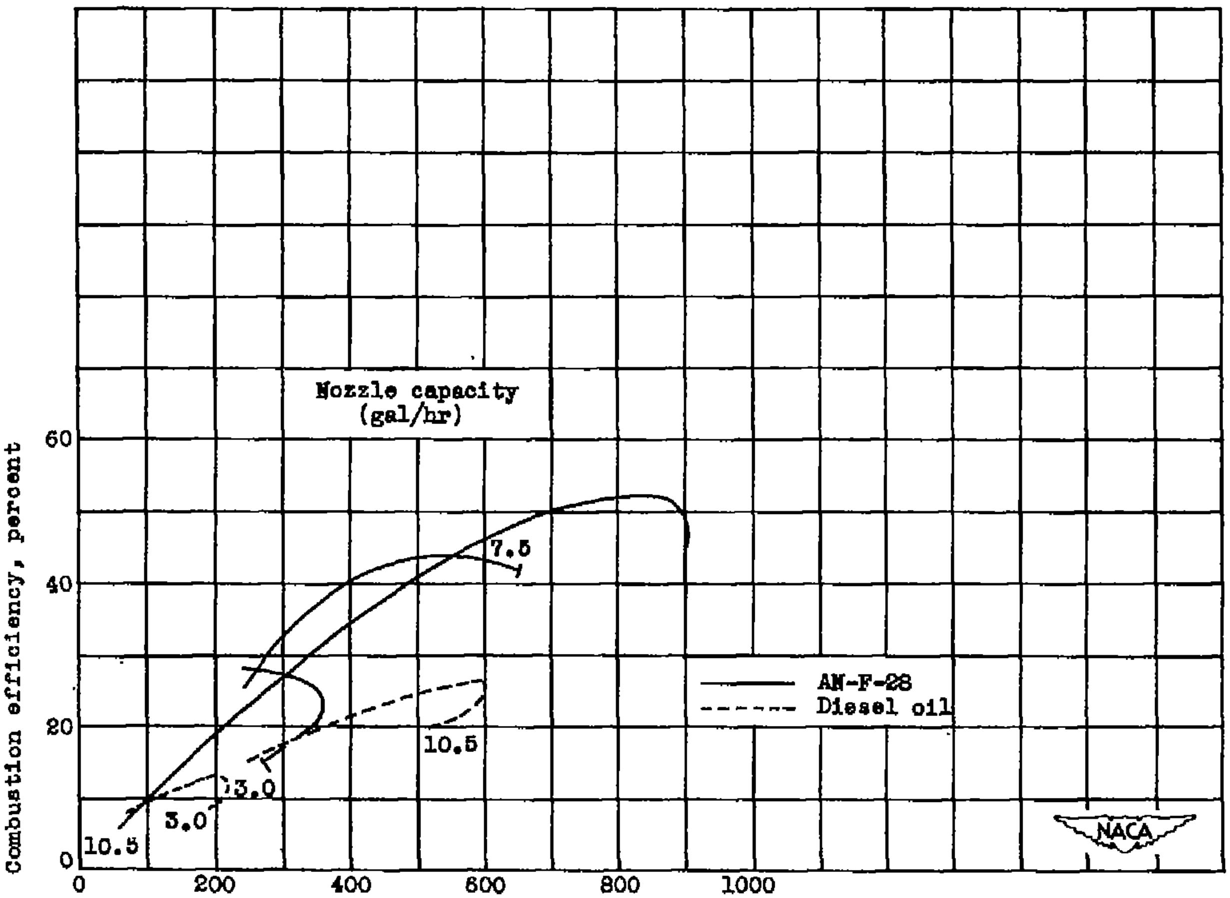

(e) Point B; inlet-air temperature, 0° F.

Figure 16. - Concluded. Comparison of combustion efficiencies obtainable for various values of mean temperature rise through annular combustor for several different-capacity fuel-injection nozzles. Simulated engine operating conditions: Point A, inlet-air static pressure, 9.2 pounds per square inch absolute; inlet-air velocity, 200 feet per second; Point B, inlet-air static pressure, 7.7 pounds per square inch; inlet-air velocity, 160 feet per second. Fuels, AN-F-28 and Diesel oil.

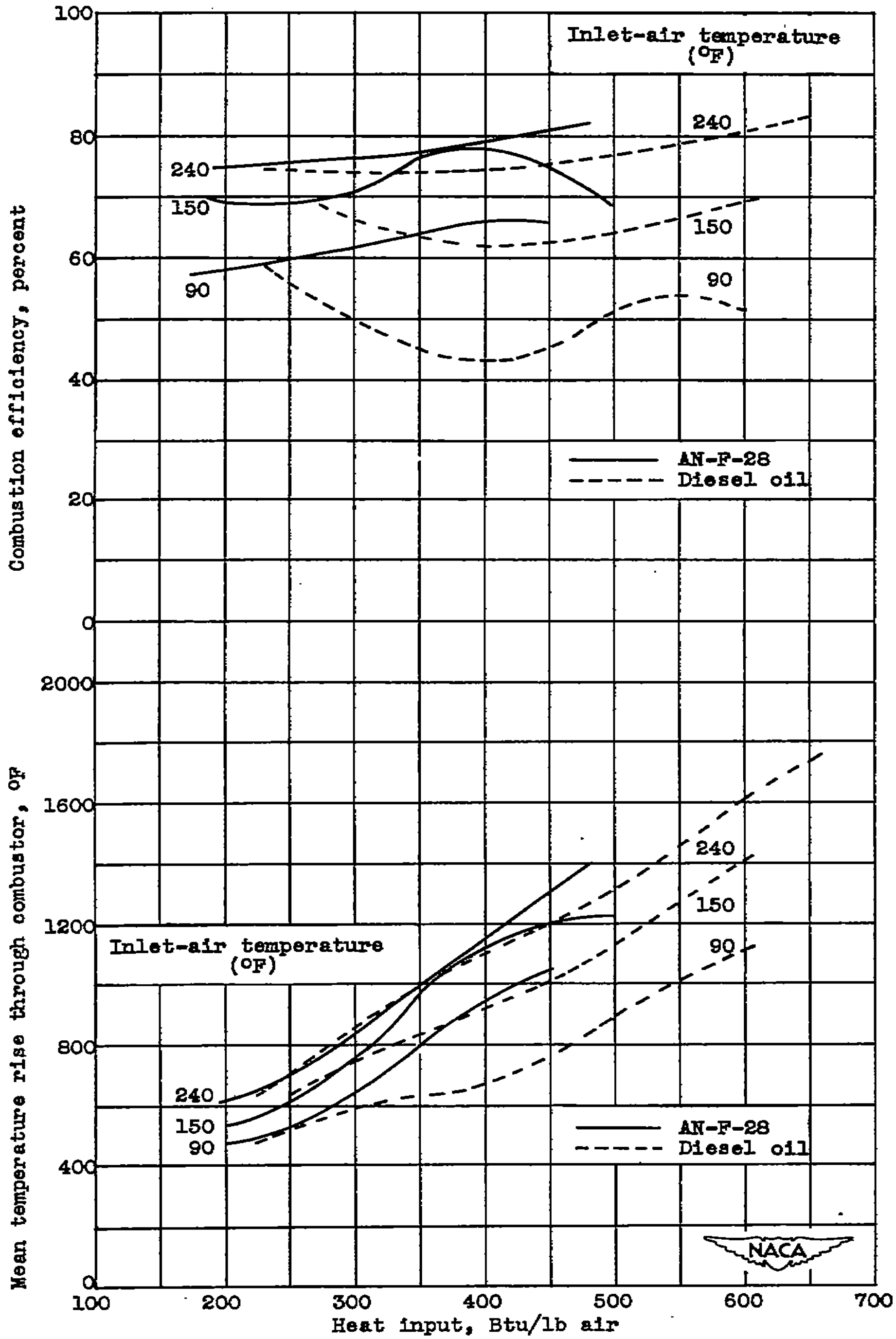

Figure 17. - Maximum combustion efficiencies and mean temperature rise available through annular combustor operating with optimum nozzle capacity for any value of heat input. Inlet-air temperatures varied from conditions simulating engine operation. Point A: inlet-air static pressure, 9.2 pounds per square inch absolute; inlet-air velocity, 200 feet per second. Fuels, AN-F-28 and Diesel oil.

933

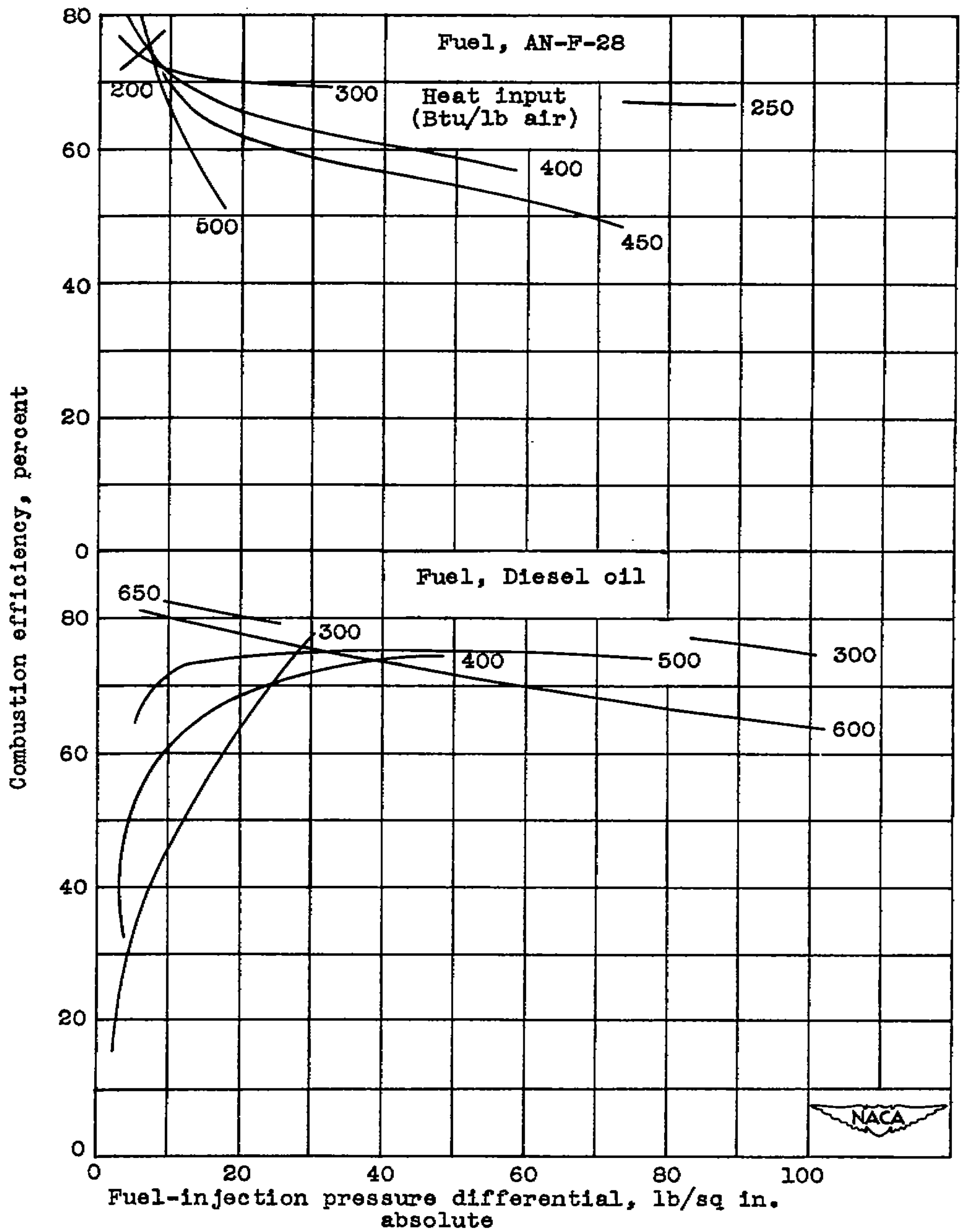

(a) Point A; inlet-air temperature, 240° F.

Figure 18. - Variation of combustion efficiency with fuel-injection pressure for several heat-input values. Simulated engine operating conditions: Point A, inlet-air static pressure, 9.2 pounds per square inch absolute; inlet-air velocity, 200 feet per second; Point B, inlet-air static pressure, 7.7 pounds per square inch absolute; inlet-air velocity, 160 feet per second. Fuels, AN-F-28 and Diesel oil.

933

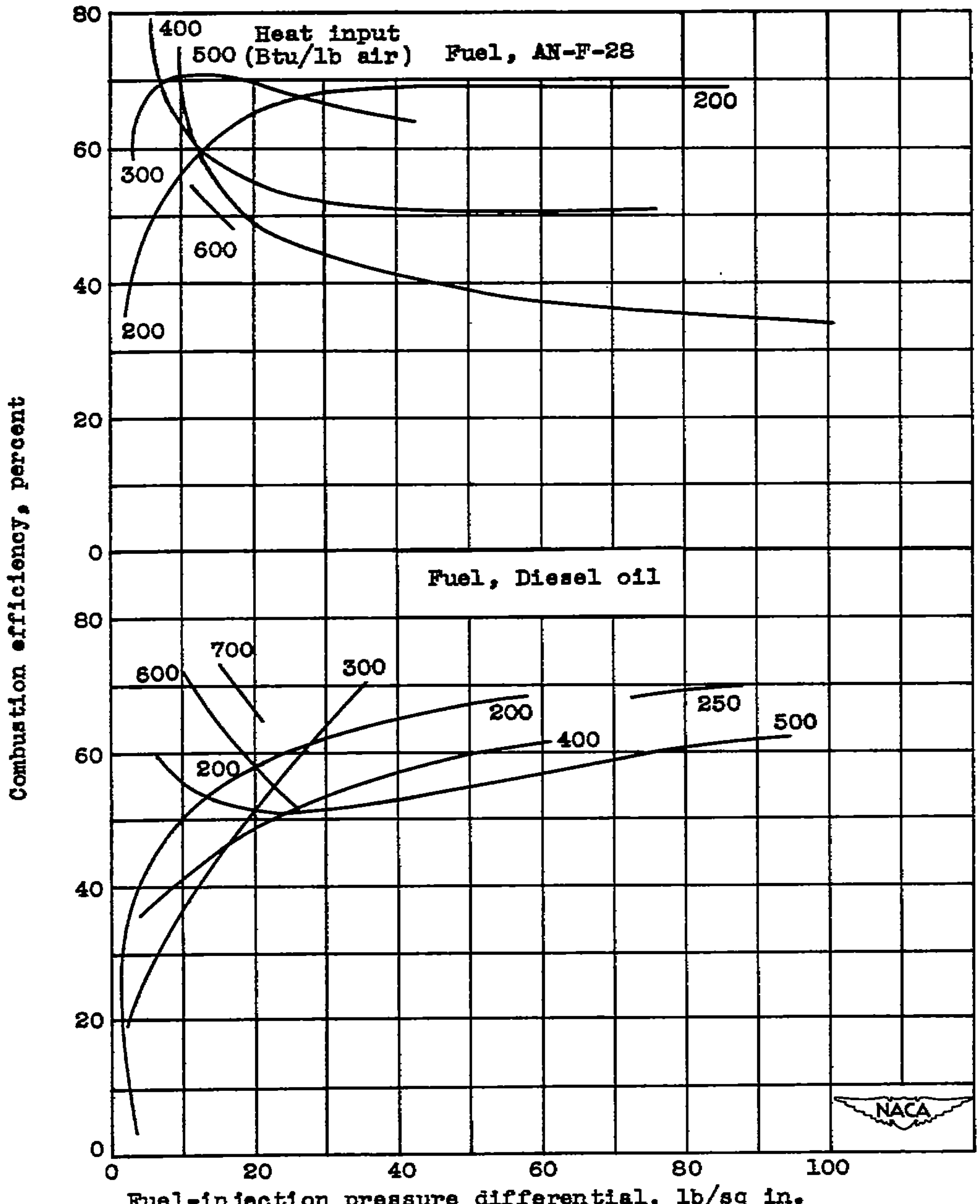

Fuel-injection pressure differential, lb/sq in. absolute

(b) Point A; inlet-air temperature, 150° F.

Figure 18. - Continued. Variation of combustion efficiency with fuel-injection pressure for several heat-input values. Simulated engine operating conditions: Point A, inlet-air static pressure, 9.2 pounds per square inch absolute; inlet-air velocity, 200 feet per second; Point B, inlet-air static pressure, 7.7 pounds per square inch absolute; inlet-air velocity, 160 feet per second. Fuels, AN-F-28 and Diesel oil.

933

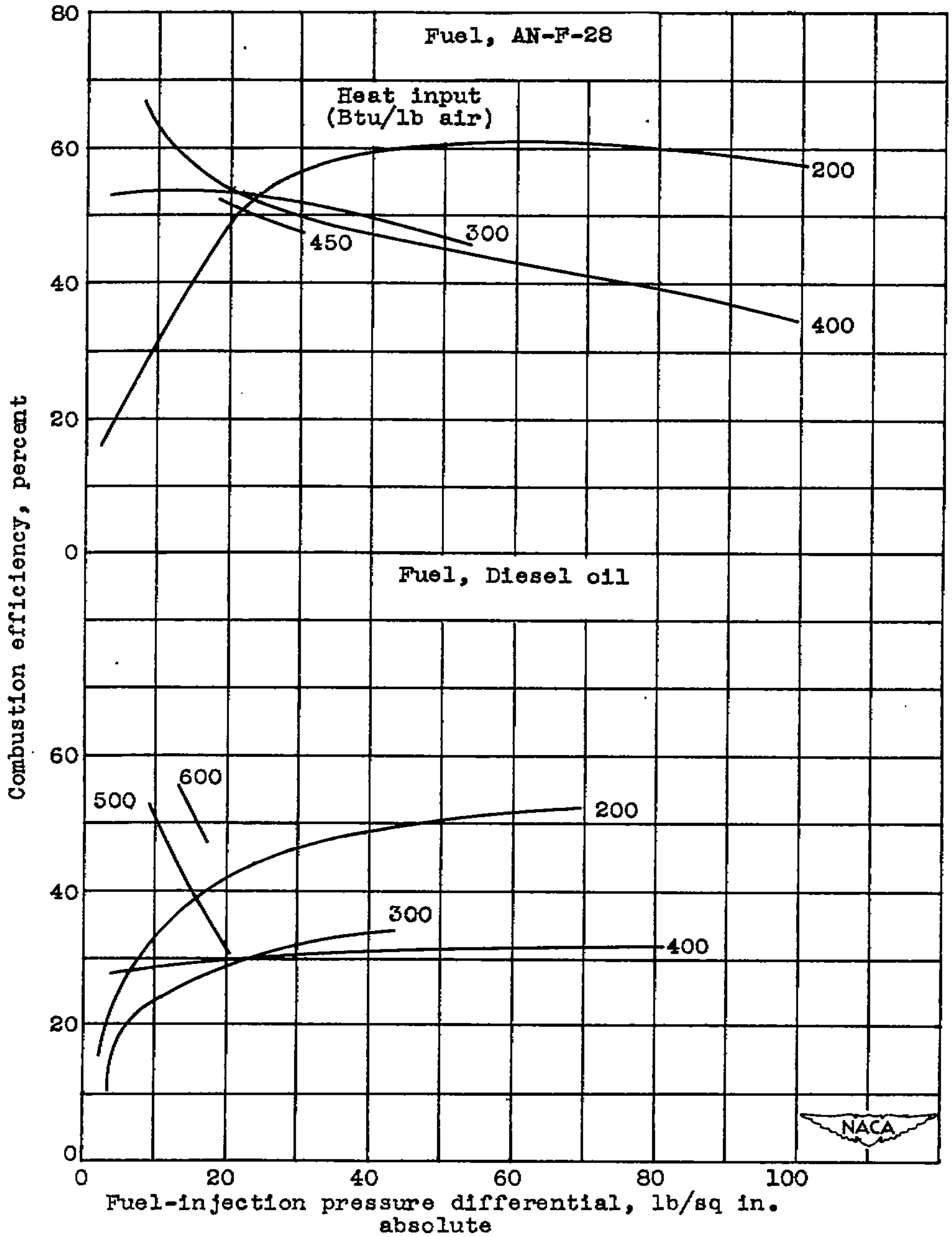

(c) Point A; inlet-air temperature, 90° F.

Figure 18. - Continued. Variation of combustion efficiency with fuel-injection pressure for several heat-input values. Simulated engine operating conditions: Point A, inlet-air static pressure, 9.2 pounds per square inch absolute; inlet-air velocity, 200 feet per second; Point B, inlet-air static pressure, 7.7 pounds per square inch absolute; inlet-air velocity, 160 feet per second. Fuels, AN-F-28 and Diesel oil.

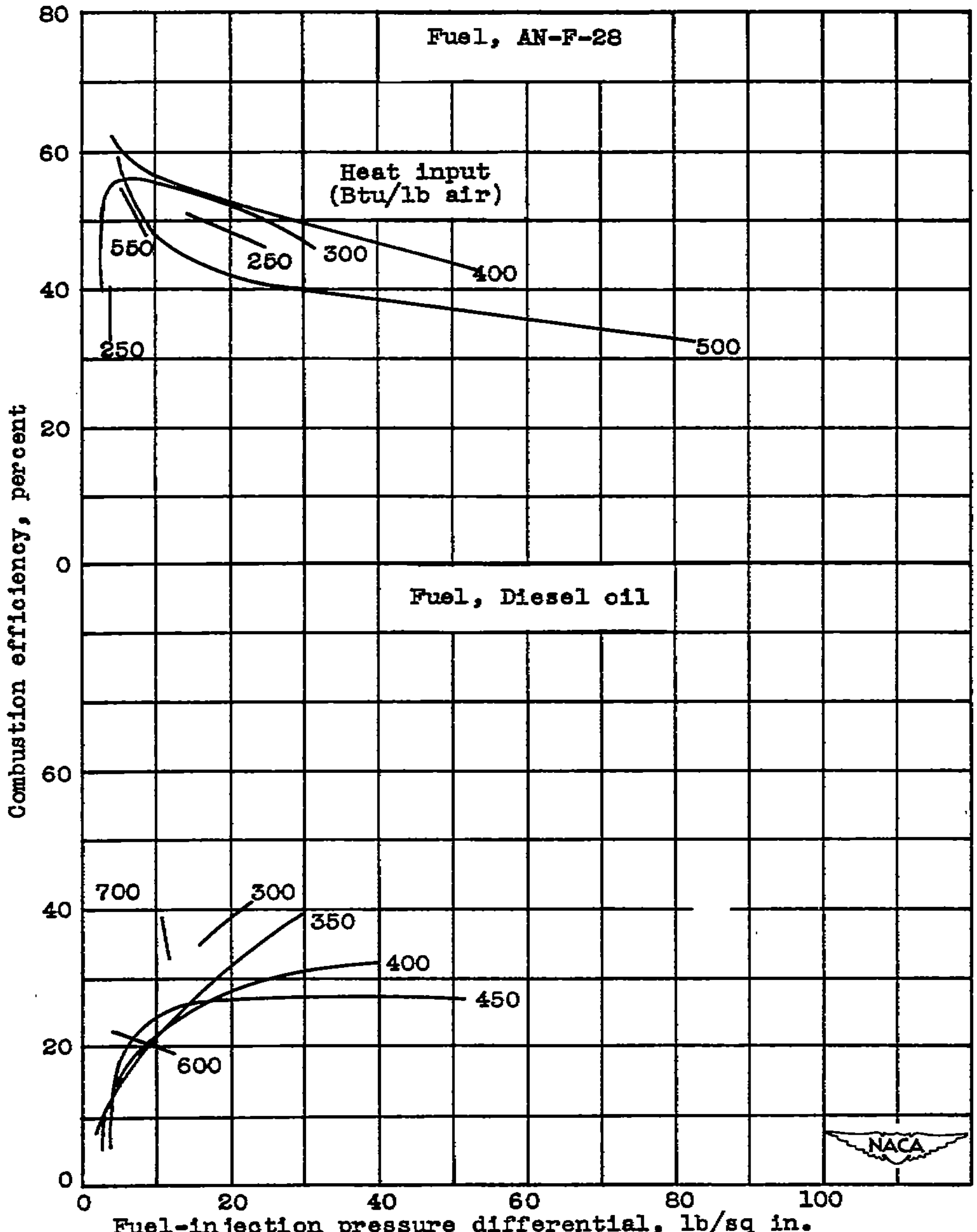

(d) Point B; inlet-air temperature, 70° F.

Figure 18. - Continued. Variation of combustion efficiency with fuel-injection pressure for several heat-input values. Simulated engine operating conditions: Point A, inlet-air static pressure, 9.2 pounds per square inch absolute; inlet-air velocity, 200 feet per second; Point B, inlet-air static pressure, 7.7 pounds per square inch absolute; inlet-air velocity, 160 feet per second. Fuels, AN-F-28 and Diesel oil.

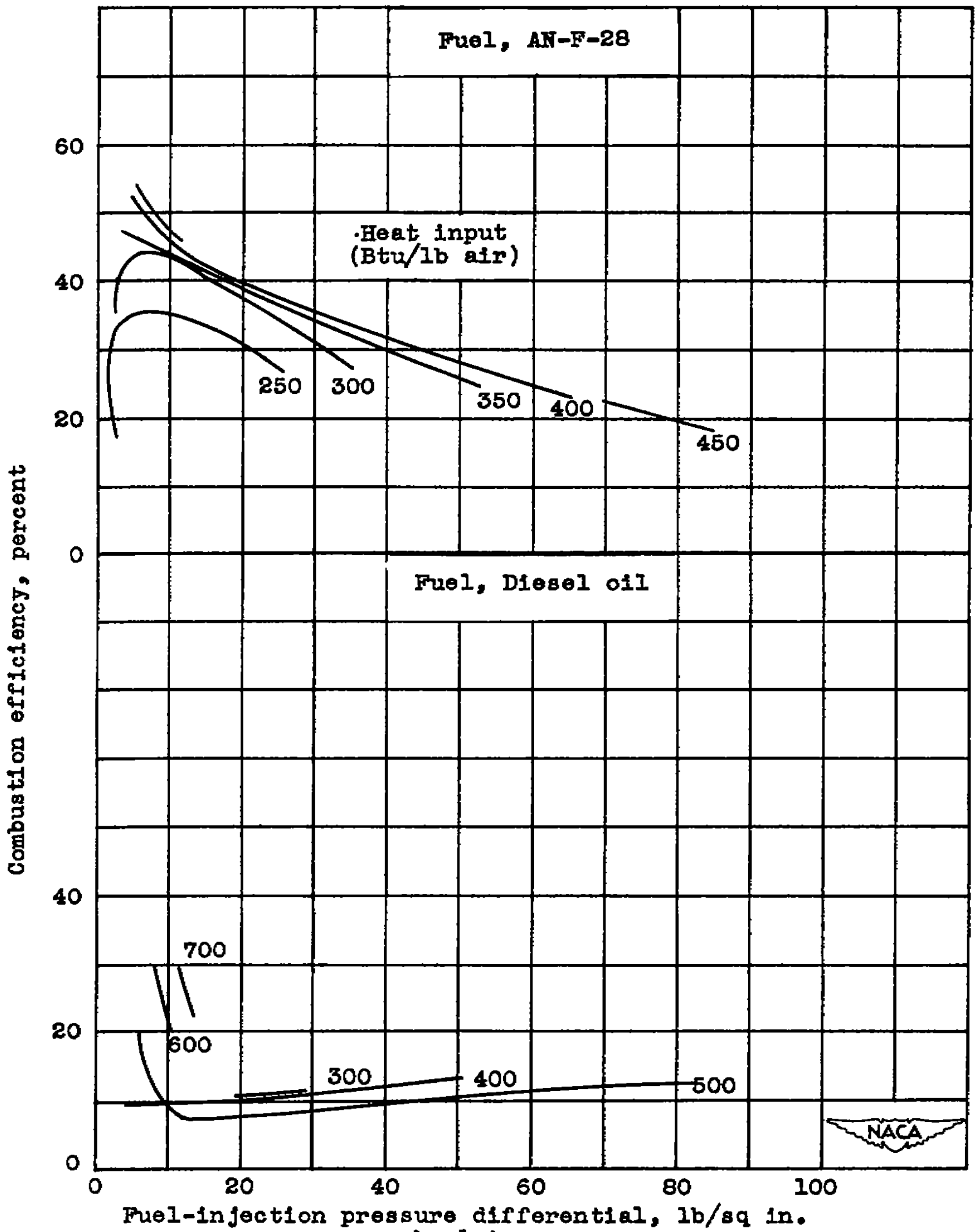

(e) Point B; inlet-air temperature, 0° F.

Figure 18. - Concluded. Variation of combustion efficiency with fuel-injection pressure for several heat-input values. Simulated engine operating conditions: Point A, inlet-air static pressure, 9.2 pounds per square inch absolute; inlet-air velocity, 200 feet per second; Point B, inlet-air static pressure, 7.7 pounds per square inch absolute; inlet-air velocity, 160 feet per second. Fuels, AN-F-28 and Diesel oil.

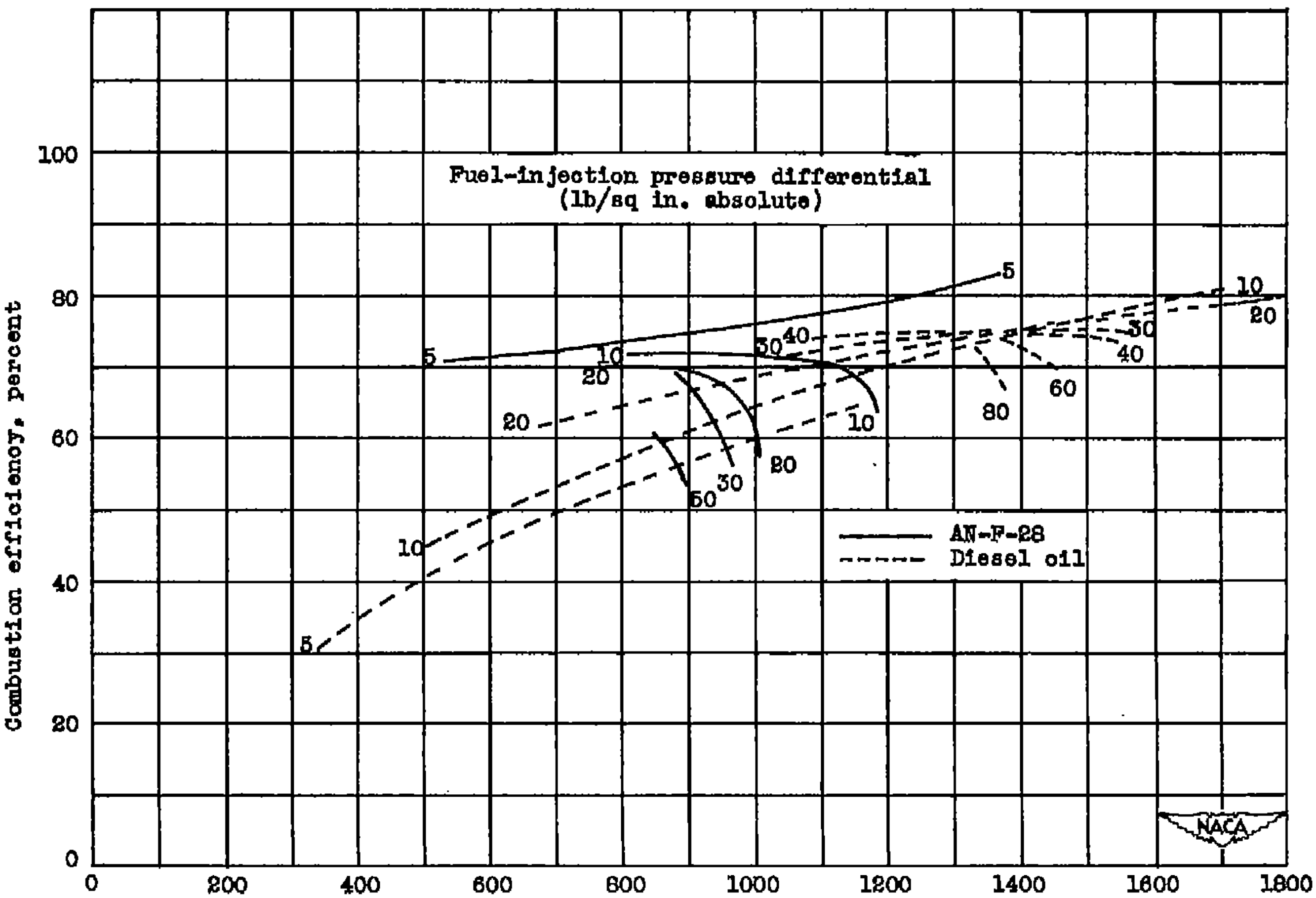

(a) Point A; inlet-air temperature, 240° F.

Figure 19. - Comparison of combustion efficiencies obtainable for various values of mean temperature rise through annular combustor for various pressure differentials across fuel-injection nozzles. Inlet-air temperatures varied from conditions simulating engine operation. Simulated engine operating conditions: Point A, inlet-air static pressure, 9.2 pounds per square inch absolute; inlet-air velocity, 200 feet per second; Point B, inlet-air static pressure, 7.7 pounds per square inch absolute; inlet-air velocity, 160 feet per second. Fuels, AN-F-28 and Diesel oil.

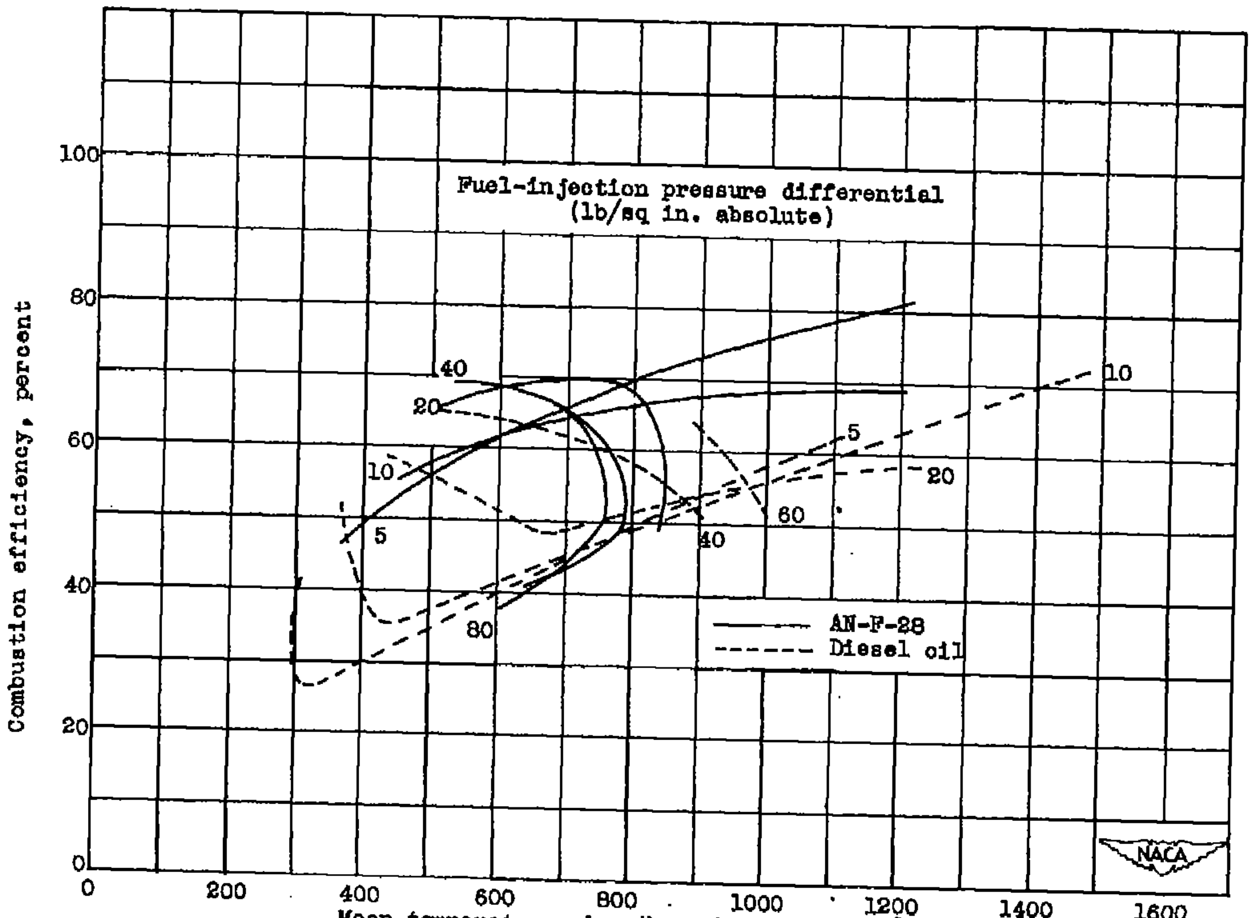

(b) Point A; inlet-air temperature, 150° F.

Figure 19. - Continued. Comparison of combustion efficiencies obtainable for various values of mean temperature rise through annular combustor for various pressure differentials across fuel-injection nozzles. Inlet-air temperatures varied from conditions simulating engine operation. Simulated engine operating conditions: Point A, inlet-air static pressure, 9.2 pounds per square inch absolute; inlet-air velocity, 200 feet per second; Point B, inlet-air static pressure, 7.7 pounds per square inch absolute; inlet-air velocity, 160 feet per second. Fuels, AN-F-28 and Diesel oil.

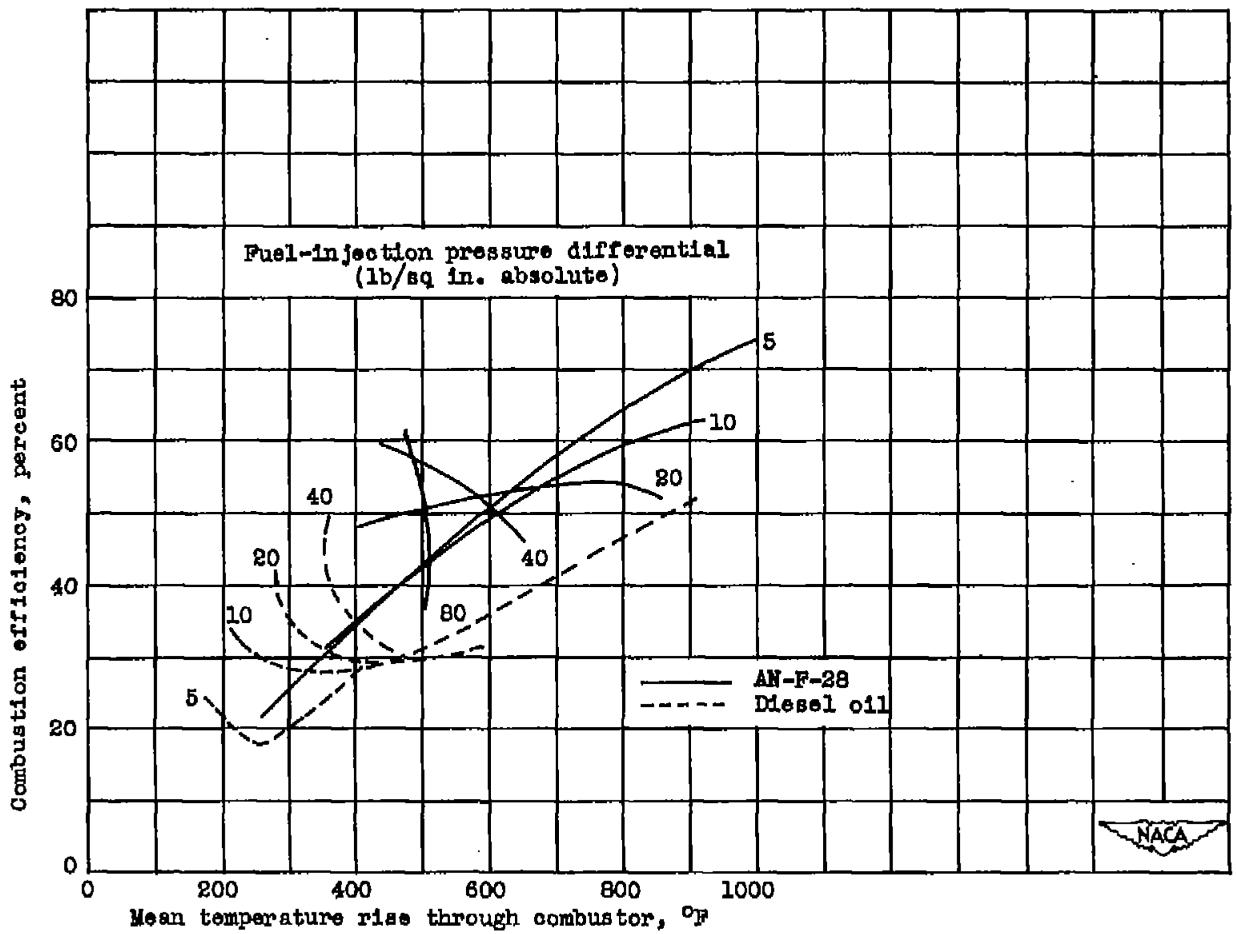

(c) Point A; inlet-air temperature, 90° F.

Figure 19. - Continued. Comparison of combustion efficiencies obtainable for various values of mean temperature rise through annular combustor for various pressure differentials across fuel-injection nozzles. Inlet-air temperatures varied from conditions simulating engine operation. Simulated engine operating conditions: Point A, inlet-air static pressure, 9.2 pounds per square inch absolute; inlet-air velocity, 200 feet per second; Point B, inlet-air static pressure, 7.7 pounds per square inch absolute; inlet-air velocity, 160 feet per second. Fuels, AN-F-28 and Diesel oil.

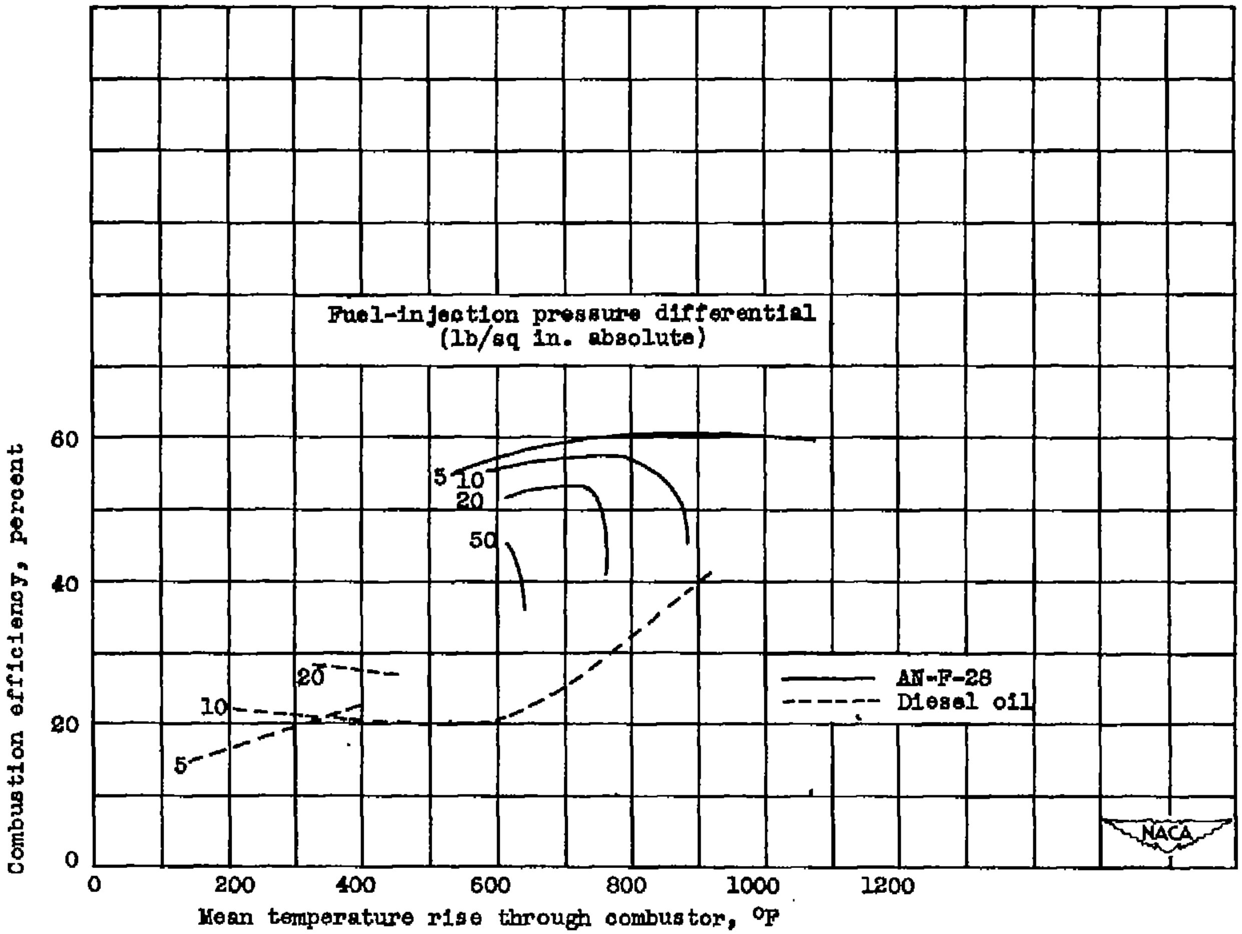

(d) Point B; inlet-air temperature, 70° F.

Figure 19. - Continued. Comparison of combustion efficiencies obtainable for various values of mean temperature rise through annular combustor for various pressure differentials across fuel-injection nozzles. Inlet-air temperatures varied from conditions simulating engine operation. Simulated engine operating conditions: Point A, inlet-air static pressure, 9.2 pounds per square inch absolute; inlet-air velocity, 200 feet per second; Point B, inlet-air static pressure, 7.7 pounds per square inch absolute; inlet-air velocity, 160 feet per second. Fuels, AN-F-28 and Diesel oil.

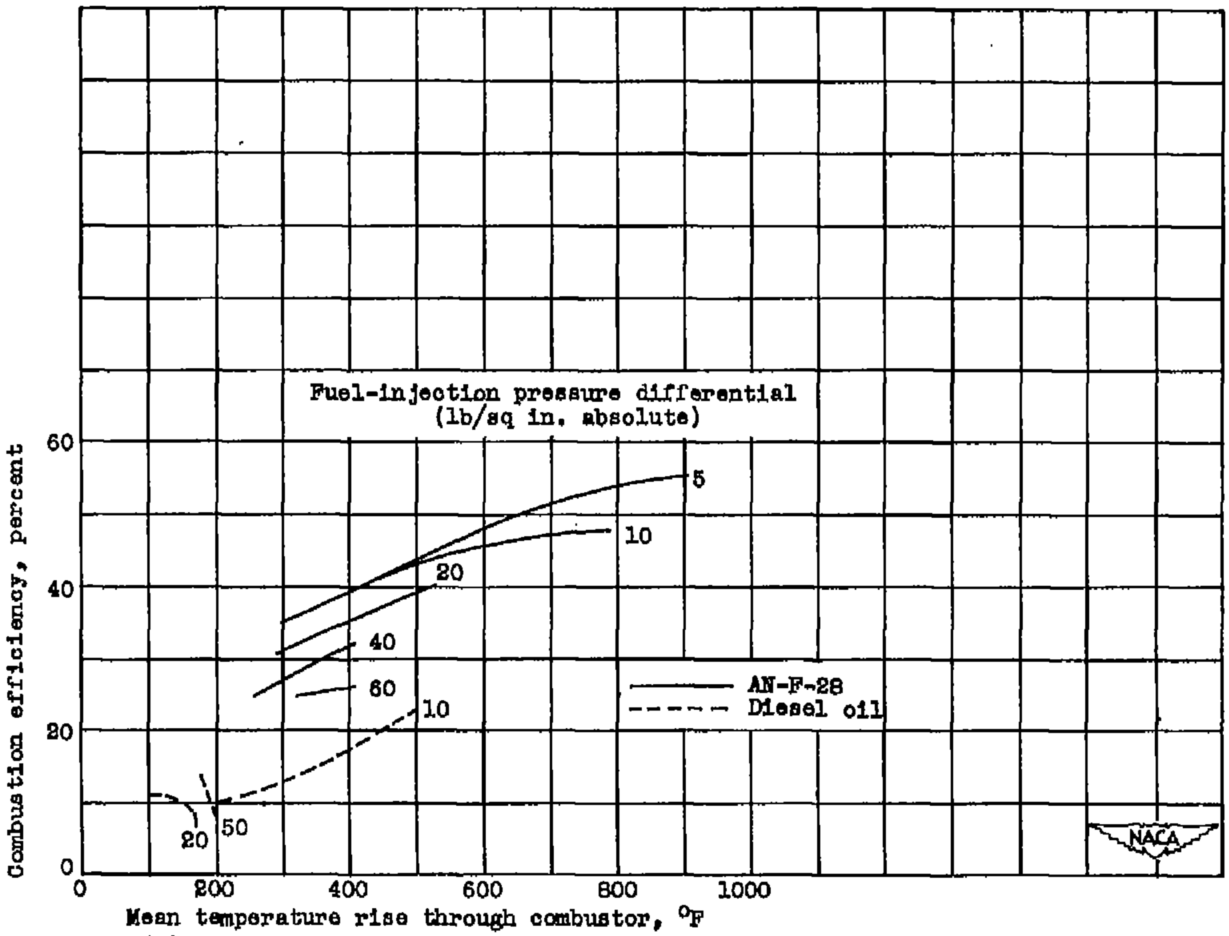

(e) Point B; inlet-air temperature, 0° F.

Figure 19. - Concluded. Comparison of combustion efficiencies obtainable for various values of mean temperature rise through annular combustor for various pressure differentials across fuel-injection nozzles. Inlet-air temperatures varied from conditions simulating engine operation. Simulated engine operating conditions: Point A, inlet-air static pressure, 9.2 pounds per square inch absolute; inlet-air velocity, 200 feet per second; Point B, inlet-air static pressure, 7.7 pounds per square inch absolute; inlet-air velocity, 160 feet per second. Fuels, AN-F-28 and Diesel oil.

933

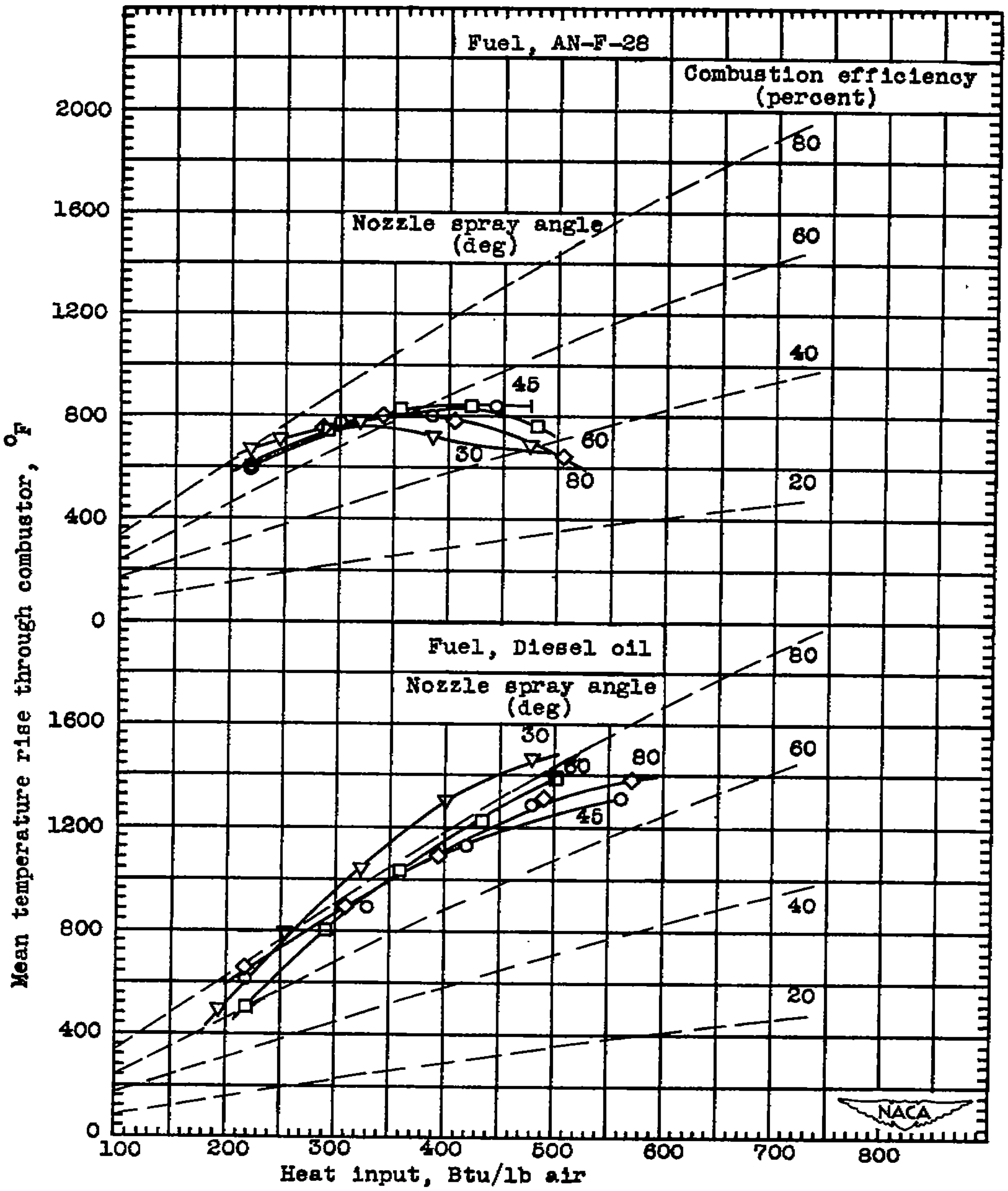

(a) Point A; inlet-air temperature, 240° F.

Figure 20. - Comparison of mean temperature rise through annular combustor for various heat-input values for four different nozzle spray angles of a 3.0-gallon-per-hour-capacity nozzle. Inlet-air temperatures independently altered from conditions simulating engine operation. Simulated engine operating conditions: Point A, inlet-air static pressure, 9.2 pounds per square inch absolute; inlet-air velocity, 200 feet per second; Point B, inlet-air static pressure, 7.7 pounds per square inch absolute; inlet-air velocity, 160 feet per second. Fuels, AN-F-28 and Diesel oil.

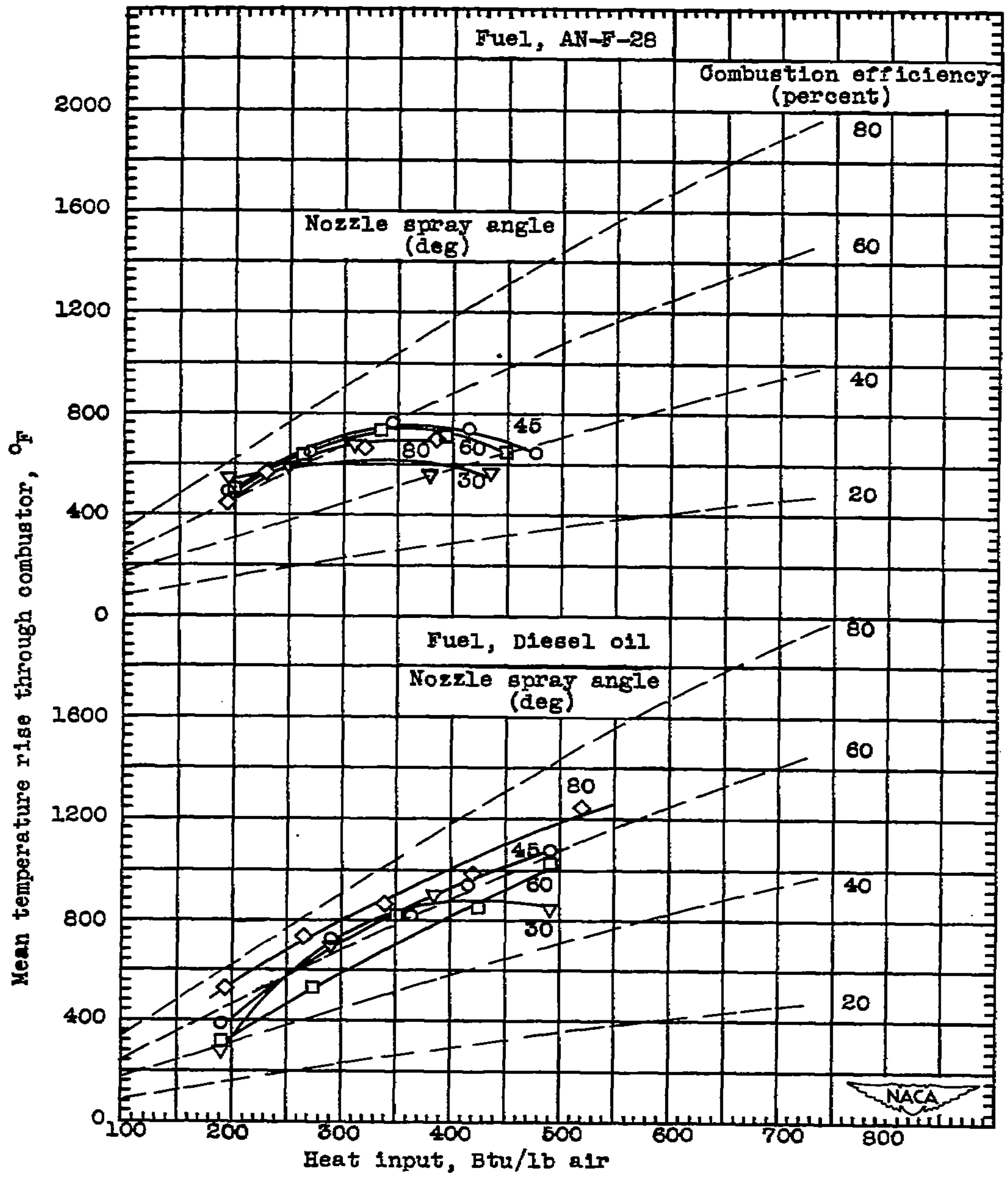

(b) Point A; inlet-air temperature, 150° F.

Figure 20. - Continued. Comparison of mean temperature rise through annular combustor for various heat-input values for four different nozzle spray angles of a 3.0-gallon-per-hour-capacity nozzle. Inlet-air temperatures independently altered from conditions simulating engine operation. Simulated engine operating conditions: Point A, inlet-air static pressure, 9.2 pounds per square inch absolute; inlet-air velocity, 200 feet per second; Point B, inlet-air static pressure, 7.7 pounds per square inch absolute; inlet-air velocity, 160 feet per second. Fuels, AN-F-28 and Diesel oil.

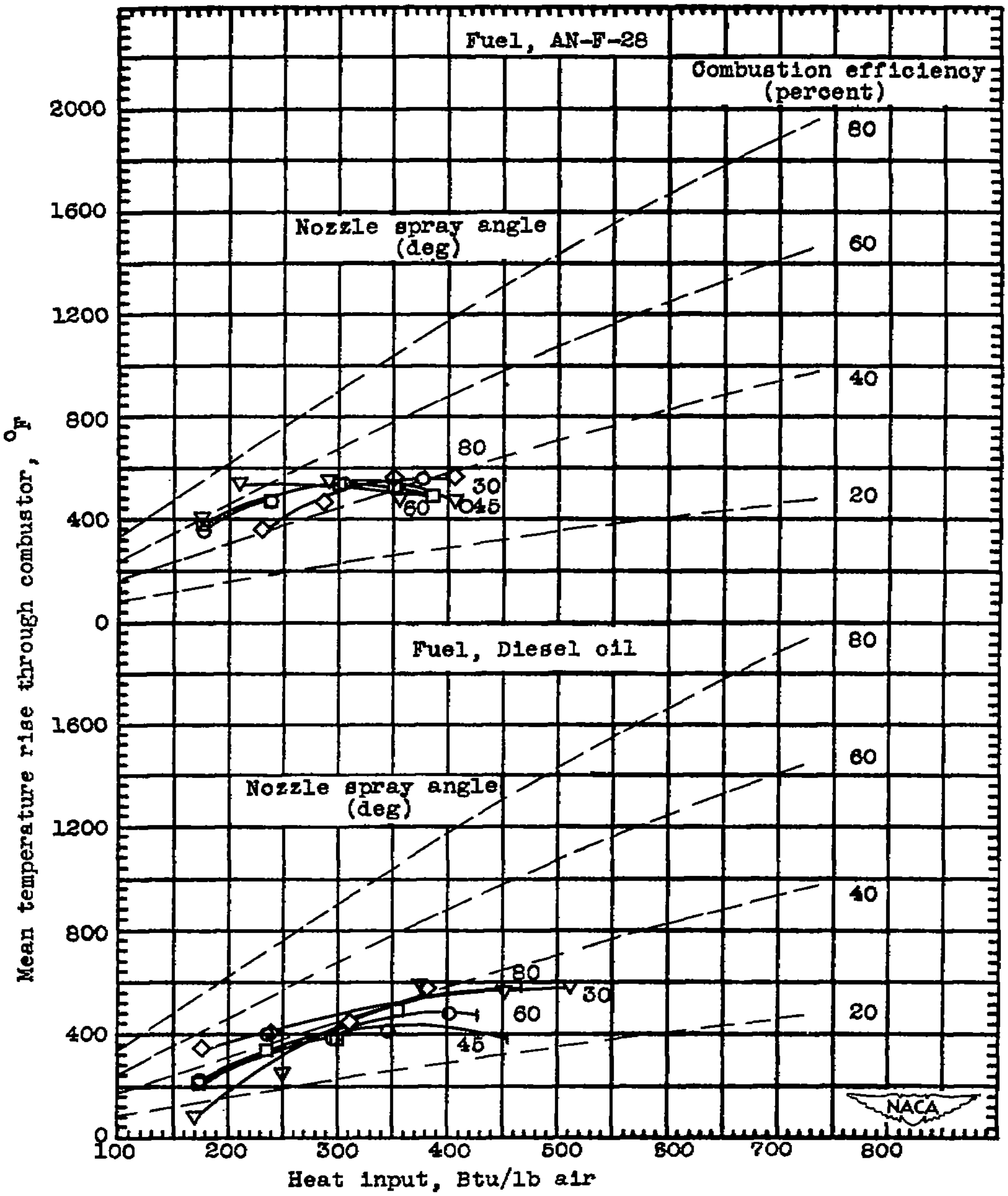

(c) Point A; inlet-air temperature, 90° F.

Figure 20. - Continued. Comparison of mean temperature rise through annular combustor for various heat-input values for four different nozzle spray angles of a 3.0-gallon-per-hour-capacity nozzle. Inlet-air temperatures independently altered from conditions simulating engine operation. Simulated engine operating conditions: Point A, inlet-air static pressure, 9.2 pounds per square inch absolute; inlet-air velocity, 200 feet per second; Point B, inlet-air static pressure, 7.7 pounds per square inch absolute; inlet-air velocity, 160 feet per second. Fuels, AN-F-28 and Diesel oil.

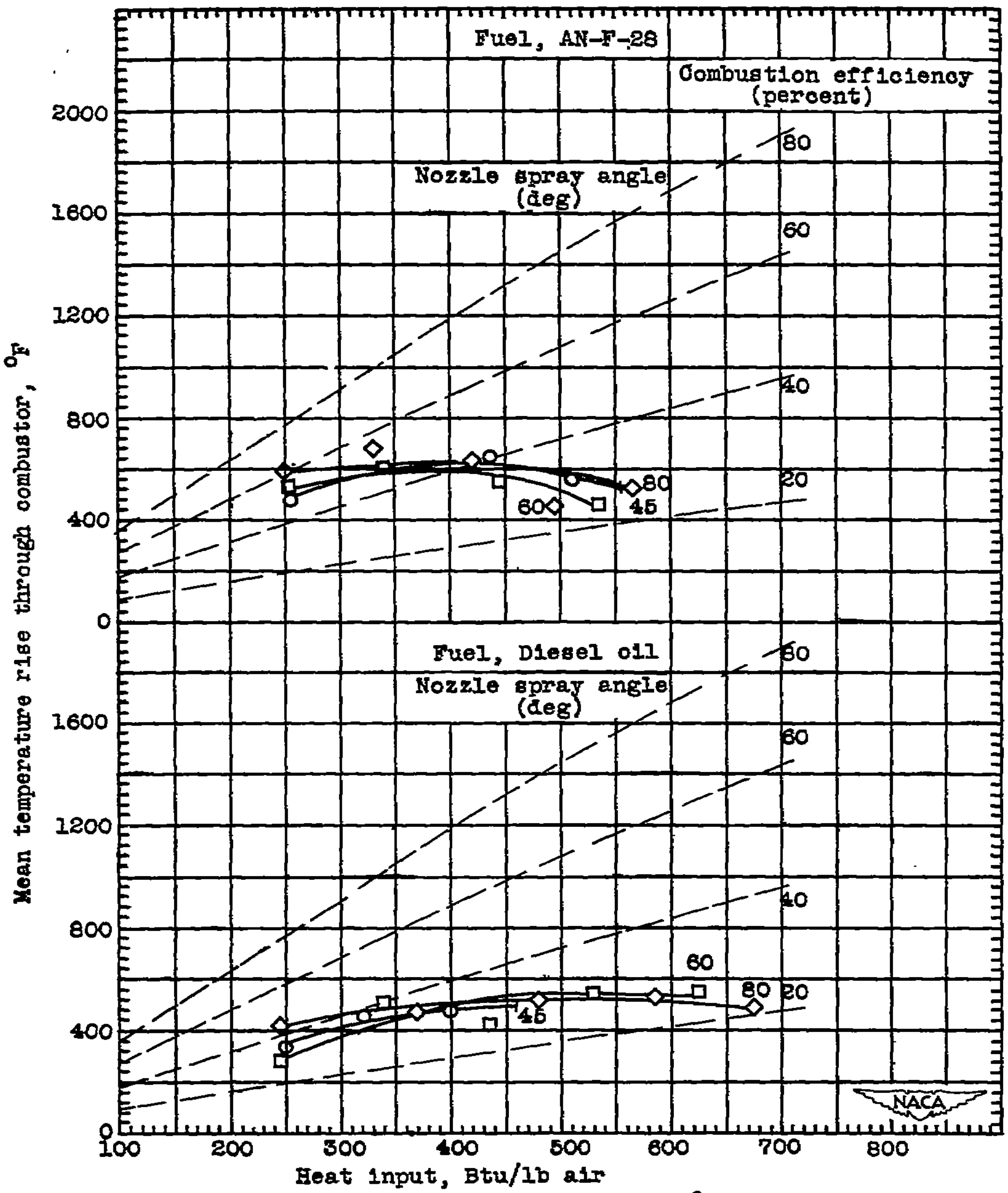

(d) Point B; inlet-air temperature, 70° F.

Figure 20. - Continued. Comparison of mean temperature rise through annular combustor for various heat-input values for four different nozzle spray angles of a 3.0-gallon-per-hour-capacity nozzle. Inlet-air temperatures independently altered from conditions simulating engine operation. Simulated engine operating conditions: Point A, inlet-air static pressure, 9.2 pounds per square inch absolute; inlet-air velocity, 200 feet per second; Point B, inlet-air static pressure, 7.7 pounds per square inch absolute; inlet-air velocity, 160 feet per second. Fuels, AN-F-28 and Diesel oil.

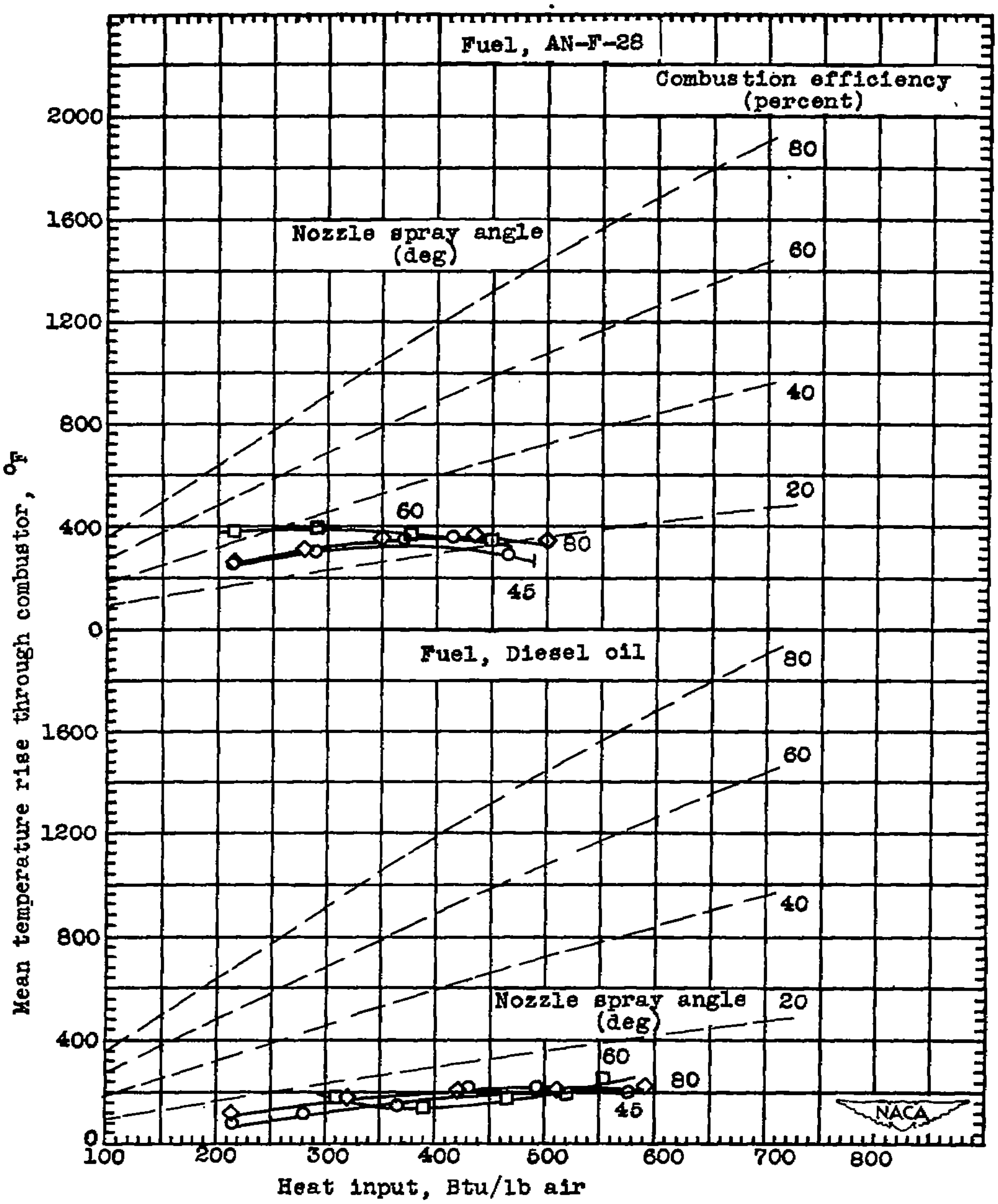

(e) Point B; inlet-air temperature, 0° F.

Figure 20. - Concluded. Comparison of mean temperature rise through annular combustor for various heat-input values for four different nozzle spray angles of a 3.0-gallon-per-hour-capacity nozzle. Inlet-air temperatures independently altered from conditions simulating engine operation. Simulated engine operating conditions: Point A, inlet-air static pressure, 9.2 pounds per square inch absolute; inlet-air velocity, 200 feet per second; Point B, inlet-air static pressure, 7.7 pounds per square inch absolute; inlet-air velocity, 160 feet per second. Fuels, AN-F-28 and Diesel oil.

933

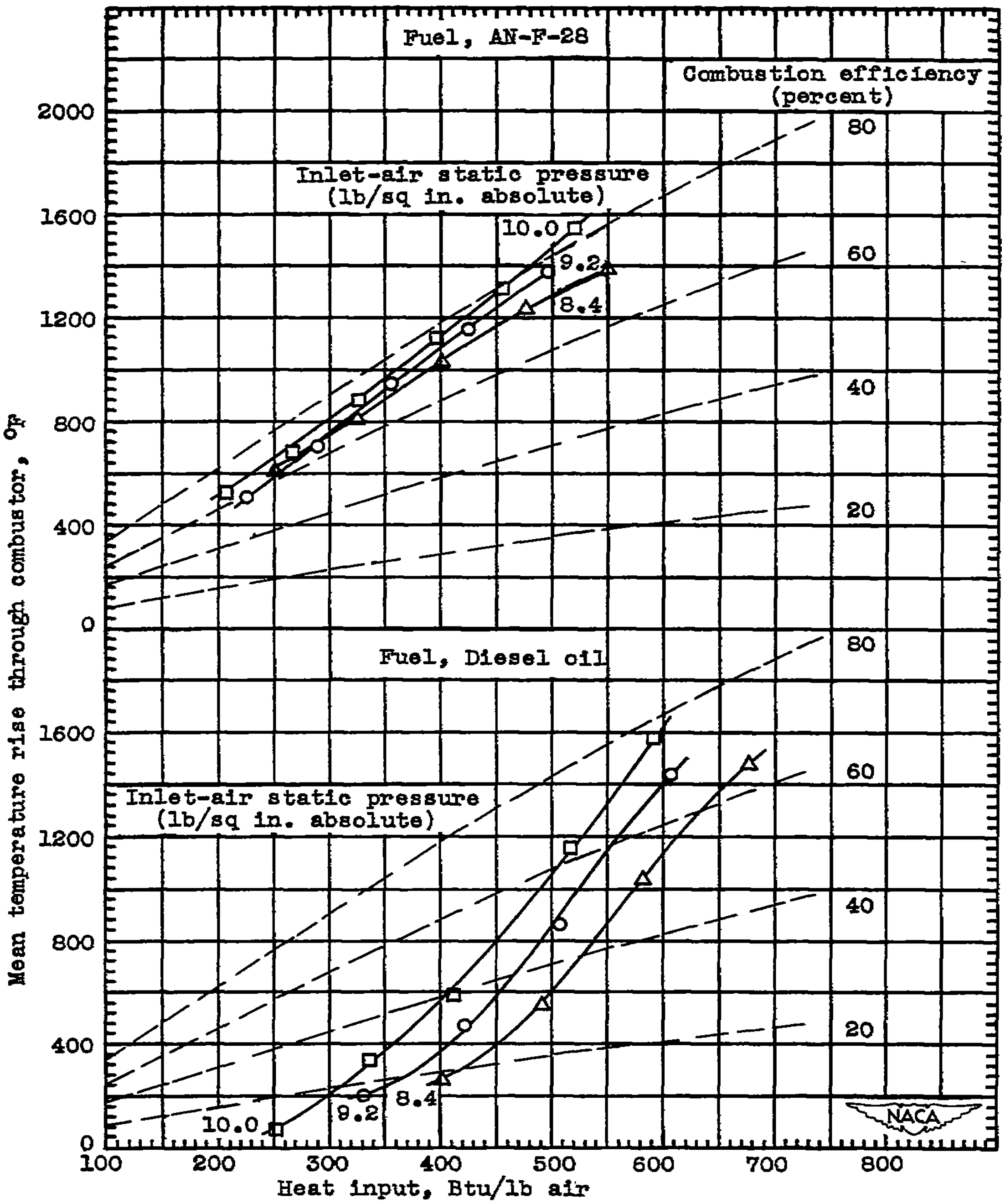

(a) Nozzle capacity, 17.5 gallons per hour.

Figure 21. - Variation of mean temperature rise through annular combustor with heat input for three different-capacity nozzles with inlet-air static pressure independently altered from conditions simulating engine operation. Point A: inlet-air temperature, 240° F; inlet-air velocity, 200 feet per second. Fuels, AN-F-28 and Diesel oil.

933

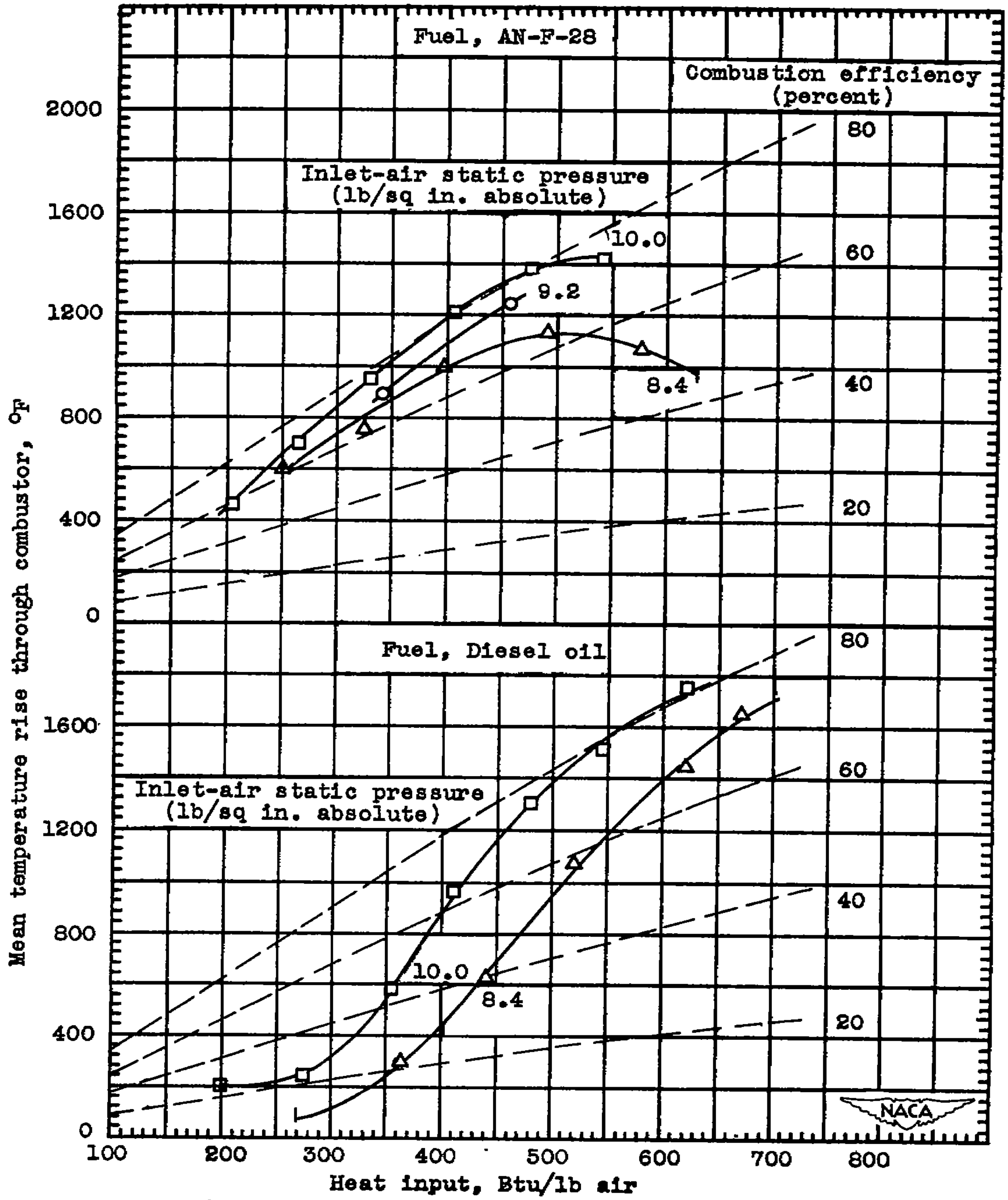

(b) Nozzle capacity, 10.5 gallons per hour.

Figure 21. - Continued. Variation of mean temperature rise through annular combustor with heat input for three different-capacity nozzles with inlet-air static pressure independently altered from conditions simulating engine operation. Point A: inlet-air temperature, 240° F; inlet-air velocity, 200 feet per second. Fuels, AN-F-28 and Diesel oil.

933

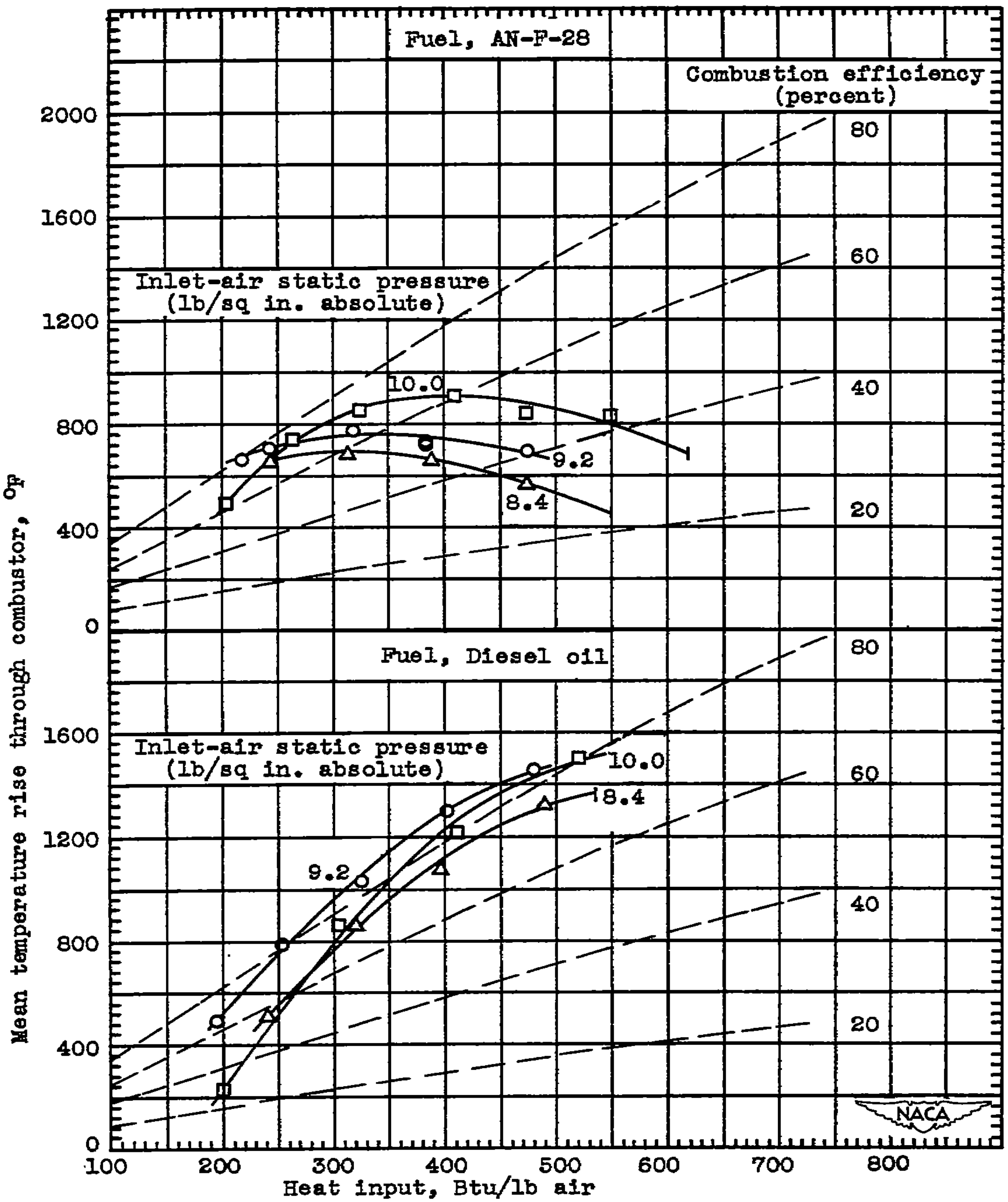

(c) Nozzle capacity, 3.0 gallons per hour.

Figure 21. - Concluded. Variation of mean temperature rise through annular combustor with heat input for three different-capacity nozzles with inlet-air static pressure independently altered from conditions simulating engine operation. Point A: inlet-air temperature, 240° F; inlet-air velocity, 200 feet per second. Fuels, AN-F-28 and Diesel oil.

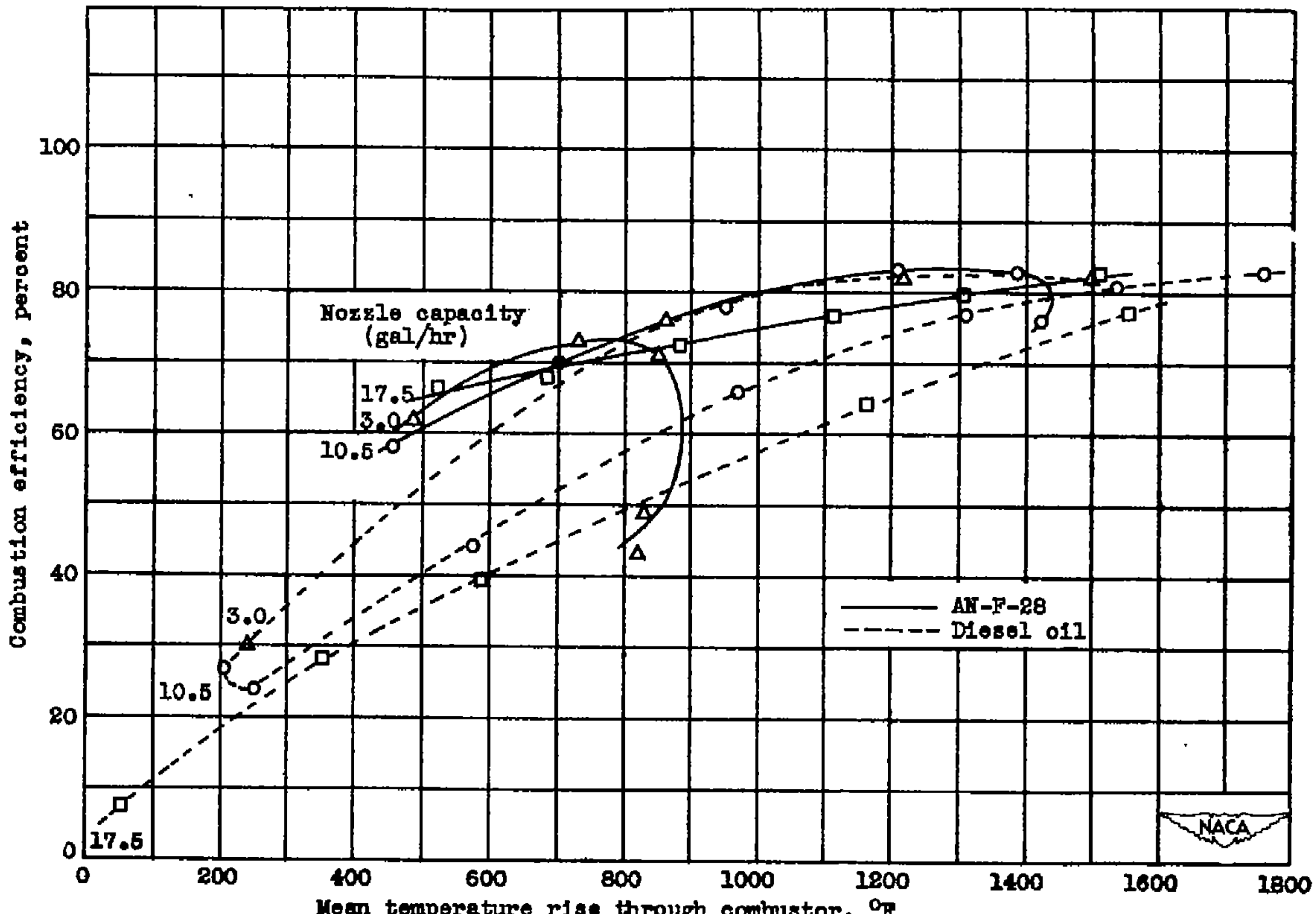

(a) Inlet-air static pressure, 10.0 pounds per square inch absolute.

Figure 22. - Comparison of combustion efficiencies obtainable for various values of mean temperature rise through annular combustor for three different-capacity nozzles with inlet-air static pressure independently altered from conditions simulating engine operation. Point A: inlet-air temperature, 240° F; inlet-air velocity, 200 feet per second. Fuels, AN-F-28 and Diesel oil.

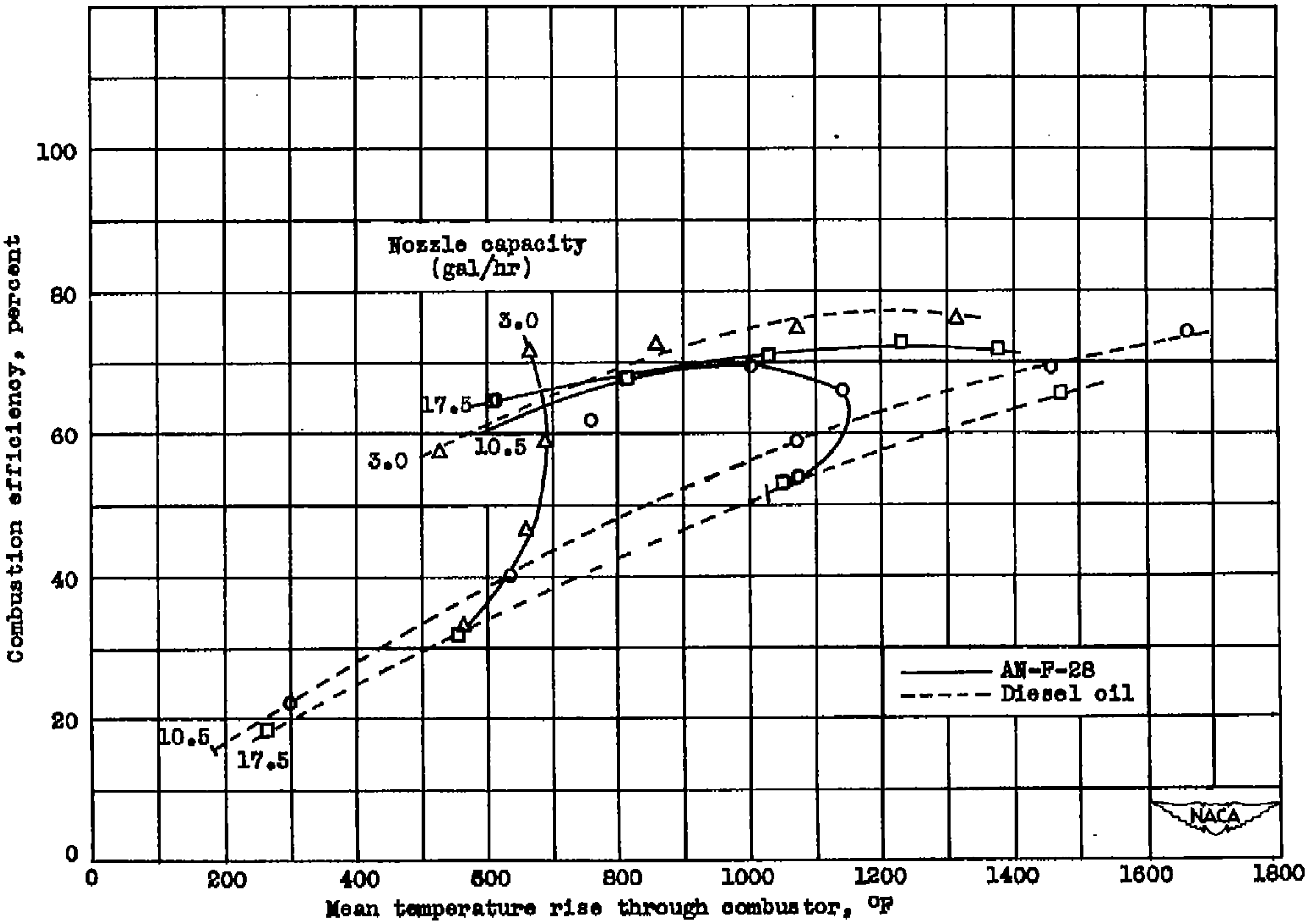

(b) Inlet-air static pressure, 8.4 pounds per square inch absolute.

Figure 22. - Concluded. Comparison of combustion efficiencies obtainable for various values of mean temperature rise through annular combustor for three different-capacity nozzles with inlet-air static pressure independently altered from conditions simulating engine operation. Point A: inlet-air temperature, 240° F; inlet-air velocity, 200 feet per second. Fuels, AN-F-28 and Diesel oil.

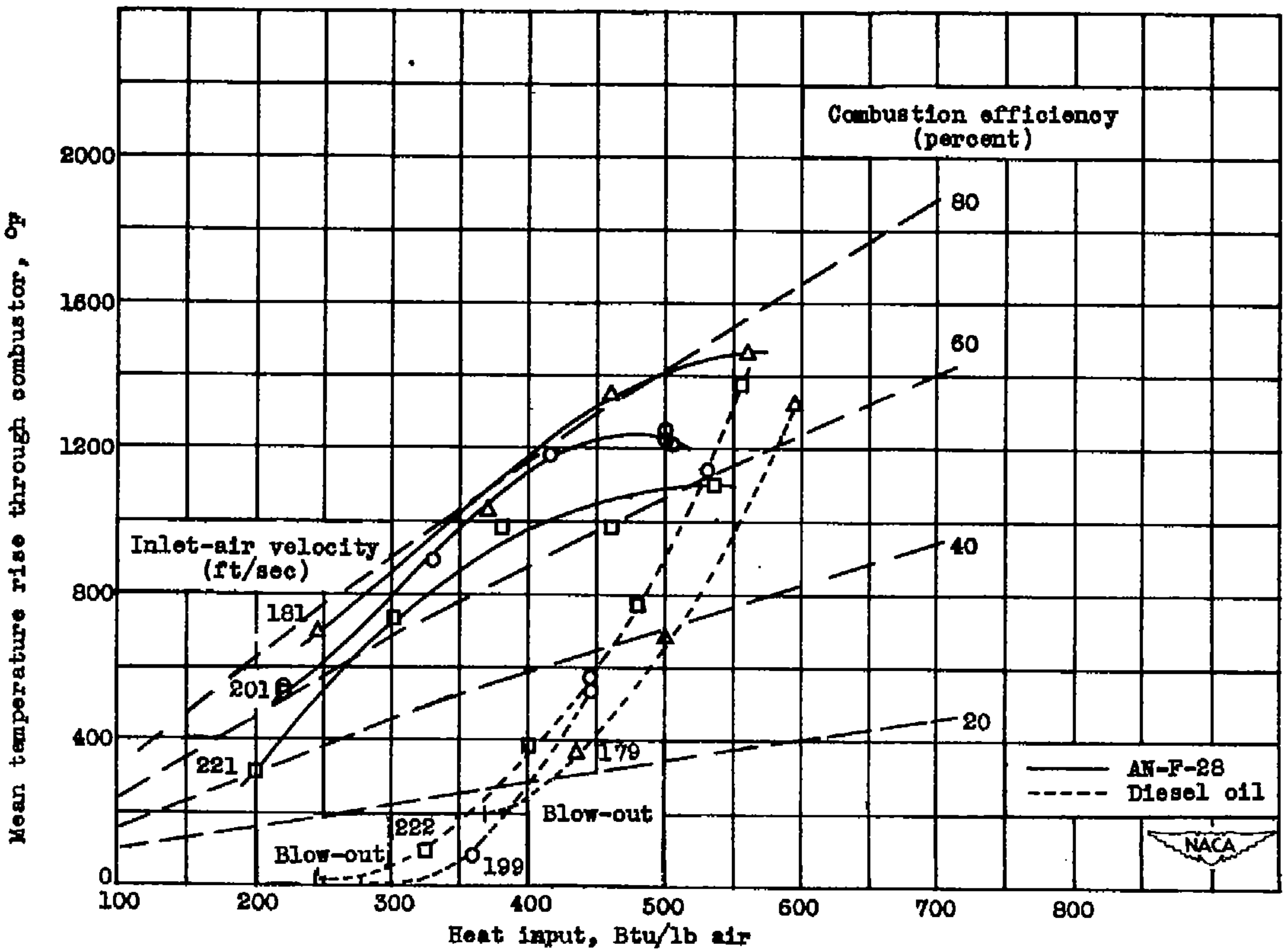

Figure 23. - Variation of mean temperature rise through annular combustor with heat input for inlet-air velocity independently altered from conditions simulating engine operation. Point A: inlet-air static pressure, 9.2 pounds per square inch absolute; inlet-air temperature, 240° F. Fuels, AN-F-28 and Diesel oil; standard combustor-flame-liner configuration (basket 1).

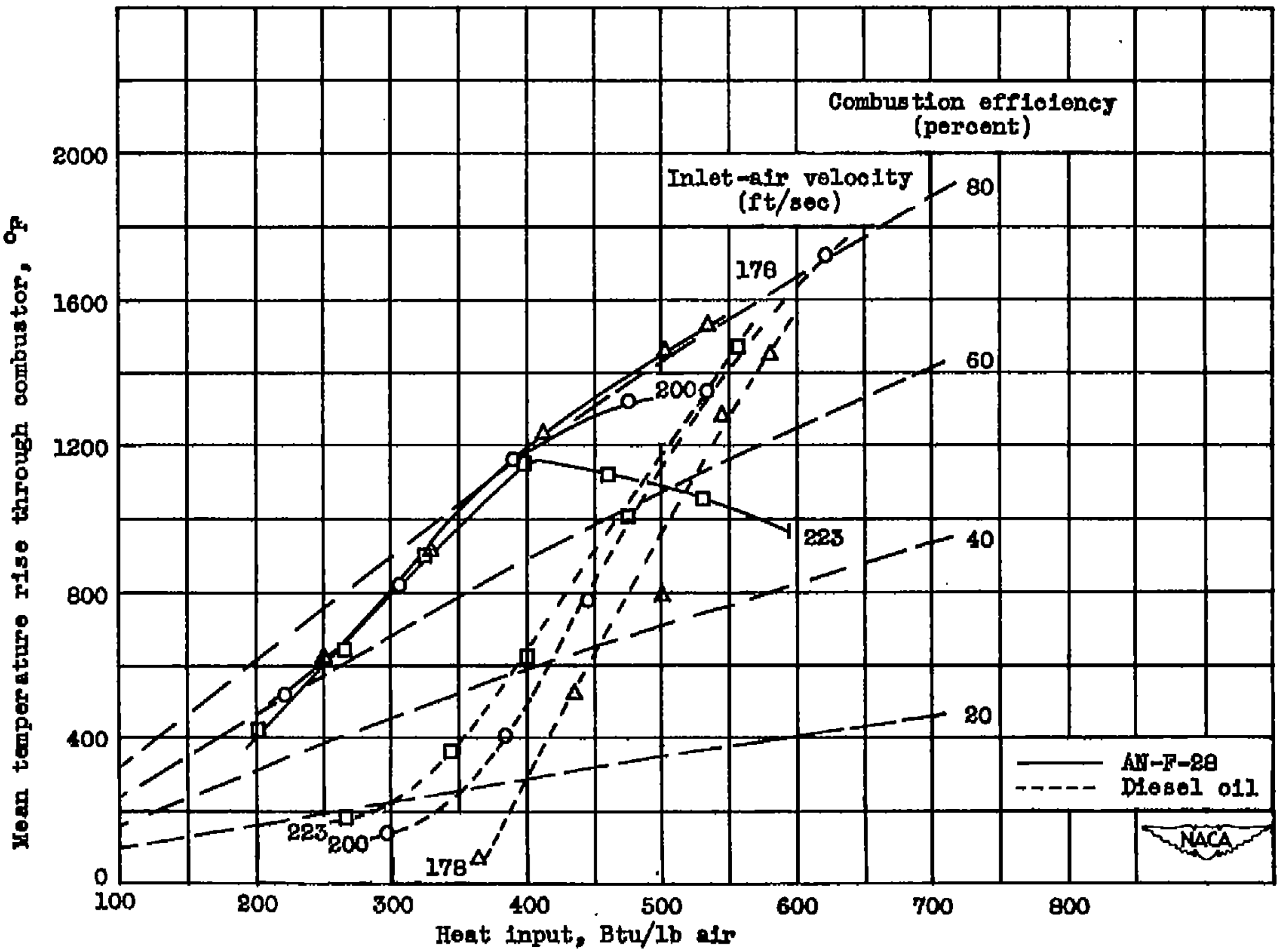

Figure 24. - Variation of mean temperature rise through annular combustor with heat input for inlet-air velocity independently altered from conditions simulating engine operation. Point A: inlet-air static pressure, 9.2 pounds per square inch absolute; inlet-air temperature, 240° F. Fuels, AN-F-28 and Diesel oil; altered combustor-flame-liner configuration (basket 2).

933

Figure 25. - View of combustor interior after completion of studies of solvent 4.

933

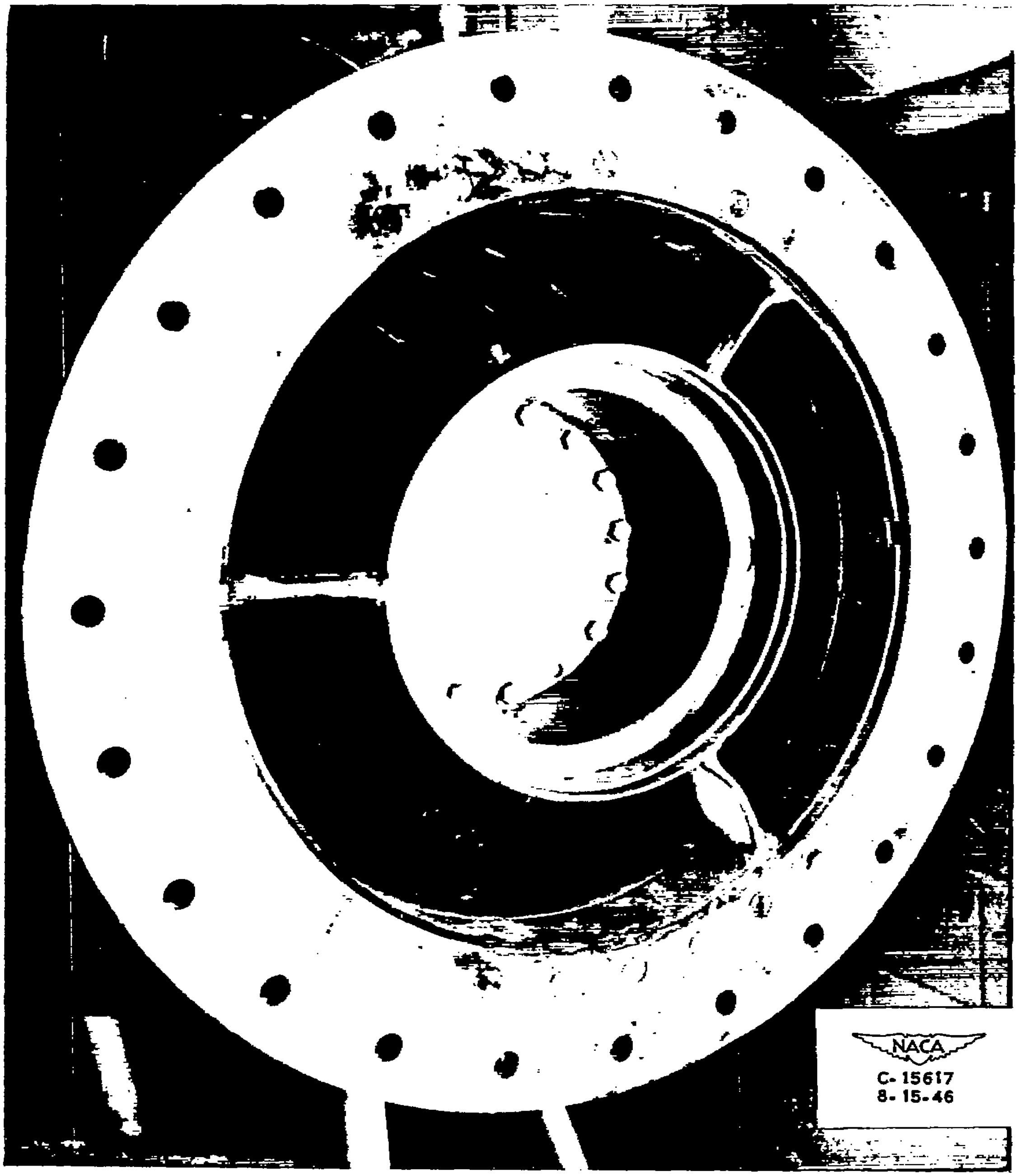

Figure 26. - View of combustor interior after completion of studies of benzene.

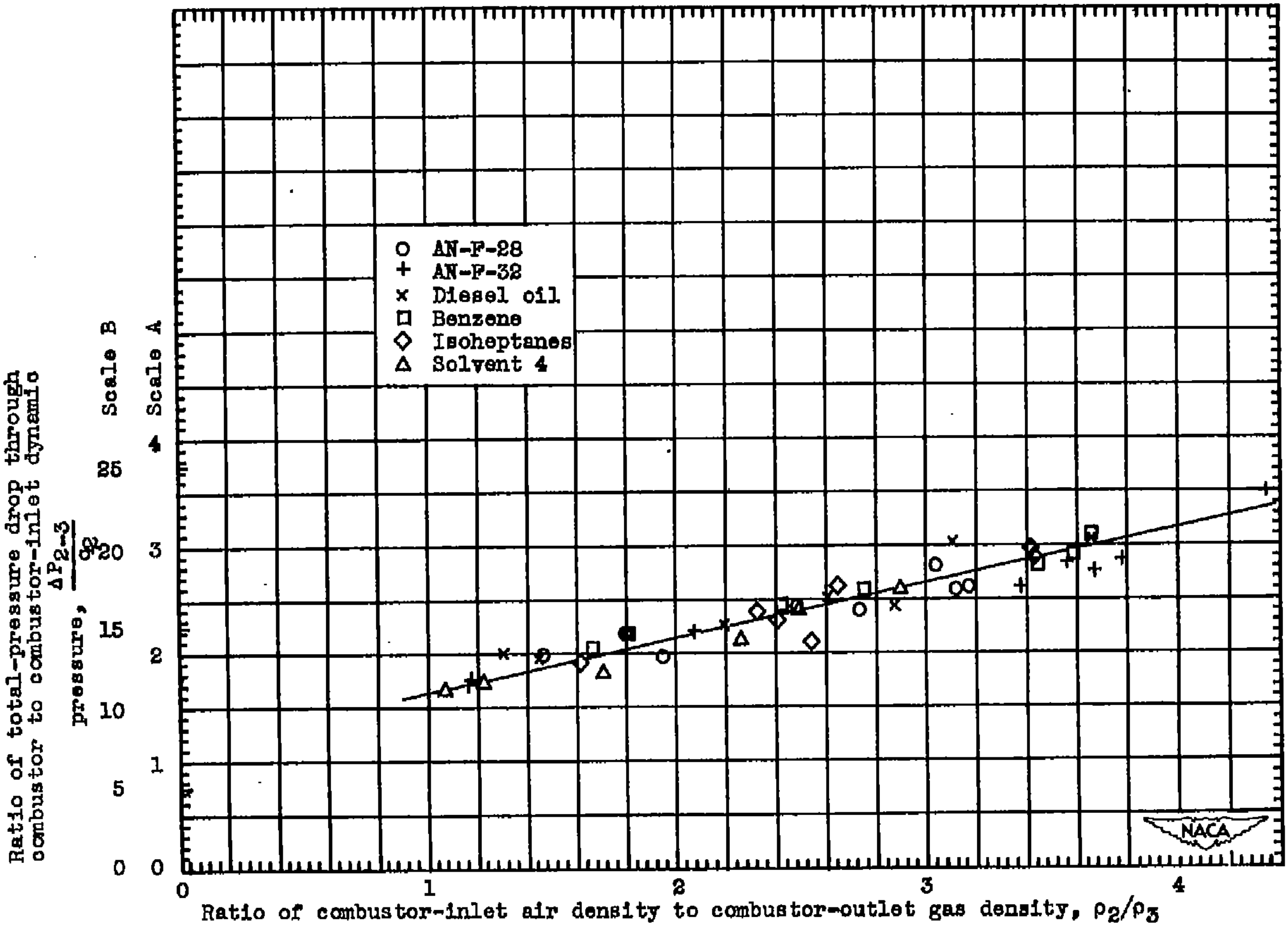

(a) With different fuels.

Figure 27. - Total-pressure drop across annular combustor expressed as function of density ratio across combustor. Scale A, q_2 based on combustor-inlet cross-sectional area; scale B, q_2 based on maximum combustor cross-sectional area.

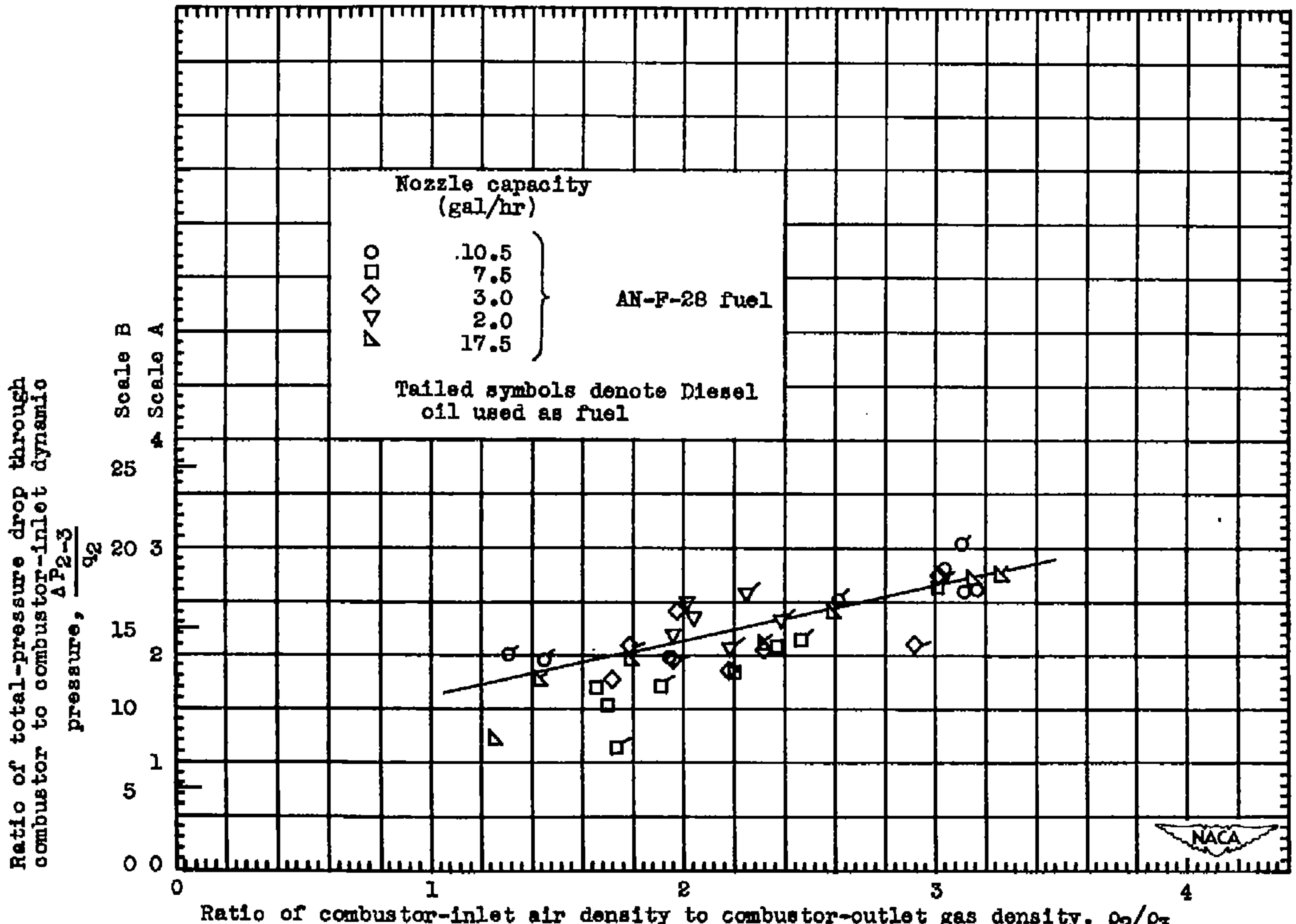

(b) With different-capacity fuel-injection nozzles.

Figure 27. - Concluded. Total-pressure drop across annular combustor expressed as function of density ratio across combustor. Scale A, q_2 based on combustor-inlet cross-sectional area; scale B, q_2 based on maximum combustor cross-sectional area.